# SOME PROBLEMS IN THE THEORY OF NONLINEAR OSCILLATIONS

YOSHISUKE UEDA

DEPARTMENT OF ELECTRICAL ENGINEERING

KYOTO UNIVERSITY

FEBRUARY, 1965

# SOME PROBLEMS IN THE THEORY OF NONLINEAR OSCILLATIONS

# SOME PROBLEMS IN THE THEORY OF NONLINEAR OSCILLATIONS

YOSHISUKE UEDA

FEBRUARY, 1965

# INTRODUCTION

The text consists of five chapters. The generation of higher harmonics in electrical systems are described in the first two chapters. The last three chapters are concerned with forced oscillations in self-oscillatory systems of the negative resistance type.

In Chap. 1 the higher-harmonic oscillations in series-resonance circuit containing saturable iron core are studied. These oscillations occur when the amplitudes of the external force is very large. The differential equation which describes the system takes the form of Duffing's equation. To a periodic solution of this equation the terms of the fundamental frequency and one or two additional components of predominant amplitudes are assumed. By using the method of harmonic balance the amplitude characteristics of the oscillations are obtained. The stability of these oscillations are discussed by solving a variational equation which characterizes small deviations from the periodic states of equilibrium. The variational equation leads to Hill's equation. The characteristic exponent of the solution [26]* is compared with the damping of the system. The conditions thus obtained secure the stability not only of the oscillation having the fundamental frequency, but also of the oscillation with higher-harmonic or subharmonic frequency. These stability criteria are derived by Prof. C. Hayashi [7, 15]. The results thus obtained are compared with the solutions obtained by analog-computer analysis and found to be in satisfactory agreement with them.

The numerical analysis is also performed by using a digital computer. A different method of analysis from that used above is developed; that is, the

---

* Numbers in brackets indicate references on pages 110 to 112.

phase plane analysis, where the coordinates are the dependent variable and its time derivative, is used. We consider the behavior of representative points on this phase plane which are prescribed at the beginning of every cycle of the external force. Mathematically, these points will be obtained as successive images of the initial point under iterations of the mapping [13, 21]. Special attention is directed toward the location of the fixed points of the mapping, since these points are correlated with the periodic solutions of the differential equation. The fixed points are sought by iterating the mapping until the successive images are converged. Because of the way of this procedure, only the stable solutions are discussed. Stable solutions thus obtained are analyzed into harmonic components with the aid of Fourier's expansion theorem.

An experimental investigation using a series-resonance circuit has been done by Prof. C. Hayashi [7, 15]. His result is cited at the end of this chapter.

Chapter 2 is concerned with the higher-harmonic oscillations in parallel-resonance circuit. It is found that, as the amplitude of the applied voltage increases, harmonics of higher orders appear successively at certain intervals of the applied voltage. The differential equation of the system is given by Mathieu's equation with an additional nonlinear term. The same method of analysis as in the preceding chapter is used.

The three chapters that follow are devoted to the study of forced oscillations in self-oscillatory systems. When a periodic force is applied to a self-oscillatory system, the frequency of the self-excited oscillation, that is, the natural frequency of the system, falls in synchronism with the driving frequency, provided these two frequencies are not far different [20, 24]. This phenomenon of frequency entrainment may also occur when the ratio of the two frequencies is in the neighborhood of an integer (different from unity) or a fraction. Thus, if the amplitude and frequency of the external force are appropriately chosen, the natural frequency of the system is entrained by a frequency which is an integral multiple or submultiple of the driving frequency [12]. If the ratio of these two frequencies is not in the neighborhood of an integer or a fraction, one may expect the occurrence of an almost periodic oscillation [14]. It is a salient feature of an almost periodic oscillation that the amplitude and phase of the oscillation vary slowly but periodically even in the steady states. However, the period of the amplitude variation is not an integral multiple of the period of the external force; the ratio of these two periods is in general incommensurable. Therefore, as a whole, there is no periodicity in the almost periodic oscillation [10, 15, 20, 24].

In Chap. 3 the system governed by van der Pol's equation with an additional term for periodic excitation is treated. At the beginning of this chapter such regions of frequency entrainment are given that, if the amplitude and frequency of the external force are prescribed in these regions, the entrainment occurs at harmonic, higher-harmonic, or subharmonic frequency of the external force. In the next place special attention is directed to the almost periodic oscillations which occur when the external force is prescribed close to the regions of entrainment. As mentioned above, the natural frequency of the system is entrained not only by the driving frequency but also by the higher-harmonic and subharmonic frequencies of the external force. Therefore, almost periodic oscillations must be discussed in connection with the entrained oscillations at these frequencies. Since an entrained oscillation at higher-harmonic or subharmonic frequency is represented by a sum of the forced and free oscillations having the driving frequency and the entrained frequency, respectively, an almost periodic oscillation which develops from it may also be expressed by the sum of these two, but the amplitude and phase of the free oscillation are allowed to vary slowly with time.

The phase-plane analysis is applied to the study of almost periodic oscillations. The coordinates of the phase plane are the time-varying amplitudes of a pair of components of the free oscillation in quadrature. Consequently, an entrained oscillation is correlated with a singular point and an almost periodic oscillation with a limit cycle in the phase plane. Some examples of limit cycle representing the almost periodic oscillation are illustrated. The transition between entrained oscillations and almost periodic oscillations is discussed by using this method.

Digital-computer analysis is also performed. As mentioned in Chap. 1, the mapping procedure is applied. Successive images of the mapping representing the almost periodic oscillation do not approach a fixed point, but move permanently and generate a closed invariant curve. Some closed invariant curves are illustrated for the same values of the external force as used in the phase-plane analysis. The limit cycles obtained by phase-plane analysis are compared with the closed invariant curves.

Chapter 4 treats the self-oscillatory system with nonlinear restoring force. Harmonic and 1/3-harmonic entrainments and almost periodic oscillations are studied for this system. The phase-plane analysis, as described in the preceding chapter, is applied for the investigation of these oscillations.

The circumstances which may occur when the detuning, that is, the difference between the frequencies of the free and the forced oscillations, is neither very small nor very large are quite complicated; for intermediate values of the detuning both the entrained and almost periodic oscillations occur depending upon different values of the initial conditions. Some description of the phenomena in such cases is given for the van der Pol's equation with forcing term [3, 5]. However, such a range of the external force is extremely narrow. On the other hand in the system under consideration, the response curves of the entrained oscillations are skewed by the nonlinearity of the restoring term. On account of this property such a range of the external force becomes broader than that of the linear case. Therefore, we can approach such phenomena by applying numerical method and computer techniques. Two examples of the phase-plane diagram having stable singularity and limit cycle are calculated. The first is the case in which harmonic entrainment and almost periodic oscillation are sustained. The second example is 1/3-harmonic entrainment and almost periodic oscillation. Special attention is directed to the transition between entrained oscillations and almost periodic oscillations which occurs under such circumstances. When the external force is varied beyond the boundary of harmonic entrainment an example of transition is illustrated by considering the generation and extinction of singularity and limit cycle on the phase plane. The theoretical results are compared with the solutions obtained by analog-computer analysis and found to be in satisfactory agreement with them.

The final Chapter 5 of the text deals with singularities and limit cycles of some autonomous system. The system under consideration arises as the fundamental equations determining the in-phase and quadrature amplitudes of the forced oscillation in a self-oscillatory system with external force. Region of harmonic entrainment, in which an entrained oscillation is represented by a stable singular point, has on either side regions in each of which an almost periodic oscillation, represented by a stable limit cycle, occurs. Between these two regions, rather complicated transitions take place such as already explained in the preceding chapter.

In this chapter is illustrated an example of phase-plane diagram having three singularities and two limit cycles. Then special attention is directed to the transformation of these singularities and limit cycles when the external force is varied beyond the boundary of entrainment.

The text is supplemented by two appendixes. In Appendix I are given the theorems of Bendixson; in Appendix II is given the theory of centers due to Poincaré. These are cited in our investigation of integral curves near the singular point in Chap. 3.

## ACKNOWLEDGMENTS

The author owes a lasting debt of gratitude to Professor Dr. C. Hayashi, who has suggested the field of research of the present thesis and given him constant and generous guidance and encouragement in promoting this work.

In the preparation of the present paper the author was greatly aided by Professor H. Shibayama of Osaka Institute of Technology, by Assistant Professor Y. Nishikawa and by Lecturer M. Abe both of Kyoto University who gave him valuable suggestions and much good advice of all kinds. Acknowledgment must also be made to Mr. S. Hiraoka and Mr. M. Kuramitsu for their excellent cooperation.

The KDC-1 Digital Computer Laboratory of Kyoto University has made time available to the author. The author wishes to acknowledge the kind considerations of the staffs of these organizations. Finally, the author appreciates the assistance he received from Miss M. Takaoka, who typed the manuscript.

CONTENTS

# CHAPTER 1

# HIGHER-HARMONIC OSCILLATIONS IN A SERIES-RESONANCE CIRCUIT

## 1.1 Introduction

Under the action of a sinusoidal external force, a nonlinear system may exhibit basically different phenomena from those found in linear systems. One of the salient features of such phenomena is the generation of higher harmonics and subharmonics. A considerable number of papers have been published concerning subharmonic oscillations in nonlinear systems [ 8, 9, 11, 13 ]; however, very few investigations have been reported on the generation of higher harmonics.

This chapter deals with higher harmonic oscillations which predominantly occur in a series-resonance circuit containing a saturable inductor and a capacitor in series. The differential equation which describes the system takes the form of Duffing's equation. The amplitude characteristics of periodic solutions are obtained by using the method of harmonic balance. Particular attention is directed to the stability investigation of these solutions by applying Hill's equation as a stability criterion. The results obtained by the above procedure are examined by using the analog and digital computers.

An experimental investigation using a series-resonance circuit has been done by Prof. C. Hayashi [ 7, pp. 39-41 ]. His result is cited at the end of this chapter. The analysis of this experimental result is a motive for the present investigation.

## 1.2 Derivation of the Fundamental Equation

The schematic diagram illustrated in Fig. 1.1 shows an electrical circuit in which the nonlinear oscillation takes place due to the saturable-core inductance L under the impression of the alternating voltage $E \sin \omega t$. As shown in the figure, the resistor R is paralleled with the capacitor C, so that the circuit is dissipative. With the notation of the figure, the equations for the circuit are written as

$$
\begin{aligned}
n \frac{d\Phi}{dt} + Ri_R &= E \sin \omega t \\
Ri_R &= \frac{1}{C} \int i_C dt \qquad (1.1) \\
i &= i_R + i_C
\end{aligned}
$$

where n is the number of turns of the inductor coil, and $\Phi$ is the magnetic flux in the core. Then, neglecting hysteresis, we may assume the saturation curve of the form

$$i = a_1 \Phi + a_3 \Phi^3 \qquad (1.2)$$

where higher powers of $\Phi$ than the third are neglected. We introduce dimensionless variables u and v, defined by

$$i = I_n \cdot u \qquad \Phi = \Phi_n \cdot v \qquad (1.3)$$

where $I_n$ and $\Phi_n$ are appropriate base quantities of the current and the flux respectively. Then Eq. (1.2) becomes

$$u = \frac{a_1 \Phi_n}{I_n} v + \frac{a_3 \Phi_n^3}{I_n} v^3 = c_1 v + c_3 v^3 \qquad (1.4)$$

Although the base quantities $I_n$ and $\Phi_n$ can be chosen quite arbitrarily, it is preferable, for the brevity of calculation, to fix them by the relations

$$n\omega^2 C\Phi_n = I_n \qquad c_1 + c_3 = 1 \tag{1.5}$$

Then, after elimination of $i_R$ and $i_C$ in Eqs. (1.1) and use of Eqs. (1.3), (1.4), and (1.5), the result in terms of v is

$$\frac{d^2v}{d\tau^2} + k\frac{dv}{d\tau} + c_1 v + c_3 v^3 = B\cos\tau \tag{1.6}$$

where $\tau = \omega t - \tan^{-1}k \qquad k = \dfrac{1}{\omega CR} \qquad B = \dfrac{E}{n\omega\Phi_n}\sqrt{1 + k^2}$

### 1.3 Periodic Solution Consisting of Odd-Order Harmonics

As the amplitude B of the external force increases, an oscillation develops in which higher harmonics may not be ignored in comparison with the fundamental component. Since the system is symmetrical, we assume, for the time being, that these higher harmonics are of odd orders;* hence a periodic solution for Eq. (1.6 may be written as

$$v_0(\tau) = x_1 \sin\tau + y_1 \cos\tau + x_3 \sin 3\tau + y_3 \cos 3\tau \tag{1.7}$$

Terms of harmonics higher than the third are certain to be present but are ignored to this order of approximation.

---

* Equation (1.6) is unchanged if the sign of v is reversed and $\tau$ is shifted by $\pi$ radians. Therefore the system governed by Eq. (1.6) is called the symmetrical system.

(a) Determination of the Coefficients of the Periodic Solution

The coefficients in the right side of Eq. (1.7) may be found by the method of harmonic balance; that is, substituting Eq. (1.7) into (1.6) and equating the coefficients of the terms containing $\sin \tau$, $\cos \tau$, $\sin 3\tau$, and $\cos 3\tau$ separately to zero, we obtain

$$
\begin{aligned}
- A_1 x_1 - k y_1 - \tfrac{3}{4} c_3[(x_1^2 - y_1^2)x_3 + 2x_1 y_1 y_3] &\equiv X_1(x_1, y_1, x_3, y_3) = 0 \\
k x_1 - A_1 y_1 + \tfrac{3}{4} c_3[2x_1 y_1 x_3 - (x_1^2 - y_1^2)y_3] &\equiv Y_1(x_1, y_1, x_3, y_3) = B \\
- A_3 x_3 - 3k y_3 - \tfrac{1}{4} c_3(x_1^2 - 3y_1^2)x_1 &\equiv X_3(x_1, y_1, x_3, y_3) = 0 \\
3k x_3 - A_3 y_3 - \tfrac{1}{4} c_3(3x_1^2 - y_1^2)y_1 &\equiv Y_3(x_1, y_1, x_3, y_3) = 0
\end{aligned}
\tag{1.8}
$$

where $A_1 = 1 - c_1 - \frac{3}{4} c_3(r_1^2 + 2r_3^2)$ $\qquad A_3 = 9 - c_1 - \frac{3}{4} c_3(2r_1^2 + r_3^2)$

$r_1^2 = x_1^2 + y_1^2$ $\qquad r_3^2 = x_3^2 + y_3^2$

Eliminating x, y components in the above equations gives

$$
\begin{aligned}
\left[\left(A_1 - \frac{3r_3^2}{r_1^2} A_3\right)^2 + k^2\left(1 + \frac{9r_3^2}{r_1^2}\right)^2\right] r_1^2 &= B^2 \\
(A_3^2 + 9k^2)\, r_3^2 &= \frac{1}{16} c_3^2 r_1^6
\end{aligned}
\tag{1.9}
$$

From these relations the steady-state components $r_1$ and $r_3$ of the periodic solution are determined. Through use of Eqs. (1.8) and (1.9) the coefficients of the periodic solution are found to be

$$
x_1 = \frac{k(r_1^2 + 9r_3^2)}{B} \qquad y = \frac{-(A_1 r_1^2 - 3A_3 r_3^2)}{B} \tag{1.10}
$$

$$x_3 = \frac{4r_3^2}{c_3 r_1^6}[-PA_3 + 3kQ] \qquad y_3 = \frac{4r_3^2}{c_3 r_1^6}[-QA_3 - 3kP]$$

and

where

$$P = (x_1^2 - 3y_1^2)x_1 \qquad Q = (3x_1^2 - y_1^2)y_1 \tag{1.11}$$

(b) Stability Investigation of the Periodic Solution*

The periodic solution as given by Eqs. (1.7), (1.10), and (1.11) actually exists only when it is stable. In this section the stability of the periodic solution will be investigated by considering the behavior of a small variation $\xi(\tau)$ from the periodic solution $v_0(\tau)$. If this variation $\xi(\tau)$ tends to zero with increasing $\tau$, the periodic solution is stable; if $\xi(\tau)$ diverges, the periodic solution is unstable. The variation $\xi(\tau)$ is defined by

$$v(\tau) = v_0(\tau) + \xi(\tau) \tag{1.12}$$

where $v_0(\tau)$ is given by Eqs. (1.7), (1.10), and (1.11). It is worth noting that $\xi(\tau)$ need not have the same frequency as the periodic solution. Substituting Eq. (1.12) into (1.6) and bearing in mind that $\xi(\tau)$ is sufficiently small, we obtain the variational equation

$$\frac{d^2\xi}{d\tau^2} + k\frac{d\xi}{d\tau} + (c_1 + 3c_3 v_0^2)\xi = 0 \tag{1.13}$$

Introducing a new variable $\eta(\tau)$ defined by

$$\xi(\tau) = e^{-\delta\tau}\cdot\eta(\tau) \qquad \delta = k/2 \tag{1.14}$$

---

* See Ref. 15 for a detailed discussion of stability in nonlinear oscillatory systems.

yields

$$\frac{d^2\eta}{d\tau^2} + (c_1 - \delta^2 + 3c_3 v_0^2)\eta = 0 \tag{1.15}$$

in which the first-derivative term is removed. Inserting $v_0(\tau)$ as given by Eq. (1.7) into (1.15) leads to a Hill's equation of the form

$$\frac{d^2\eta}{d\tau^2} + [\,\theta_0 + 2\sum_{n=1}^{3}\theta_{ns}\sin 2n\tau + 2\sum_{n=1}^{3}\theta_{nc}\cos 2n\tau]\eta = 0$$

where

$$\theta_0 = c_1 - \delta^2 + \frac{3}{2}c_3(r_1^2 + r_3^2) \tag{1.16}$$

$$\theta_{1s} = \frac{3}{2}c_3(x_1y_1 - x_1y_3 + y_1x_3), \quad \theta_{1c} = -\frac{3}{4}c_3(x_1^2 - y_1^2) + \frac{3}{2}c_3(x_1x_3 + y_1y_3)$$

$$\theta_{2s} = \frac{3}{2}c_3(x_1y_3 + y_1x_3), \quad \theta_{2c} = \frac{3}{2}c_3(-x_1x_3 + y_1y_3)$$

$$\theta_{3s} = \frac{3}{2}c_3x_3y_3\,, \quad \theta_{3c} = -\frac{3}{4}c_3(x_3^2 - y_3^2)$$

By Floquet's theorem [ 4 ], the general solution of Eq. (1.16) takes the form

$$\eta(\tau) = Ae^{\mu\tau}\phi(\tau) + Be^{-\mu\tau}\psi(\tau) \tag{1.17}$$

where A and B are arbitrary constants, $\Phi(\tau)$ and $\Psi(\tau)$ are periodic functions of $\tau$ of period $\pi$ or $2\pi$, and $\mu$ is the characteristic exponent to be determined by the parameters $\theta$'s. From the theory of Hill's equation [16, 18, 25, 26] one sees that there are regions of parameters $\theta$'s in which the solution, Eq. (1.17), is either stable or unstable, and that these regions of stability and instability appear alternately as parameter $\theta_0$ increases. For convenience, we shall call the regions of instability as the first, the second, ··· unstable regions as parameter $\theta_0$ increases from zero. It is known that the periodic functions $\Phi(\tau)$ and $\Psi(\tau)$ in Eq. (1.17) contain odd-order harmonics in the regions of odd orders and even-order harmonics in the regions of even orders and that, in the $n$th unstable region, the $n$th harmonic component predominates over other harmonics.

Since Eq. (1.7) is an approximate solution of Eq. (1.6), a solution of Eq. (1.16) may reasonably be an approximation of the same order. Therefore we assume that a particular solution in the first and the third unstable regions is given by

$$\eta(\tau) = e^{\mu\tau}\phi(\tau) = e^{\mu\tau}[b_1 \sin(\tau - \sigma_1) + b_3 \sin(3\tau - \sigma_3)]^* \quad (1.18)$$

We substitute this into Eq. (1.16) and apply the method of harmonic balance to obtain

$$\Delta_1(\mu) \equiv \begin{vmatrix} \theta_0 + \mu^2 - 1 - \theta_{1c} & \theta_{1s} - 2\mu & \theta_{1c} - \theta_{2c} & -\theta_{1s} + \theta_{2s} \\ \theta_{1s} + 2\mu & \theta_0 + \mu^2 - 1 + \theta_{1c} & \theta_{1s} + \theta_{2s} & \theta_{1c} + \theta_{2c} \\ \theta_{1c} - \theta_{2c} & \theta_{1s} + \theta_{2s} & \theta_0 + \mu^2 - 9 - \theta_{3c} & \theta_{3s} - 6\mu \\ -\theta_{1s} + \theta_{2s} & \theta_{1c} + \theta_{2c} & \theta_{3s} + 6\mu & \theta_0 + \mu^2 - 9 + \theta_{3c} \end{vmatrix} = 0 \quad (1.19)$$

From Eq. (1.14) and (1.17) one sees that the variation $\xi$ tends to zero with increasing $\tau$ provided that $|\mu| < \delta$. Hence the stability condition for the first and the third unstable region is given by

$$\Delta_1(\delta) > 0 \quad (1.20)$$

Substitution of parameters $\theta$'s given by Eqs. (1.16) into the condition (1.20) yields

---

* This form of solution was introduced by E. T. Whittaker [26].

$$\Delta_1(\delta) \equiv \begin{vmatrix} \frac{\partial X_1}{\partial x_1} & \frac{\partial X_1}{\partial y_1} & \frac{\partial X_1}{\partial x_3} & \frac{\partial X_1}{\partial y_3} \\ \frac{\partial Y_1}{\partial x_1} & \frac{\partial Y_1}{\partial y_1} & \frac{\partial Y_1}{\partial x_3} & \frac{\partial Y_1}{\partial y_3} \\ \frac{\partial X_3}{\partial x_1} & \frac{\partial X_3}{\partial y_1} & \frac{\partial X_3}{\partial x_3} & \frac{\partial X_3}{\partial y_3} \\ \frac{\partial Y_3}{\partial x_1} & \frac{\partial Y_3}{\partial y_1} & \frac{\partial Y_3}{\partial x_3} & \frac{\partial Y_3}{\partial y_3} \end{vmatrix} \equiv \frac{\partial(X_1, Y_1, X_3, Y_3)}{\partial(x_1, y_1, x_3, y_3)} > 0 \qquad (1.21)$$

**Differentiating Eqs. (1.8) with respect to B, we obtain**

$$\begin{aligned} \frac{\partial X_1}{\partial x_1}\frac{dx_1}{dB} + \frac{\partial X_1}{\partial y_1}\frac{dy_1}{dB} + \frac{\partial X_1}{\partial x_3}\frac{dx_3}{dB} + \frac{\partial X_1}{\partial y_3}\frac{dy_3}{dB} &= 0 \\ \frac{\partial Y_1}{\partial x_1}\frac{dx_1}{dB} + \frac{\partial Y_1}{\partial y_1}\frac{dy_1}{dB} + \frac{\partial Y_1}{\partial x_3}\frac{dx_3}{dB} + \frac{\partial Y_1}{\partial y_3}\frac{dy_3}{dB} &= 1 \\ \frac{\partial X_3}{\partial x_1}\frac{dx_1}{dB} + \frac{\partial X_3}{\partial y_1}\frac{dy_1}{dB} + \frac{\partial X_3}{\partial x_3}\frac{dx_3}{dB} + \frac{\partial X_3}{\partial y_3}\frac{dy_3}{dB} &= 0 \\ \frac{\partial Y_3}{\partial x_1}\frac{dx_1}{dB} + \frac{\partial Y_3}{\partial y_1}\frac{dy_1}{dB} + \frac{\partial Y_3}{\partial x_3}\frac{dx_3}{dB} + \frac{\partial Y_3}{\partial y_3}\frac{dy_3}{dB} &= 0 \end{aligned} \qquad (1.22)$$

Solving these simultaneous equations gives

$$\frac{dx_1}{dB} = \frac{\Delta_{21}}{\Delta} \qquad \frac{dy_1}{dB} = \frac{\Delta_{22}}{\Delta} \qquad \frac{dx_3}{dB} = \frac{\Delta_{23}}{\Delta} \qquad \frac{dy_3}{dB} = \frac{\Delta_{24}}{\Delta} \qquad (1.23)$$

where $\Delta_{2i}$ ($i = 1 \sim 4$) is the cofactor of row 2 and column i of the determinant $\Delta$ ($\equiv \Delta_1(\delta)$). Consequently,

$$\frac{dr_1}{dB} = \frac{1}{r_1\Delta}(x_1\Delta_{21} + y_1\Delta_{22})$$

$$\frac{dr_3}{dB} = \frac{1}{r_3\Delta}\,(x_3\Delta_{23} + y_3\Delta_{24}) \tag{1.24}$$

where $\quad r_1^2 = x_1^2 + y_1^2 \qquad r_3^2 = x_3^2 + y_3^2$

Hence the vertical tangency of the characteristic curves ($Br_1$ and $Br_3$ relations) occurs at the stability limit $\Delta = 0$ of the first and the third unstable regions.

A particular solution of Eq. (1.16) in the second unstable region may preferably be written as

$$\eta(\tau) = e^{\mu\tau}\phi(\tau) = e^{\mu\tau}[b_0 + b_2 \sin(2\tau - \sigma_2)] \tag{1.25}$$

Proceeding analogously as above, the characteristic exponent $\mu$ is determined by

$$\Delta_2(\mu) \equiv \begin{vmatrix} \theta_0 + \mu^2 & \theta_{1s} & \theta_{1c} \\ 2\theta_{1s} & \theta_0 + \mu^2 - 4 - \theta_{2c} & \theta_{2s} - 4\mu \\ 2\theta_{1c} & \theta_{2s} + 4\mu & \theta_0 + \mu^2 - 4 + \theta_{2c} \end{vmatrix} = 0 \tag{1.26}$$

and the stability condition for the second unstable region, i.e., $|\mu| < \delta$, is given by

$$\Delta_2(\delta) > 0 \tag{1.27}$$

(c) Numerical Example

Putting $k = 0.4$, $c_1 = 0$, and $c_3 = 1$ in Eq. (1.6) gives

$$\frac{d^2v}{d\tau^2} + 0.4\,\frac{dv}{d\tau} + v^3 = B\cos\tau$$

By use of Eqs. (1.9) the amplitude characteristics of Eq. (1.7) were calculated for this particular case and plotted against B in Fig. 1.2. The dotted portions of the characteristic curves represent unstable states, since the stability condition (1.20) or (1.27) is not satisfied in these intervals.

## 1.4 Occurrence of Even-Order Harmonics

It has been pointed out in Sec. 1.3b that even-order harmonics are self-excited in the second unstable region (see Fig. 1.2). In this region, the self-excited oscillation would gradually build up with increasing amplitude taking the form

$$e^{(\mu - \delta)\tau}\,[b_0 + b_2 \sin(2\tau - \sigma_2)] \qquad \text{with} \qquad \mu - \delta > 0$$

and ultimately get to the steady state with a constant amplitude which is limited by the nonlinearity of the system. This implies that, under certain intervals of B, such even-order harmonics must be considered in the periodic solution.

### (a) Periodic Solution and Condition for Stability

From the above consideration, a periodic solution for Eq. (1.6) may be assumed as

$$v_0(\tau) = z + x_1 \sin\tau + y_1 \cos\tau + x_2 \sin 2\tau + y_2 \cos 2\tau \tag{1.28}$$

Terms of harmonics higher than the second, especially the third harmonic, are certain to be present but are ignored to avoid unwieldy calculations. The unknown coefficients in the right side of Eq. (1.28) are determined in much the same manner as before; that is, substituting Eq. (1.28) into (1.6) and equating the coefficients of the nonoscillatory term and of the terms containing $\sin\tau$, $\cos\tau$, $\sin 2\tau$, and $\cos 2\tau$ separately to zero, we obtain

$$-A_0 z + \frac{3}{4} c_3\,[2x_1y_1x_2 - (x_1^2 - y_1^2)y_2] \equiv Z(z, x_1, y_1, x_2, y_2) = 0$$

$$- A_1x_1 - ky_1 + 3c_3z\ (y_1x_2 - x_1y_2) \equiv X_1(z,\ x_1,\ y_1,\ x_2,\ y_2) = 0$$

$$kx_1 - A_1y_1 + 3c_3z\ (x_1x_2 + y_1y_2) \equiv Y_1(z,\ x_1,\ y_1,\ x_2,\ y_2) = B$$

$$- A_2x_2 - 2ky_2 + 3c_3zx_1y_1 \equiv X_2(z,\ x_1,\ y_1,\ x_2,\ y_2) = 0$$

$$2kx_2 - A_2y_2 - \frac{3}{2}\, c_3z\ (x_1^2 - y_1^2) \equiv Y_2(z,\ x_1,\ y_1,\ x_2,\ y_2) = 0 \qquad (1.29)$$

where $A_0 = - c_1 - c_3\ [z^2 + \frac{3}{2}\ (r_1^2 + r_2^2)]$

$$A_1 = 1 - c_1 - \frac{3}{4}\, c_3\ (4z^2 + r_1^2 + 2r_2^2) \qquad A_2 = 4 - c_1 - \frac{3}{4}\, c_3\ (4z^2 + 2r_1^2 + r_2^2)$$

$$r_1^2 = x_1^2 + y_1^2 \qquad\qquad r_2^2 = x_2^2 + y_2^2$$

Eliminating x, y components in the above equations gives

$$[(A_1 - \frac{2r_2^2}{r_1^2}\, A_2)^2 + k^2(1 + \frac{4r_2^2}{r_1^2})^2]\ r_1^2 = B^2$$

$$- A_0z^2 + \frac{1}{2}\, A_2r_2^2 = 0 \qquad (1.30)$$

$$(A_2^2 + 4k^2)r_2^2 = \frac{9}{4}\, c_3^2z^2r_1^4$$

From these relations z, $r_1$, and $r_2$ are determined. Through use of Eqs. (1.29) and (1.30) the coefficients of the periodic solution are found to be

$$x_1 = \frac{k(r_1^2 + 4r_2^2)}{B} \qquad y_1 = \frac{- (A_1r_1^2 - 2A_2r_2^2)}{B} \qquad (1.31)$$

and

$$x_2 = \frac{4r_2^2}{3c_3zr_1^4}\ [A_2x_1y_1 + k(x_1^2 - y_1^2)]$$

$$y_2 = \frac{4r_2^2}{3c_3zr_1^4}\ [2kx_1y_1 - \frac{1}{2}\, A_2(x_1^2 - y_1^2)] \qquad (1.32)$$

Proceeding analogously as in Sec. 1.3b, the condition for stability may also be derived ; namely, inserting $v_0(\tau)$ as given by Eq. (1.28) into (1.15) leads to a Hill's equation of the form

$$\frac{d^2\eta}{d\tau^2} + [\theta_0 + 2\sum_{n=1}^{4} \theta_{ns} \sin n\tau + 2\sum_{n=1}^{4} \theta_{nc} \cos n\tau]\eta = 0 \tag{1.33}$$

where $\xi\ (= v - v_0) = e^{-\delta\tau} \cdot \eta$

A particular solution of Eq. (1.33) in the first and second unstable regions may be assumed as

$$\eta(\tau) = e^{\mu\tau}\phi(\tau) = e^{\mu\tau}[b_0 + b_1 \sin(\tau - \sigma_1) + b_2 \sin(2\tau - \sigma_2)] \tag{1.34}$$

Through use of Eqs. (1.29) the stability condition is obtained as*

$$\Delta(\delta) \equiv \frac{\partial(Z, X_1, Y_1, X_2, Y_2)}{\partial(z, x_1, y_1, x_2, y_2)} > 0 \tag{1.35}$$

(b) Numerical Example

By use of Eqs. (1.30) the amplitude characteristics of Eq. (1.28) were calculated and plotted in Fig. 1.3. The system parameters are the same as in Fig. 1.2, i.e., $k = 0.4$, $c_1 = 0$, and $c_3 = 1$. The dotted portions represent

---

* As the coefficient of $\eta$ in Eq. (1.33) contains even and odd harmonics, there are regions of parameters $\theta$'s in which the subharmonics of order 1/2, 3/2, ... are excited. This implies that in the second unstable region of Fig. 1.2 there may exist intervals of B such that subharmonics of order 1/2, 3/2, ... develop. A detailed investigation of such a case is, however, omitted here (cf. Secs. 1.5, 1.6b).

unstable state since condition (1.35) is not satisfied. One sees that the second unstable region of Fig. 1.3 became narrower than that of Fig. 1.2 and was shifted to the left. This fact results from the neglection of the third harmonic in Eq. (1.28). It is worth mentioning that the second harmonic is maintained in the second unstable region even though the system is symmetrical.

## 1.5 Analog-Computer Analysis

The theoretical results obtained in the preceding sections will be compared with the solutions obtained by using an analog computer. The block diagram of Fig. 1.4 shows an analog-computer setup for the solution of Eq. (1.6), in which the system parameters k, $c_1$, and $c_3$ are set equal to the values as given in Secs. 1.3c and 1.4b; i.e.,

$$\frac{d^2v}{d\tau^2} + 0.4\,\frac{dv}{d\tau} + v^3 = B\,\cos\tau \tag{1.36}$$

The symbols in the figure follow the conventional notation.* The solutions of Eq. (1.36) are sought for various values of B, i.e., the amplitude of the external force. From the solutions obtained in this way, each harmonic component is calculated and plotted against B in Fig. 1.5. The first unstable region ranges from B = 0.45 to 0.53; jump phenomenon takes place in the direction of arrows. The second unstable region extends from B = 2.7 to 12.6. In this region the concurrence of the subharmonics of order 1/2, 3/2, ··· is confirmed in the intervals of B approximately from 7 to 11. However, since the solutions accom-

---

* The integral amplifiers in the block diagram integrate their inputs with respect to the machine time (in second), which is, in this particular case, 5 times the independent variable $\tau$.

panied with such subharmonics are extremely sensitive to the external disturbance, the result obtained by computer analysis was not very accurate. Therefore, we indicate such region by broken lines in Fig. 1.5. The third unstable region occurs between $B = 12.6$ to $14.9$, and the oscillation jumps into another stable state on the borders of this region. These results show the qualitative agreement with the theoretical results obtained in the preceding sections.

## 1.6 Numerical Analysis by Using a Digital Computer

In the preceding sections we investigated the approximate solutions of Eq. (1.6) both by using the harmonic balance method and by using an analog computer. The results thus obtained state that there are such regions of B that in the first and the third unstable regions there exist two stable states (see Fig. 1.2) and in the second unstable region there is the only stable state (see Fig. 1.3).*

In this section we shall seek for the numerical solution in each unstable region by using the KDC-1 digital computer.

The periodic solutions of Eq. (1.6), that is,

$$\frac{d^2v}{d\tau^2} + k\frac{dv}{d\tau} + c_1 v + c_3 v^3 = B\cos\tau$$

is determined by the following procedure.

The second-order differential equation (1.6) can be rewritten as the simultaneous equations of the first order

$$\frac{dv}{d\tau} = \dot{v}$$

* In the second unstable region, there are two oscillations differing in sign and in phase by $\pi$ radians, but their amplitudes are the same.

$$\frac{d\dot{v}}{d\tau} = - k\dot{v} - c_1 v - c_3 v^3 + B \cos\tau \tag{1.37}$$

We consider the location of the points whose coordinates are given by $v(\tau)$ and $\dot{v}(\tau)$ at the instants of $\tau = 0, 2\pi, 4\pi, \cdots$ in the $v\dot{v}$ plane, since the right sides of Eqs. (1.37) are periodic functions in $\tau$ of period $2\pi$. Mathematically, these points $P_n(v(2n\pi), \dot{v}(2n\pi))$ are defined as the successive images of the initial point $P_0(v(0), \dot{v}(0))$ under iterations of the mapping T from $\tau = 0$ to $2n\pi$; and we denote this by the notation

$$P_n = T^n(P_0) \tag{1.38}$$

where $n = 1, 2, 3, \cdots$.

Actually, these points can be obtained approximately by performing the numerical integration of Eqs. (1.37) from $\tau = 0$ to $2n\pi$. Special attention is directed toward the location of the fixed point and of the periodic point of Eqs. (1.37).*

---

* The point whose location is invariant under the mapping is called the fixed point; i.e.,

$$P_0 = P_1(= T(P_0))$$

and the corresponding solution $v(\tau)$ is periodic in $\tau$ with the period $2\pi$. While the periodic points are defined by the following relations,

$$P_0 \neq P_i \quad (1 \leq i \leq m - 1) \qquad\qquad P_0 = P_m(= T^m(P_0))$$

namely, periodic points are invariant under every $\underline{m}$th iterate of the mapping. The corresponding solution $v(\tau)$, in this case, is also periodic in $\tau$ but its least period is equal to $2m\pi$.

When an initial point $P_0$, the initial condition $(v(0), \dot{v}(0))$, is chosen sufficiently near the fixed (periodic) point, the point sequence $\{P_n\}$ converges to the fixed (periodic) point as $n \to \infty$ provided the fixed (periodic) point is completely stable. In order to determine the location of the stable fixed (periodic) point, we estimate the initial condition by making use of the values obtained in the preceding sections.

Then numerical integration of Eqs. (1.37) is performed from the above initial condition until the following condition is reached; i.e.,

$$\begin{aligned} &|P_n - P_{n+1}| < \varepsilon \qquad \text{for the fixed point} \\ \text{or} \qquad &|P_n - P_{n+m}| < \varepsilon \qquad \text{for the periodic point} \end{aligned} \tag{1.39}$$

where $\varepsilon$ is small positive constant.* Because of the way of this procedure, only the stable solutions are obtained.

Once the stable fixed (periodic) point is determined, we seek the time response values of $v(\tau)$ and $\dot{v}(\tau)$ at the instants of $\tau = nh$, where $n = 0, 1, \cdots, 2N-1$ (or $2mN-1$), and $h$ $(= \pi/N)$ is a chosen time increment. From the data obtained in this way, we can calculate the desired harmonic components of $v(\tau)$ with the aid of Fourier's expansion theorem:

$$v(\tau) = \frac{1}{2} a_0 + \sum_{n=1}^{\infty} \left(a_{n/p} \cos \frac{n}{p}\tau + b_{n/p} \sin \frac{n}{p}\tau\right)$$

$$\text{where} \qquad a_{n/p} = \frac{1}{p\pi}\int_0^{2p\pi} v(\tau) \cos \frac{n}{p}\tau d\tau \qquad n = 0, 1, 2, \cdots \tag{1.40}$$

---

* We shall show the numerical examples afterwards, where the value of $\varepsilon$ is taken equal to $10^{-5}$.

$$b_{n/p} = \frac{1}{p\pi}\int_0^{2p\pi} v(\tau)\ \sin\frac{n}{p}\tau\, d\tau \qquad n = 1, 2, 3, \cdots$$

and p = 1 for fixed point and p = m for periodic point.

By using the method above-described we show some examples of numerical solution of Eq. (1.6) with the system parameters $k = 0.4$, $c_1 = 0$, and $c_3 = 1$; i.e.,

$$\frac{d^2v}{d\tau^2} + 0.4\frac{dv}{d\tau} + v^3 = B \cos\tau \tag{1.41}$$

for several values of B.

(a) Numerical Solutions in the First Unstable Region

We consider the equation

$$\frac{d^2v}{d\tau^2} + 0.4\frac{dv}{d\tau} + v^3 = 0.5 \cos\tau \tag{1.42}$$

For this particular value of the amplitude of the external force (B = 0.5), there are two stable states of the periodic solution; see Fig. 1.2. In order to distinguish these two stable states, we shall call them the resonant and the nonresonant states, respectively, as the amplitude of the oscillation is large or small. The numerical solutions for Eq. (1.42) are determined. They are as follows.

For Resonant Oscillation:

$$\begin{aligned} v(\tau) = \; & 0.298 \cos\tau + 1.145 \sin\tau \\ & - 0.048 \cos 3\tau - 0.035 \sin 3\tau \\ & + 0.003 \cos 5\tau + 0.000 \sin 5\tau \\ & + \cdots \end{aligned} \tag{1.43}$$

For Nonresonant Oscillation:

$$v(\tau) = -0.530\cos\tau + 0.294\sin\tau + 0.001\cos 3\tau + 0.006\sin 3\tau + \cdots \tag{1.44}$$

The phase trajectories in the $v\dot{v}$ plane of the solutions, given by Eqs. (1.43) and (1.44), are plotted in Fig. 1.6a by thick and fine lines, respectively. Figure 1.6b shows the waveforms $v(\tau)$ converted from the trajectories of Fig. 1.6a. The small circles on the trajectories in Fig. 1.6a indicate the location of the stable fixed points of the mapping. In performing the numerical integration of Eqs. (1.37), we used the Runge-Kutta-Gill's method (with the step h equal to $\pi/30$). We also employed the trapezoidal formula for calculating the second and the third definite integrals of (1.40).

(b) Numerical Solutions in the Second Unstable Region

Case 1:
$$\frac{d^2v}{d\tau^2} + 0.4\frac{dv}{d\tau} + v^3 = 4\cos\tau \tag{1.45}$$

There are two stable solutions for Eq. (1.45); one of them is

$$\begin{aligned} v(\tau) = \; & 0.314 \\ & + 1.591\cos\tau + 0.597\sin\tau \\ & - 0.201\cos 2\tau - 0.730\sin 2\tau \\ & + 0.148\cos 3\tau + 0.115\sin 3\tau \\ & + 0.036\cos 4\tau - 0.154\sin 4\tau \\ & - 0.034\cos 5\tau + 0.025\sin 5\tau \\ & + 0.017\cos 6\tau - 0.015\sin 6\tau \\ & - 0.011\cos 7\tau - 0.001\sin 7\tau \end{aligned}$$

$$+ 0.003 \cos 8\tau + 0.002 \sin 8\tau$$
$$- 0.002 \cos 9\tau - 0.002 \sin 9\tau$$
$$+ 0.000 \cos 10\tau + 0.001 \sin 10\tau$$
$$+ \cdots \tag{1.46}$$

The other solution can be represented by $-v(\tau + \pi)$, where $v(\tau)$ is given by Eq. (1.46). Figure 1.7a and b show the phase trajectories and the waveforms of $v(\tau)$, respectively.

As we have already predicted the occurrence of subharmonics of order 1/2, 3/2, ··· in Sec. 1.4a, this type of solutions was observed in Sec. 1.5. We shall show below the numerical solution.

Case 2:
$$\frac{d^2v}{d\tau^2} + 0.4\frac{dv}{d\tau} + v^3 = 9 \cos \tau \tag{1.47}$$

There are four stable solutions for Eq. (1.47). If we indicate one of them by $v(\tau)$, the remaining three solutions are represented by $v(\tau + 2\pi)$, $-v(\tau + \pi)$, and $-v(\tau + 3\pi)$. Therefore only one of them is shown below.

$$\begin{aligned} v(\tau) = &- 0.314 \\ &+ 0.007 \cos \tfrac{1}{2}\tau - 0.062 \sin \tfrac{1}{2}\tau \\ &+ 1.839 \cos \tau + 0.585 \sin \tau \\ &+ 0.007 \cos \tfrac{3}{2}\tau - 0.000 \sin \tfrac{3}{2}\tau \\ &+ 0.337 \cos 2\tau + 0.258 \sin 2\tau \\ &- 0.069 \cos \tfrac{5}{2}\tau + 0.096 \sin \tfrac{5}{2}\tau \\ &+ 0.889 \cos 3\tau + 0.043 \sin 3\tau \\ &+ 0.021 \cos \tfrac{7}{2}\tau + 0.015 \sin \tfrac{7}{2}\tau \\ &+ 0.048 \cos 4\tau + 0.114 \sin 4\tau \end{aligned}$$

$$
\begin{aligned}
&- 0.025 \cos \tfrac{9}{2}\tau + 0.026 \sin \tfrac{9}{2}\tau \\
&+ 0.184 \cos 5\tau + 0.058 \sin 5\tau \\
&+ 0.001 \cos \tfrac{11}{2}\tau + 0.002 \sin \tfrac{11}{2}\tau \\
&+ 0.019 \cos 6\tau + 0.050 \sin 6\tau \\
&- 0.012 \cos \tfrac{13}{2}\tau + 0.010 \sin \tfrac{13}{2}\tau \\
&+ 0.046 \cos 7\tau + 0.023 \sin 7\tau \\
&- 0.001 \cos \tfrac{15}{2}\tau + 0.001 \sin \tfrac{15}{2}\tau \\
&+ 0.005 \cos 8\tau + 0.017 \sin 8\tau \\
&- 0.004 \cos \tfrac{17}{2}\tau + 0.003 \sin \tfrac{17}{2}\tau \\
&+ 0.010 \cos 9\tau + 0.008 \sin 9\tau \\
&- 0.001 \cos \tfrac{19}{2}\tau + 0.000 \sin \tfrac{19}{2}\tau \\
&+ 0.001 \cos 10\tau + 0.006 \sin 10\tau \\
&+ \cdots \qquad\qquad (1.48)
\end{aligned}
$$

Figure 1.8a shows the trajectories of the stable solutions for Eq. (1.47). The small circles in the figure indicate the location of the periodic points which are correlated with the subharmonic oscillation of order 1/2. The periodic points 1 and 2 (or 3 and 4) lie on the same trajectory and, under iterations of the mapping, these points are transferred successively to the points that follow in the direction of the arrows. In order to distinguish clearly the trajectory of the point 1 to 2 (or 3 to 4) from that of the point 2 to 1 (or 4 to 3), we show the former by full lines and the latter by dotted lines. The waveforms corresponding to the trajectories $1 \rightarrow 2 \rightarrow 1$ and $3 \rightarrow 4 \rightarrow 3$ are shown in Fig. 1.8b.

### (c) Numerical Solutions in the Third Unstable Region

$$\frac{d^2v}{d\tau^2} + 0.4\,\frac{dv}{d\tau} + v^3 = 13\cos\tau \tag{1.49}$$

For this particular value of B, i.e., B = 13 in Eq. (1.41), two stable solutions are obtained. They are

$$\begin{aligned} v(\tau) = {} & 2.477\cos\tau + 0.773\sin\tau \\ & - 0.513\cos 3\tau - 1.213\sin 3\tau \\ & - 0.083\cos 5\tau - 0.285\sin 5\tau \\ & - 0.092\cos 7\tau + 0.046\sin 7\tau \\ & - 0.015\cos 9\tau + 0.017\sin 9\tau \\ & + 0.006\cos 11\tau + 0.007\sin 11\tau \\ & + 0.002\cos 13\tau + 0.000\sin 13\tau \\ & + \cdots \end{aligned} \tag{1.50}$$

and

$$\begin{aligned} v(\tau) = {} & 1.669\cos\tau + 0.781\sin\tau \\ & + 1.404\cos 3\tau + 0.074\sin 3\tau \\ & + 0.350\cos 5\tau + 0.090\sin 5\tau \\ & + 0.115\cos 7\tau + 0.047\sin 7\tau \\ & + 0.038\cos 9\tau + 0.018\sin 9\tau \\ & + 0.012\cos 11\tau + 0.007\sin 11\tau \\ & + 0.004\cos 13\tau + 0.003\sin 13\tau \\ & + 0.001\cos 15\tau + 0.001\sin 15\tau \\ & + \cdots \end{aligned} \tag{1.51}$$

The phase trajectories of $v(\tau)$, given by Eqs. (1.50) and (1.51) are depicted in Fig. 1.9a by thick and fine lines, respectively. Figure 1.9b shows the

Table 1.1 Stable fixed and periodic points for Eq. (1.41) and the chosen step h.

| Value of B | Point | v | $\dot{v}$ | Value of h | Classification |
|---|---|---|---|---|---|
| 0.5 | Fig. 1.6a 1 | 0.2526 | 1.0398 | $\pi/30$ | Fixed point |
| | 2 | -0.5290 | 0.3134 | " | " |
| 4 | Fig. 1.7a 1 | 1.5220 | 3.1810 | $\pi/30$ | Fixed point |
| | 2 | 1.8626 | -1.1065 | " | " |
| 9 | Fig. 1.8a 1 | 2.9857 | 3.2769 | $\pi/60$ | Periodic point |
| | 2 | 3.1460 | 2.2806 | " | " |
| | 3 | 2.8192 | -0.7005 | " | " |
| | 4 | 2.9310 | 0.2684 | " | " |
| 13 | Fig. 1.9a 1 | 1.7823 | -3.7474 | $\pi/60$ | Fixed point |
| | 2 | 3.5927 | 2.0913 | " | " |

waveforms of $v(\tau)$ converted from the trajectories of Fig. 1.9a. As one sees from the magnitudes of the fundamental components in Eqs. (1.50) and (1.51), the solution given by Eq. (1.50) corresponds to the upper branch of the characteristic curve $r_1$ in the third unstable region (see Fig. 1.2).

The values of the coordinates of the stable fixed and periodic points appeared in the above examples are summed up and listed in Table 1.1. The values of the time increment h which is employed for finding the corresponding fixed (periodic) point are also shown.

## 1.7 Experimental Result

An experiment using a series-resonance circuit as illustrated in Fig. 1.1 has been performed [ 7, pp. 39-41 ]. The result is as follows.

Since B is proportional to the amplitude E of the applied voltage, varying E will bring about the excitation of higher harmonic oscillations. This is observed in Fig. 1.10, in which the effective value of the oscillating current is plotted (in thick line) for a wide range of the applied voltage. By making use of a heterodyne harmonic analyser, this current is analyzed into harmonic components. These are shown by fine line, the numbers on which indicate the order of the harmonics. The first unstable region ranges between 24 and 40 volts of the applied voltage; the jump phenomenon in this region has been called the ferro-resonance. The second unstable region extends from 180 to 580 volts. As expected from the preceding analysis, the occurrence of even harmonics is a salient feature of this region. The third unstable region occurs between 660 and 670 volts, exhibiting another jump in amplitude.

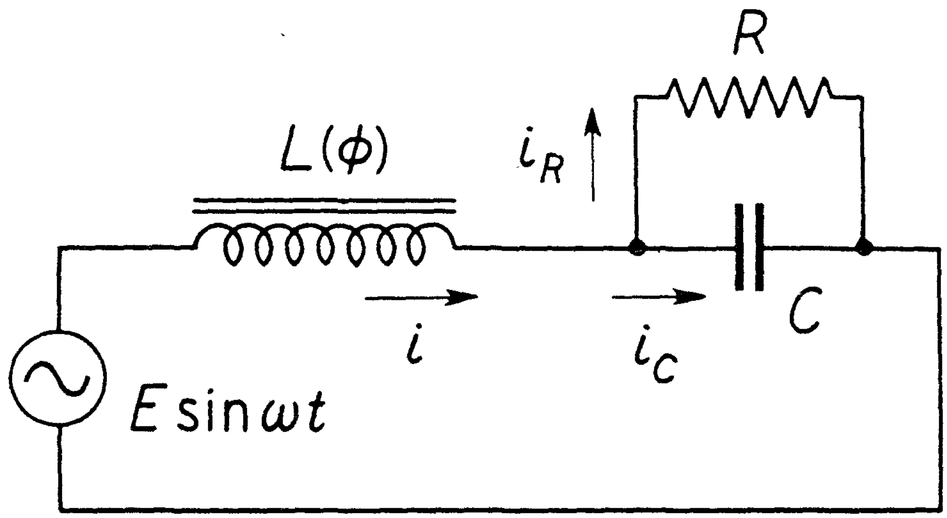


Fig. 1.1. Series-resonance circuit with nonlinear inductance.

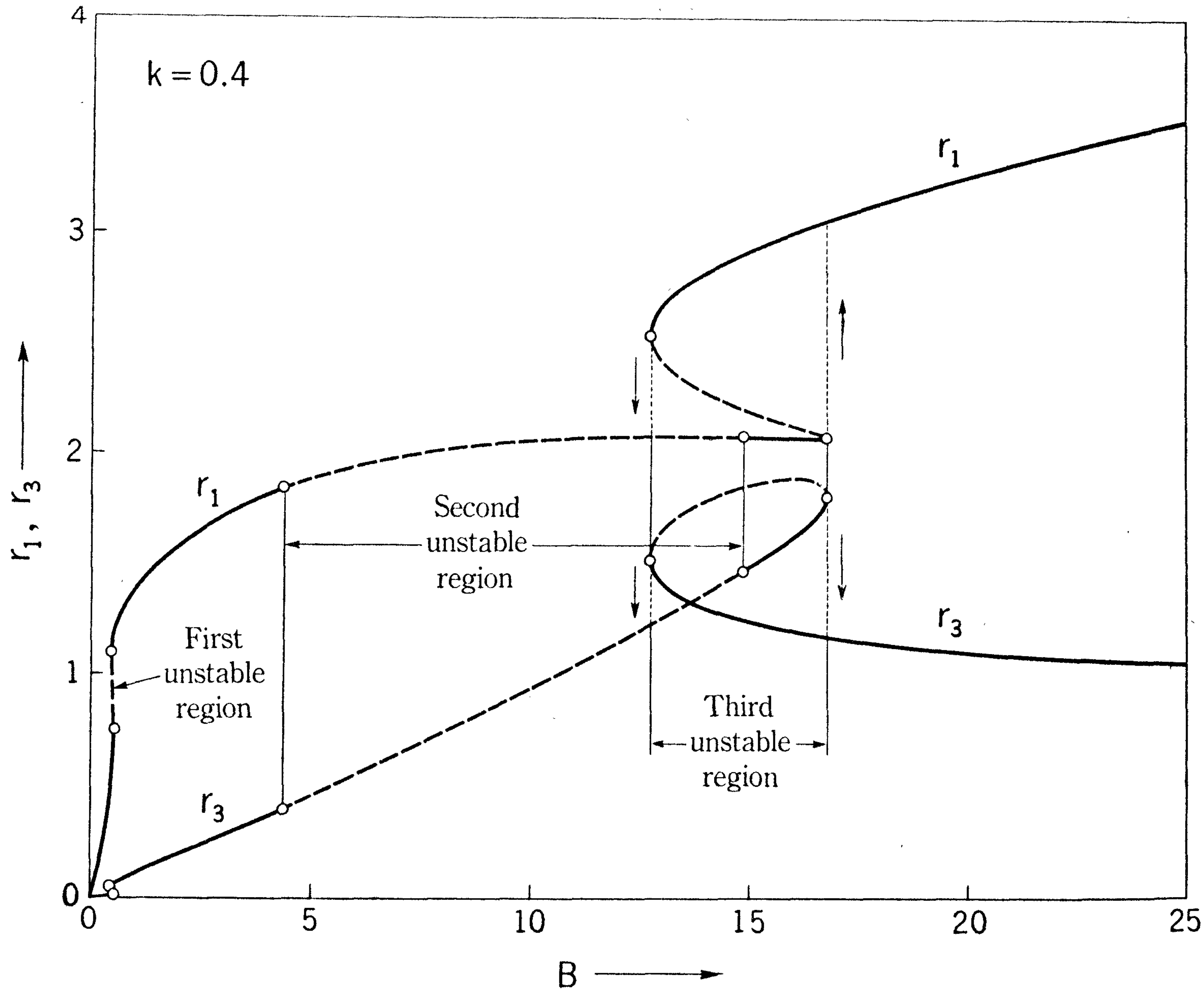


Fig. 1.2. Amplitude characteristics of the periodic solution as given by Eq. (1.7).

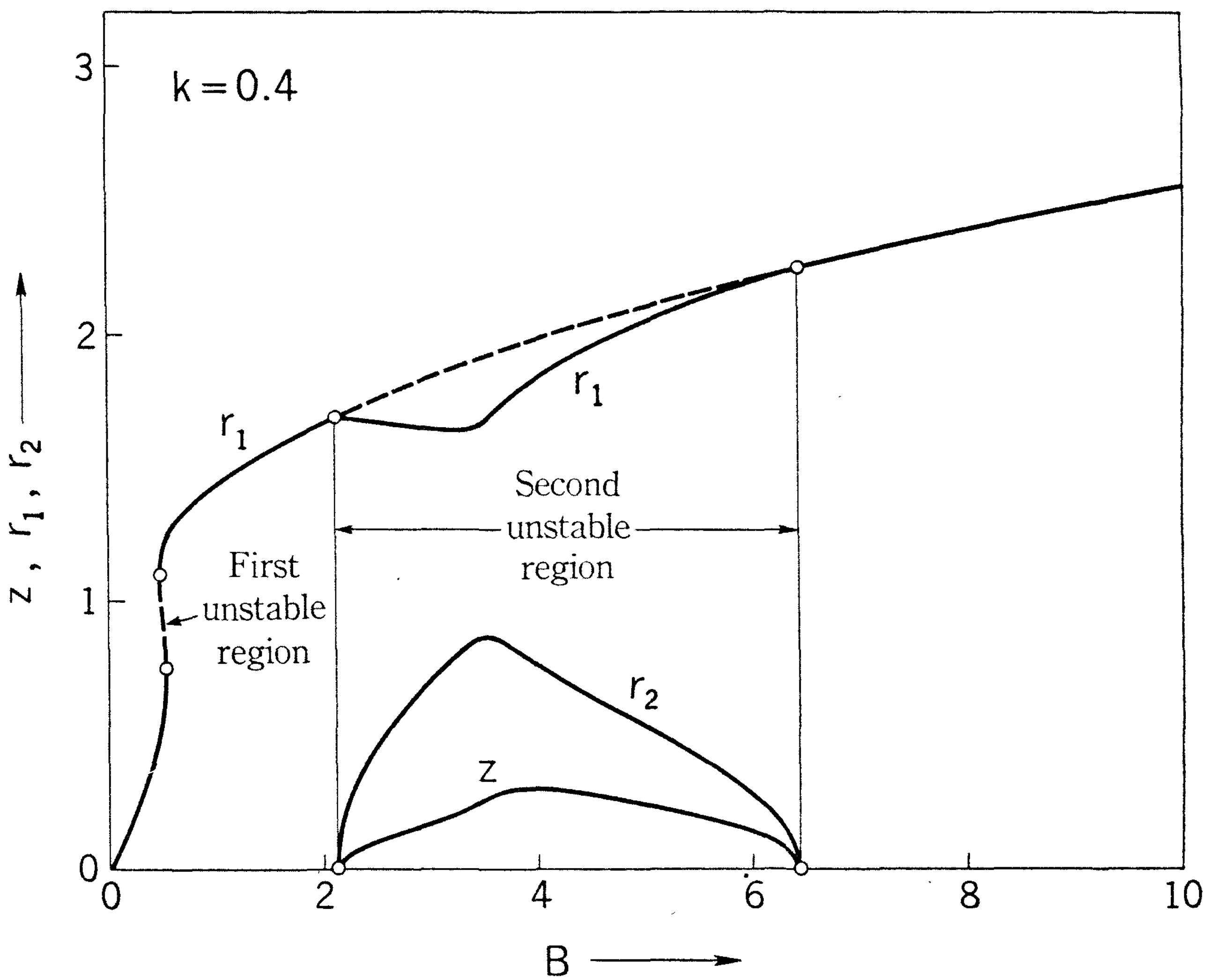


Fig. 1.3. Amplitude characteristics of the periodic solution as given by Eq. (1.28).

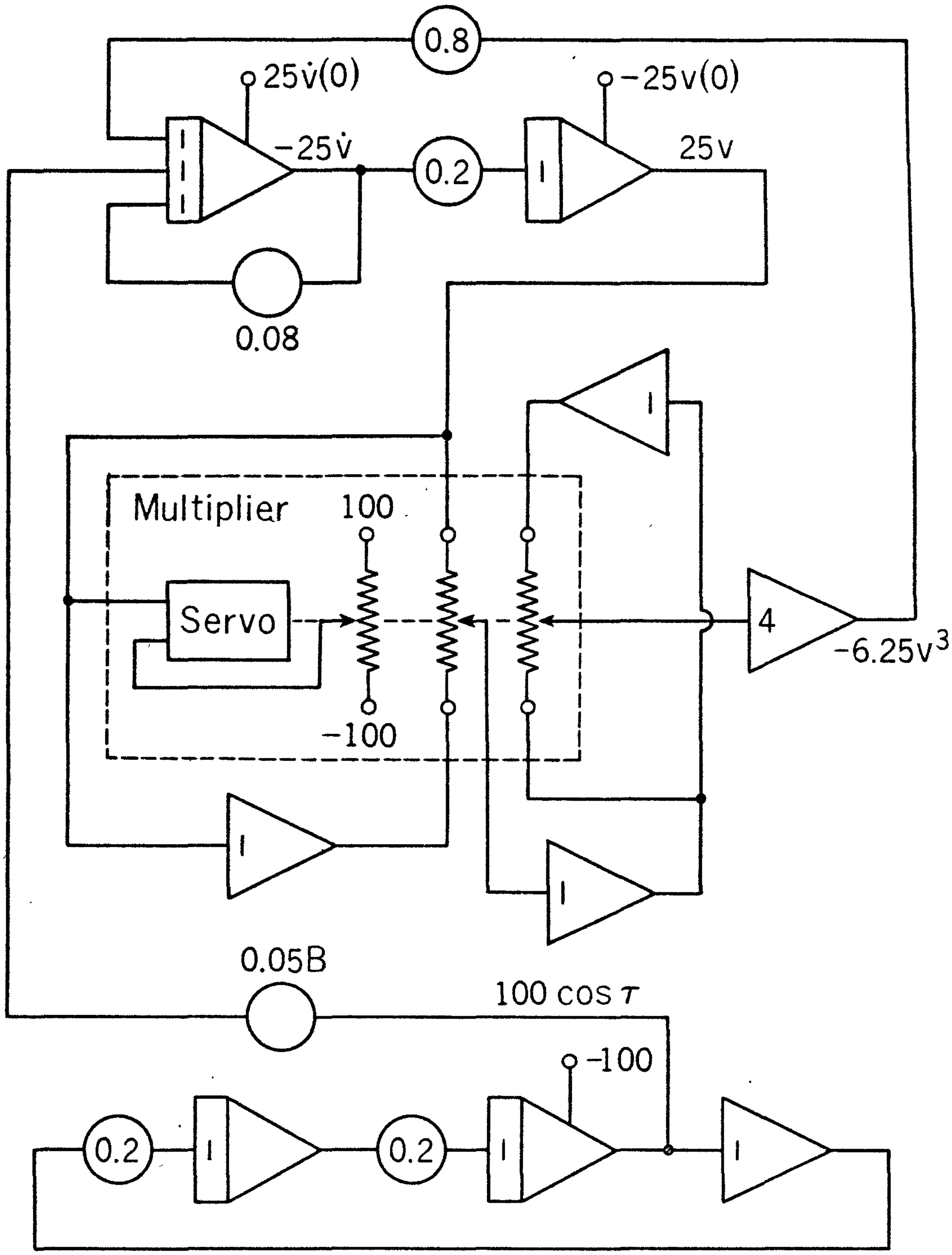


Fig. 1.4. Computer block diagram for Eq. (1.36).

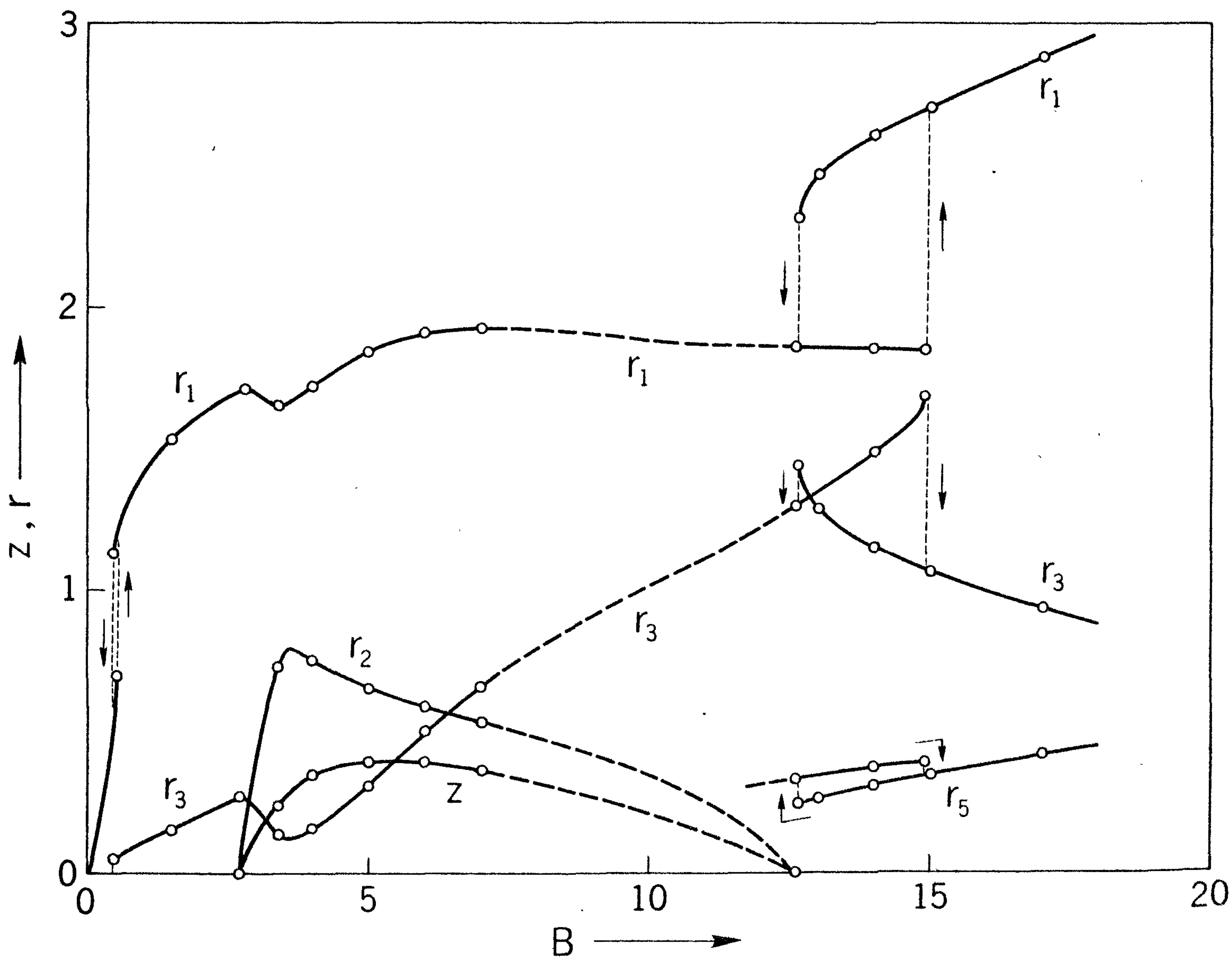


Fig. 1.5. Amplitude characteristics obtained by analog-computer analysis.

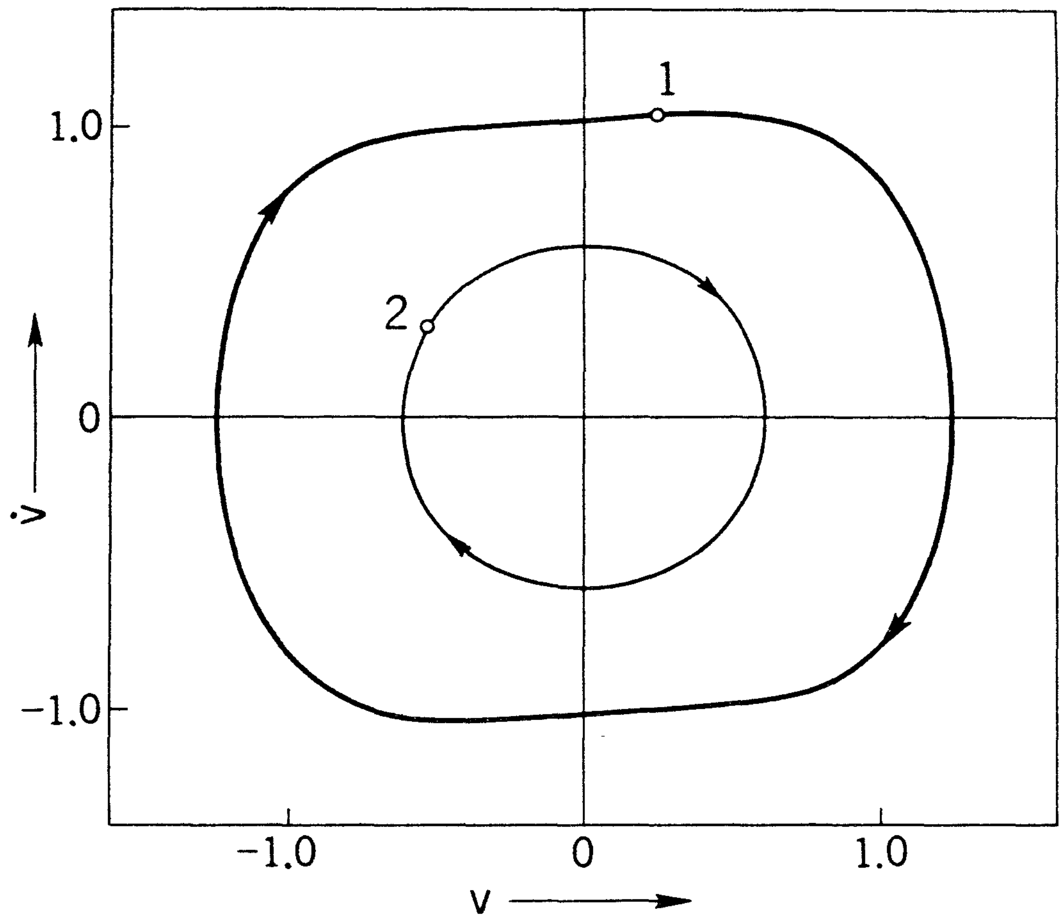


Fig. 1.6(a). Trajectories of the stable solutions for Eq. (1.42).

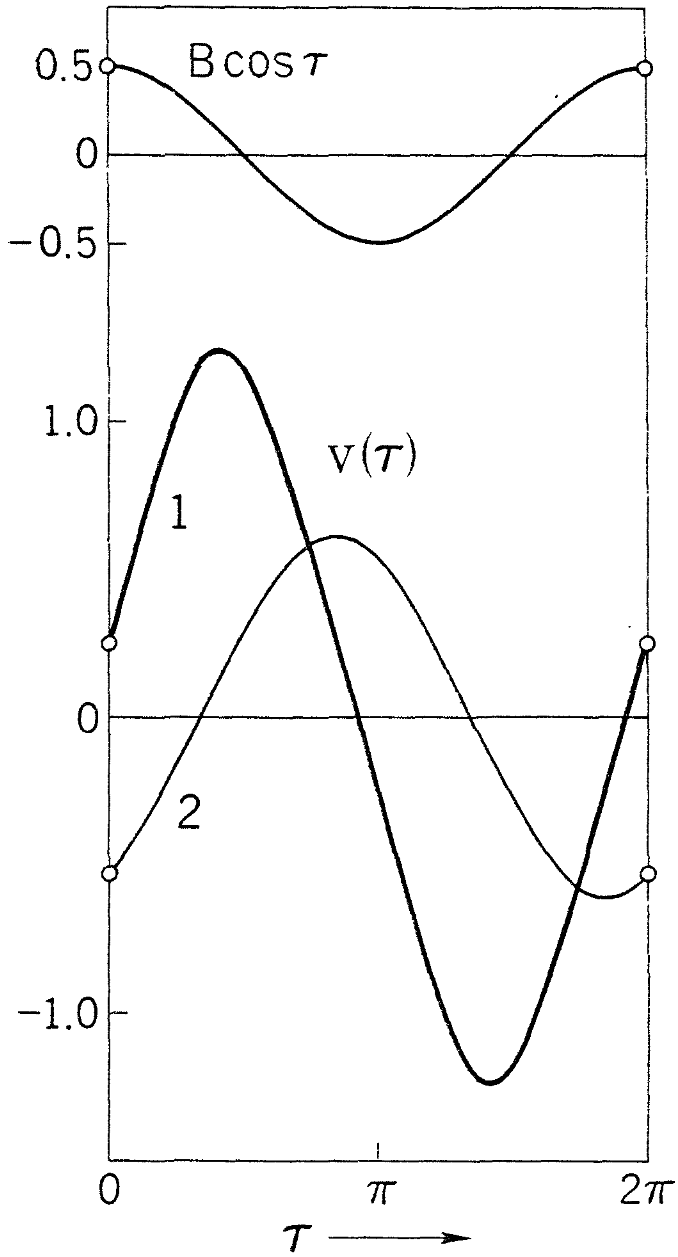


Fig. 1.6(b). Waveforms of v(τ) converted from the trajectories of Fig. 1.6a.

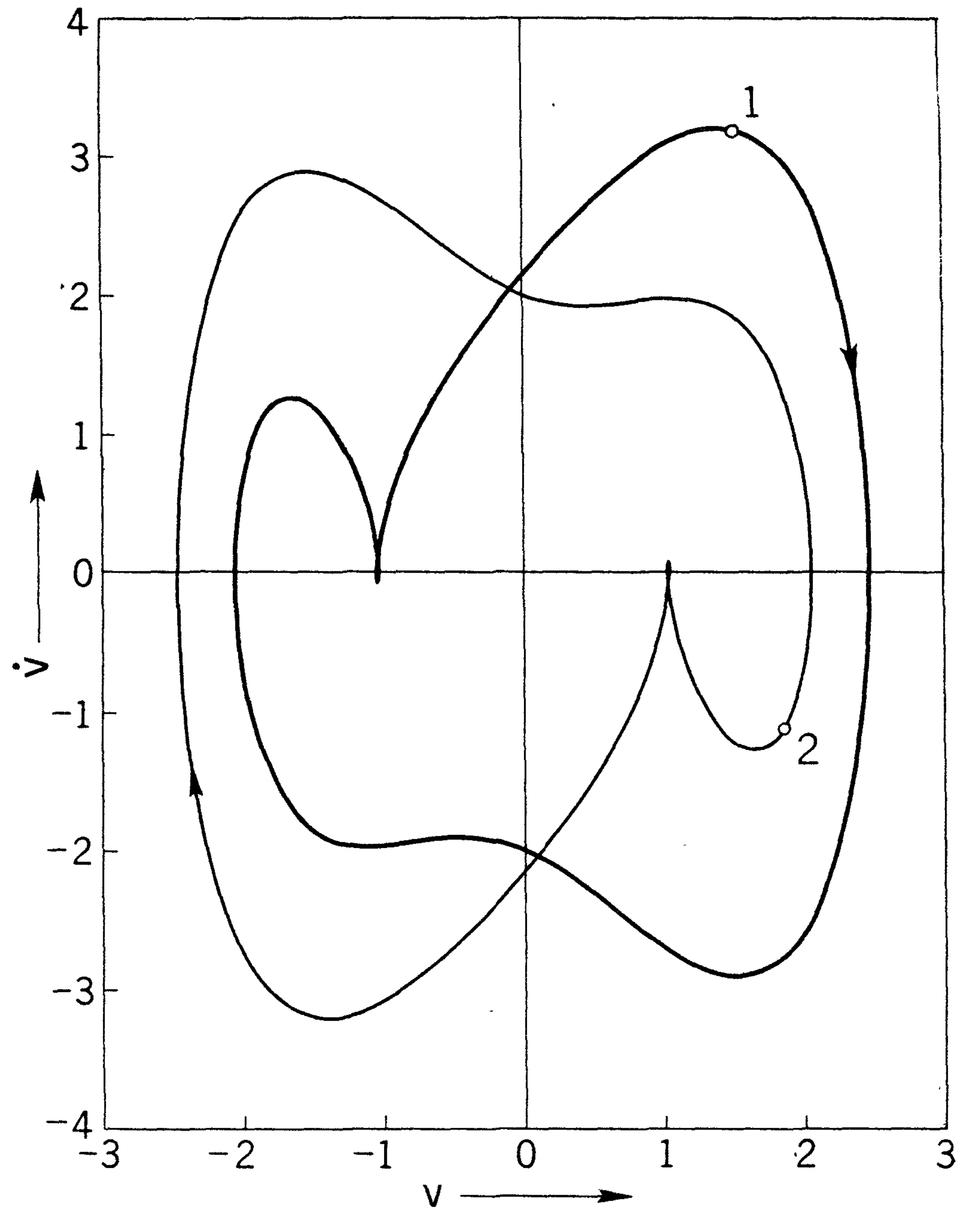


Fig. 1.7(a). Trajectories of the stable solutions for Eq. (1.45).

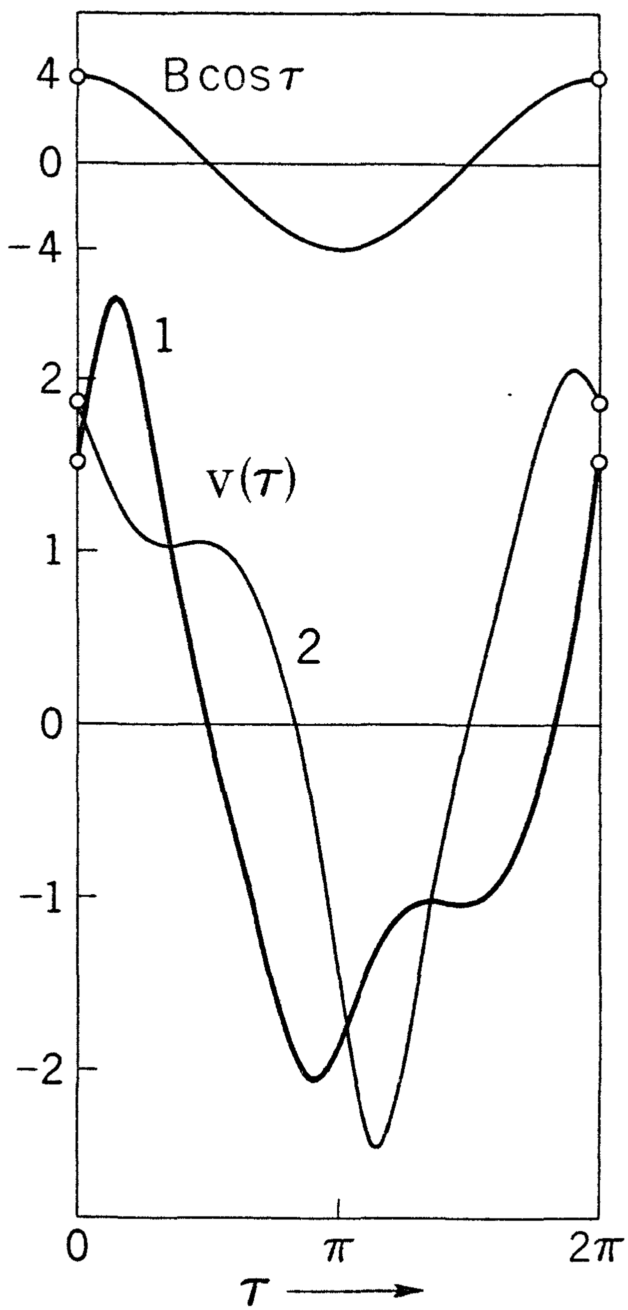


Fig. 1.7(b). Waveforms of v(τ) converted from the trajectories of Fig. 1.7a.

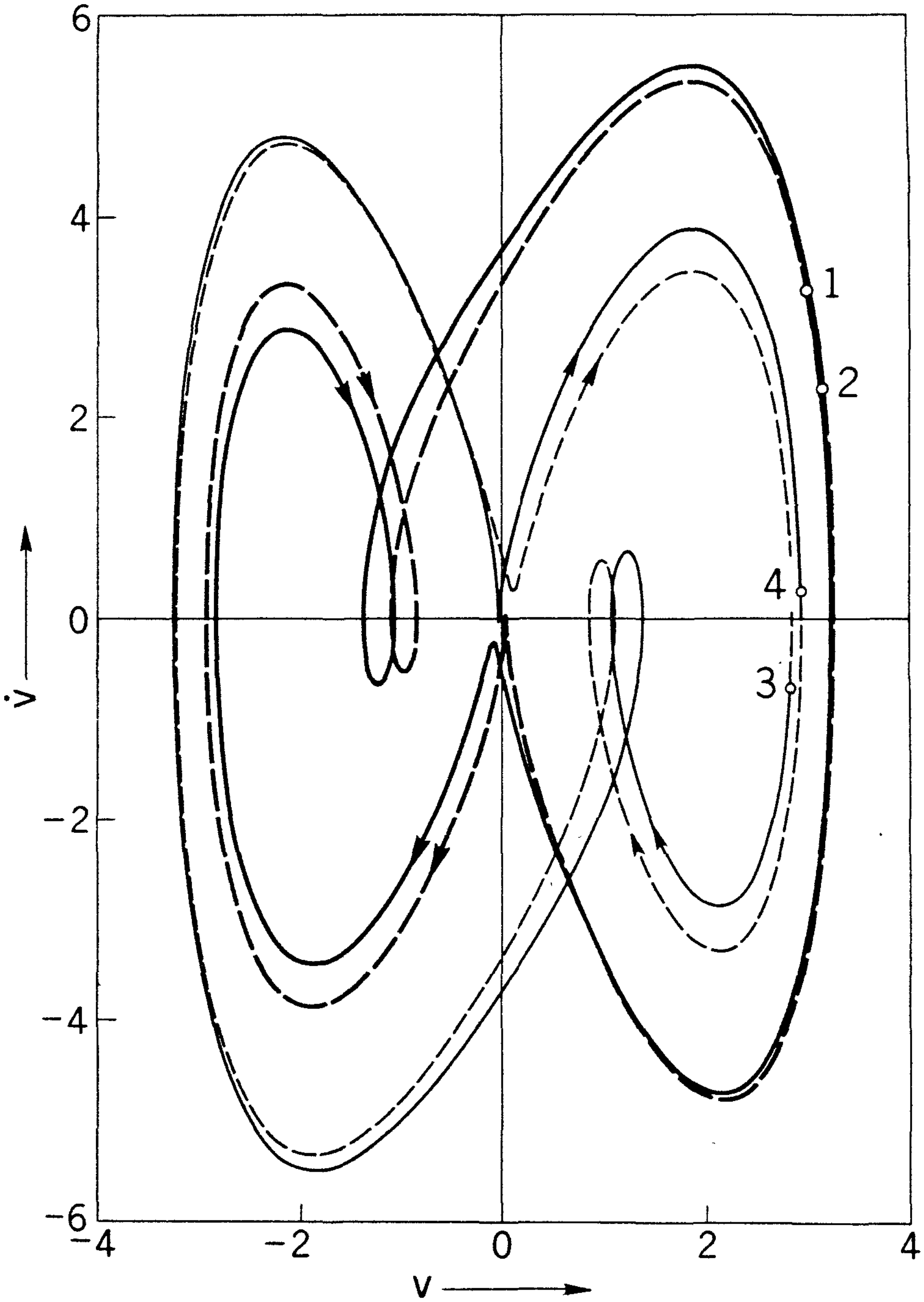


Fig. 1.8(a). Trajectories of the stable solutions for Eq. (1.47).

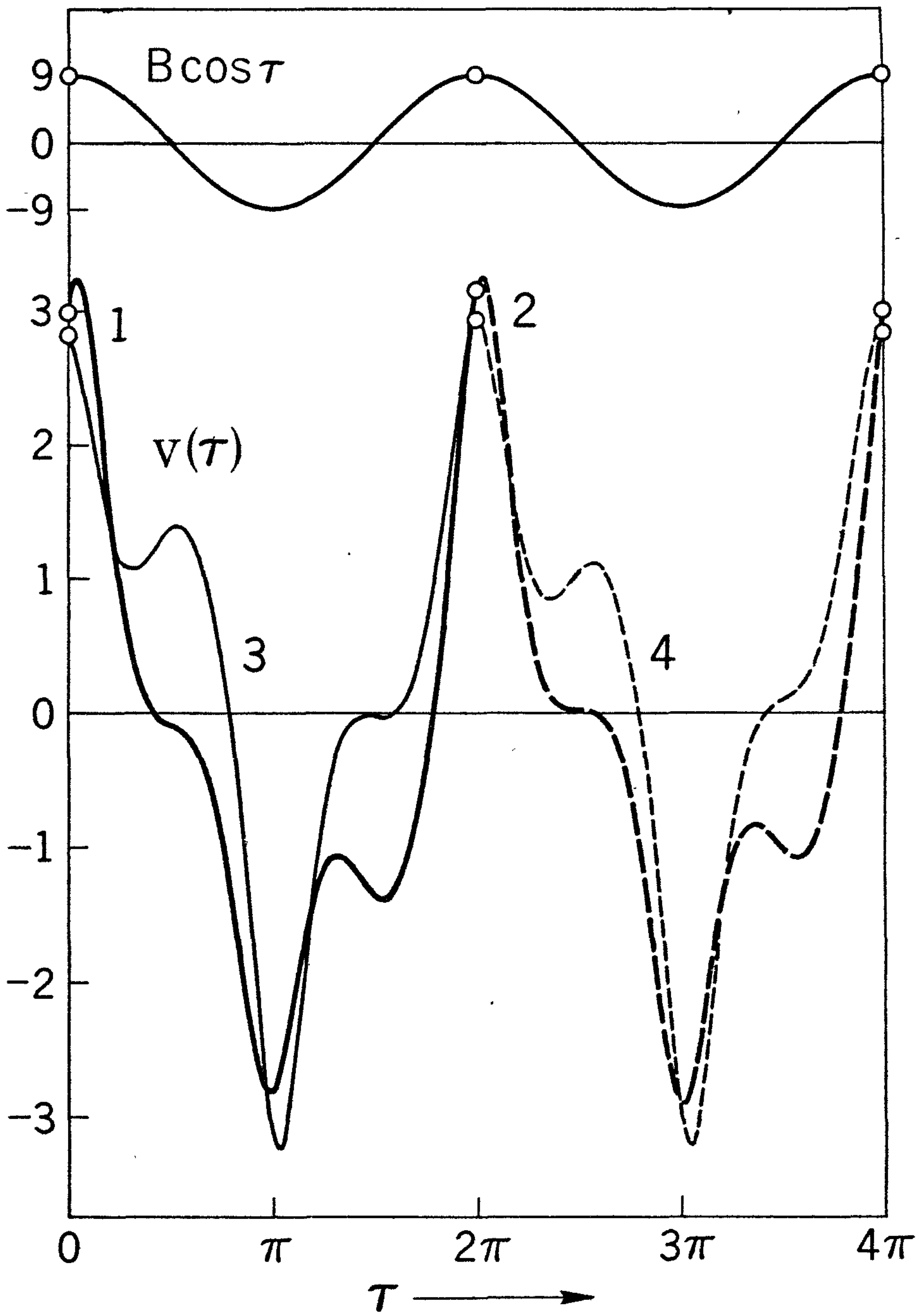


Fig. 1.8(b). Waveforms of the 1/2-harmonic oscillations converted from the trajectories of Fig. 1.8a.

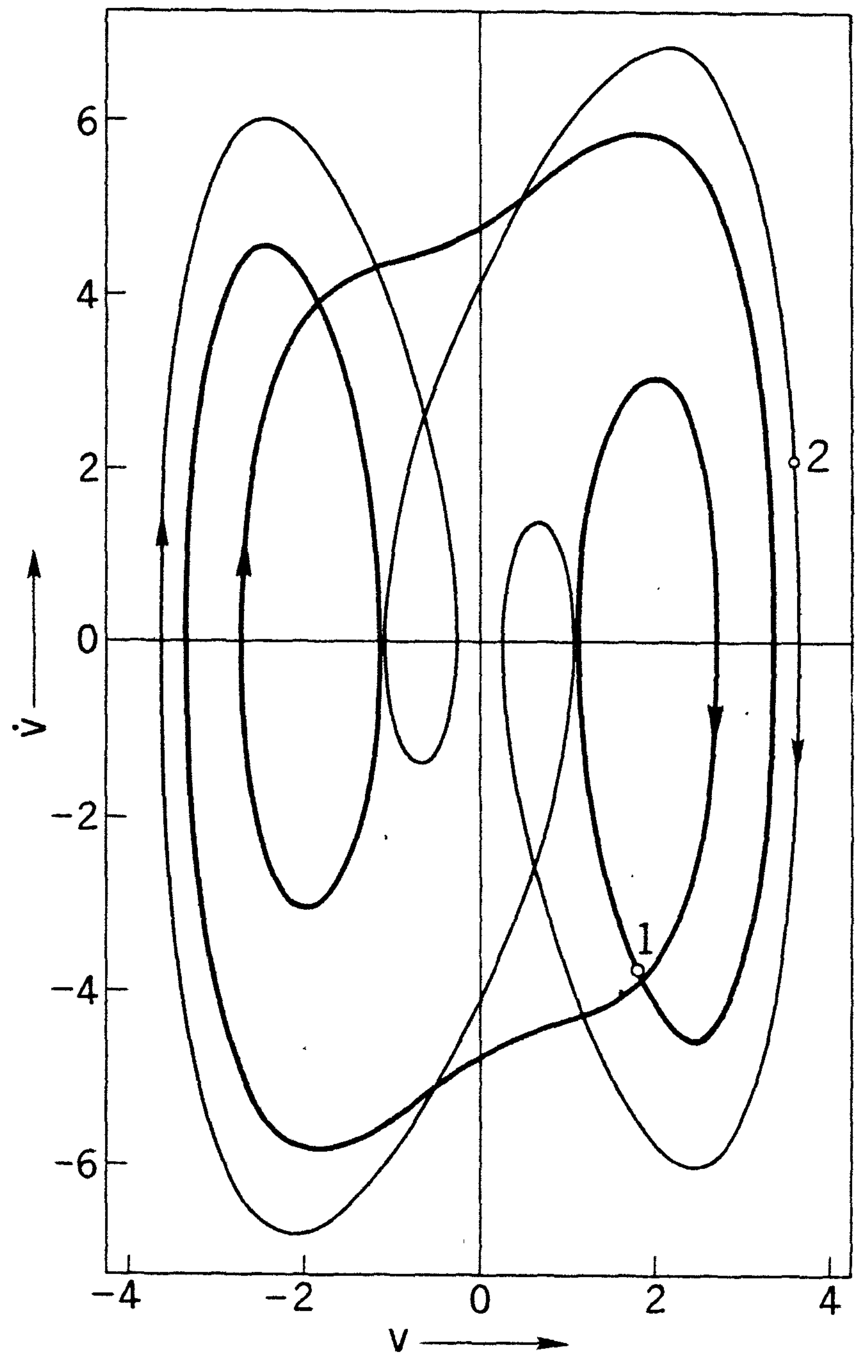


Fig. 1.9(a). Trajectories of the stable solutions for Eq. (1.49).

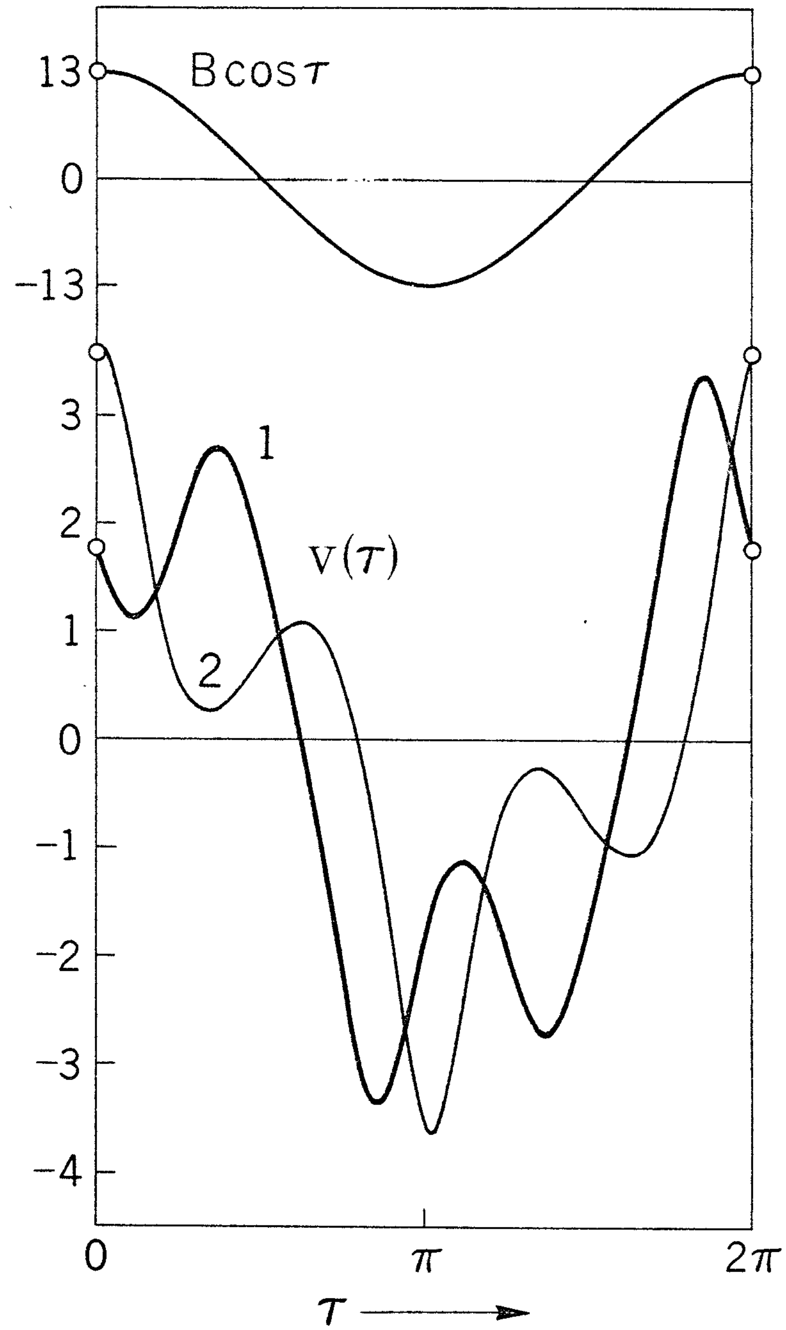


Fig. 1.9(b). Waveforms of $v(\tau)$ converted from the trajectories of Fig. 1.9a.

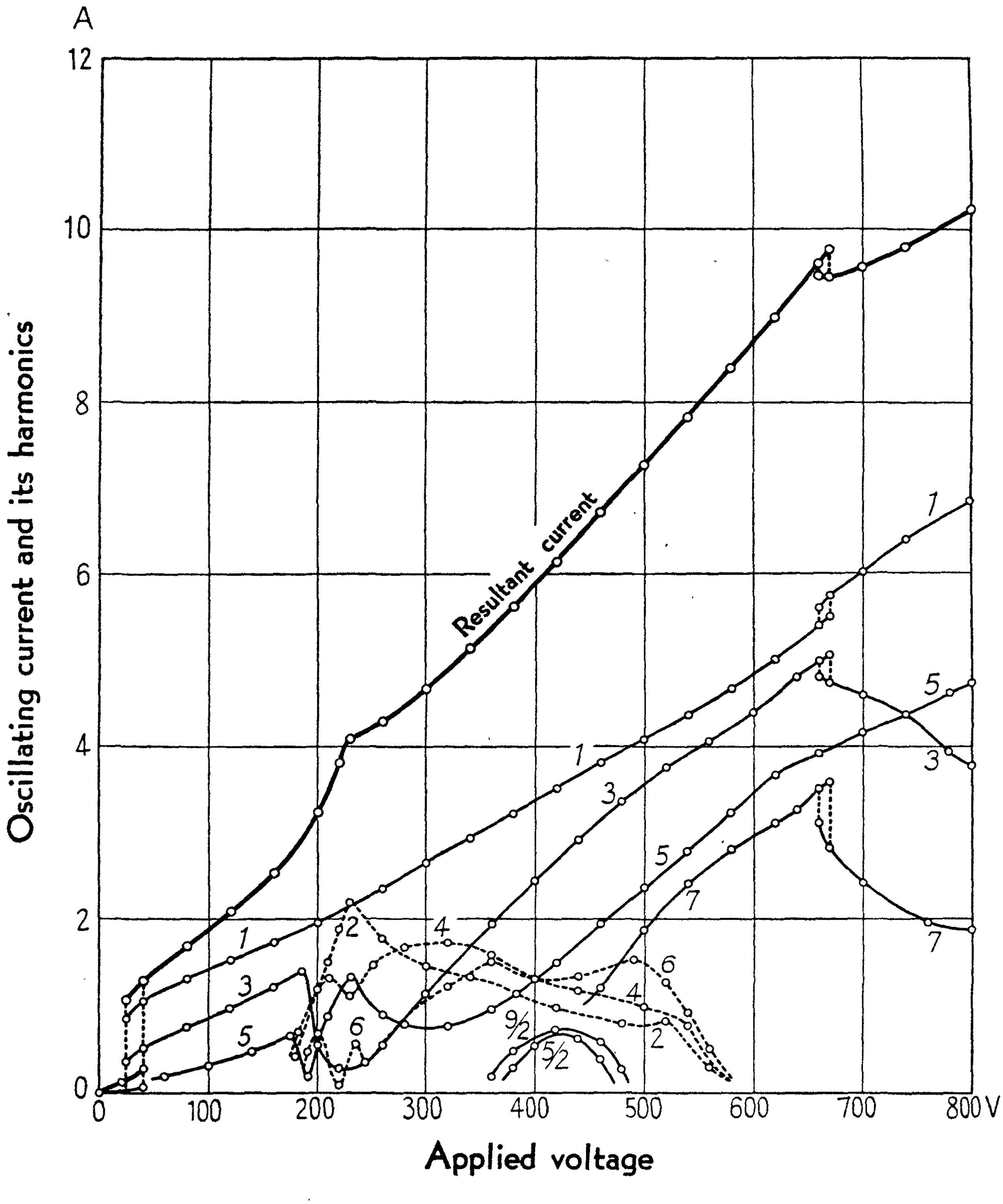


Fig. 1.10. Oscillating current and its harmonic components in the case where the iron core is highly saturated.

# CHAPTER 2

# HIGHER-HARMONIC OSCILLATIONS IN A PARALLEL-RESONANCE CIRCUIT

## 2.1 Introduction

In the preceding chapter, we investigated the higher-harmonic oscillations in a series-resonance circuit. Since the series condenser limits the current which magnetizes the reactor core, the applied voltage must be exceedingly raised in order to bring the oscillation into the unstable regions of higher order. Hence we may expect that a higher harmonic oscillation is likely to occur in a parallel-resonance circuit because the reactor core is readily saturated under the impression of a comparatively low voltage; and this will be investigated in the present chapter. The differential equation which describes the system takes the form of Mathieu's equation with additional terms of linear damping and nonlinear restoring force. The experimental result is also given at the end of this chapter.

## 2.2 Derivation of the Fundamental Equation

Figure 2.1 shows the schematic diagram of a parallel-resonance circuit, in which two oscillation circuits are connected in series, each having equal values of L, R, and C, respectively. Using the notation of the figure, the equations for the circuit are written as

$$\begin{aligned} n\frac{d\Phi_1}{dt} &= Ri_{R1} = \frac{1}{C}\int i_{C1}dt \\ n\frac{d\Phi_2}{dt} &= Ri_{R2} = \frac{1}{C}\int i_{C2}dt \\ n\frac{d\Phi_1}{dt} + n\frac{d\Phi_2}{dt} &= E\sin\omega t \end{aligned} \qquad (2.1)$$

$$i = i_{L1} + i_{R1} + i_{C1} = i_{L2} + i_{R2} + i_{C2}$$

The same saturation curve is assumed for both of the inductors $L(\phi_1)$ and $L(\phi_2)$; i.e.,

$$i_{L1} = a_1\phi_1 + a_3\phi_1^3 \qquad i_{L2} = a_1\phi_2 + a_3\phi_2^3 \tag{2.2}$$

If the two oscillation circuits behave identically, one has, from the third member of Eqs. (2.1),

$$\phi_1 = \phi_2 = -\frac{E}{2n\omega}\cos\omega t$$

An increase of the flux $\phi_1$ by $\phi$ results in the decrease of $\phi_2$ by the same amount; i.e.,

$$\phi_1 = -\frac{E}{2n\omega}\cos\omega t + \phi \qquad \phi_2 = -\frac{E}{2n\omega}\cos\omega t - \phi \tag{2.3}$$

After elimination of $i_{R1}$, $i_{R2}$, $i_{C1}$, and $i_{C2}$ in Eqs. (2.1) and by using Eqs. (2.3), we obtain

$$\frac{d^2\phi}{dt^2} + \frac{1}{CR}\frac{d\phi}{dt} + \frac{1}{2nC}(i_{L1} - i_{L2}) = 0 \tag{2.4}$$

Proceeding in the same manner as in Sec. 1.2, we introduce dimensionless variables defined by

$$i_{L1} = I_n \cdot u_{L1} \qquad i_{L2} = I_n \cdot u_{L2} \qquad \phi = \Phi_n \cdot v \tag{2.5}$$

and fix the base quantities, $I_n$ and $\Phi_n$ by the following relations:

$$n\omega^2 C\Phi_n = I_n \qquad c_1 + c_3 = 1$$

where

$$c_1 = \frac{a_1\Phi_n}{I_n} \qquad c_3 = \frac{a_3\Phi_n^3}{I_n} \tag{2.6}$$

Then, through use of Eqs. (2.2), (2.3), (2.5), and (2.6), Eq. (2.4) may be written in normalized form as

$$\frac{d^2v}{d\tau^2} + k\frac{dv}{d\tau} + (c_1 + \frac{3}{2}c_3B^2 + \frac{3}{2}c_3B^2 \cos 2\tau)v + c_3v^3 = 0 \tag{2.7}$$

where $\tau = \omega t$ $\qquad k = \frac{1}{\omega CR}$ $\qquad B = \frac{E}{2n\omega\Phi_n}$

## 2.3 Periodic Solutions

We assume for a moment that $k = 0$ and $v$ is so small that we may neglect the nonlinear term in Eq. (2.7). Then Eq. (2.7) reduces to a Mathieu's equation

$$\frac{d^2v}{d\tau^2} + (\theta_0 + 2\theta_1 \cos 2\tau)v = 0 \tag{2.8}$$

where $\theta_0 = c_1 + \frac{3}{2}c_3B^2$ $\qquad \theta_1 = \frac{3}{4}c_3B^2$

From the theory of Mathieu's equation [ 18, 19, 25, 26 ] one sees that there are regions of parameters, $\theta_0$ and $\theta_1$, in which the solution for Eq. (2.8) is either stable (remains bounded as $\tau$ increases) or unstable (diverges unboundedly), and that these regions of stability and instability appear alternately as parameter $\theta_0$ increases. We shall call such regions of instability as the first, the second, $\cdots$ unstable regions as parameter $\theta_0$ increases from zero. When the parameters $\theta_0$ and $\theta_1$ lie in the _n_th unstable region, a higher harmonic of the _n_th order is predominantly excited. Once the oscillation builds up, the nonlinear term $c_3v^3$ in Eq. (2.7) may not be ignored. It is this term that finally prevents the amplitude of the oscillation from growing up unboundedly.

After these preliminary remarks, we now proceed to investigate the solution of Eq. (2.7) and assume the following form of the solution.

Harmonic: $\qquad v_0(\tau) = x_1 \sin\tau + y_1 \cos\tau \qquad (2.9)$

Second-harmonic: $v_0(\tau) = z + x_2 \sin 2\tau + y_2 \cos 2\tau$ (2.10)

Third-harmonic: $v_0(\tau) = x_1 \sin \tau + y_1 \cos \tau + x_3 \sin 3\tau + y_3 \cos 3\tau$ (2.11)

(a) Harmonic Oscillation

In order to determine the coefficients in the right side of Eq. (2.9), we use the method of harmonic balance; namely, substituting Eq. (2.9) into (2.7) and equating the coefficients of the terms containing $\sin\tau$ and $\cos\tau$ separately to zero, we obtain

$$-\left(A_1 + \frac{3}{4} c_3 B^2\right)x_1 - ky_1 \equiv X_1(x_1, y_1) = 0$$

$$kx_1 - \left(A_1 - \frac{3}{4} c_3 B^2\right)y_1 \equiv Y_1(x_1, y_1) = 0 \qquad (2.12)$$

where $\quad A_1 = 1 - c_1 - \frac{3}{4} c_3(2B^2 + r_1^2) \qquad r_1^2 = x_1^2 + y_1^2$ .

Eliminating x, y components in the above equations gives

$$\left[A_1^2 + k^2 - \left(\frac{3}{4} c_3 B^2\right)^2\right] r_1^2 = 0 \qquad (2.13)$$

from which the amplitude $r_1$ is found to be

$$r_1^2 = 0 \qquad (2.14)$$

or

$$r_1^2 = \left(\frac{4}{3} - 2B^2\right) \pm \sqrt{B^4 - \left(\frac{4k}{3c_3}\right)^2} \qquad (2.15)$$

(b) Second-Harmonic Oscillation

After substitution of Eq. (2.10) into (2.7), equating the coefficients of the nonoscillatory term and of the terms containing $\sin 2\tau$ and $\cos 2\tau$ separately to zero gives

$$
\begin{aligned}
- A_0 z + \tfrac{3}{4} c_3 B^2 y_2 &\equiv Z(z,\ x_2,\ y_2) = 0 \\
- A_2 x_2 - 2k y_2 &\equiv X_2(z,\ x_2,\ y_2) = 0 \\
2k x_2 - A_2 y_2 + \tfrac{3}{2} c_3 B^2 z &\equiv Y_2(z,\ x_2,\ y_2) = 0
\end{aligned}
\tag{2.16}
$$

where
$$
\begin{aligned}
A_0 &= - c_1 - c_3[z^2 + \tfrac{3}{2}(B^2 + r_2^2)] \\
A_2 &= 4 - c_1 - \tfrac{3}{4} c_3(2B^2 + 4z^2 + r_2^2) \\
r_2^2 &= x_2^2 + y_2^2
\end{aligned}
$$

Eliminating x, y components in the above equations gives

$$
\begin{aligned}
- A_0 z^2 + \tfrac{1}{2} A_2 r_2^2 &= 0 \\
(A_2^2 + 4k^2) r_2^2 &= (\tfrac{3}{2} c_3 B^2)^2 z^2
\end{aligned}
\tag{2.17}
$$

from which the unknown quantities z and $r_2$ are determined.

(c) Third-Harmonic Oscillation

By substituting Eq. (2.11) into (2.7), and equating the terms containing sin $\tau$, cos $\tau$, sin $3\tau$, and cos $3\tau$ separately to zero, we obtain

$$
\begin{aligned}
&- (A_1 + \tfrac{3}{4} c_3 B^2) x_1 - k y_1 - \tfrac{3}{4} c_3[(x_1^2 - y_1^2 - B^2) x_3 + 2 x_1 y_1 y_3] \\
&\qquad\qquad \equiv X_1(x_1,\ y_1,\ x_3,\ y_3) = 0 \\
&k x_1 - (A_1 - \tfrac{3}{4} c_3 B^2) y_1 + \tfrac{3}{4} c_3[2 x_1 y_1 x_3 - (x_1^2 - y_1^2 - B^2) y_3] \\
&\qquad\qquad \equiv Y_1(x_1,\ y_1,\ x_3,\ y_3) = 0 \\
&- A_3 x_3 - 3k y_3 + \tfrac{1}{4} c_3[3B^2 - (x_1^2 - 3y_1^2)] x_1 \equiv X_3(x_1,\ y_1,\ x_3,\ y_3) = 0
\end{aligned}
$$

$$3kx_3 - A_3y_3 + \frac{1}{4} c_3[3B^2 - (3x_1^2 - y_1^2)]y_1 \equiv Y_3(x_1, y_1, x_3, y_3) = 0$$

where

$$A_1 = 1 - c_1 - \frac{3}{4} c_3(2B^2 + r_1^2 + 2r_3^2) \tag{2.18}$$

$$A_3 = 9 - c_1 - \frac{3}{4} c_3(2B^2 + 2r_1^2 + r_3^2)$$

$$r_1^2 = x_1^2 + y_1^2 \qquad r_3^2 = x_3^2 + y_3^2$$

from which unknown quantities $x_1$, $y_1$, $x_3$, and $y_3$, and consequently the amplitudes $r_1$ and $r_3$, are determined.

## 2.4 Stability Investigation of the Periodic Solutions

The periodic solutions as given in the preceding section actually exist only when they are stable. In this section the stability of the periodic solutions will be investigated in the same manner as we have done in Sec. 1.3b. We consider a small variation $\xi(\tau)$ from the periodic solution $v_0(\tau)$. Then the behavior of $\xi(\tau)$ is described by the following variational equation:

$$\frac{d^2\xi}{d\tau^2} + k\frac{d\xi}{d\tau} + (c_1 + \frac{3}{2} c_3B^2 + \frac{3}{2} c_3B^2 \cos 2\tau + 3c_3v_0^2)\xi = 0 \tag{2.19}$$

Furthermore we introduce a new variable $\eta(\tau)$ defined by

$$\xi(\tau) = e^{-\delta\tau} \cdot \eta(\tau) \qquad \delta = k/2 \tag{2.20}$$

to remove the first-derivative term. Then we obtain

$$\frac{d^2\eta}{d\tau^2} + (c_1 - \delta^2 + \frac{3}{2} c_3B^2 + \frac{3}{2} c_3B^2 \cos 2\tau + 3c_3v_0^2)\eta = 0 \tag{2.21}$$

### (a) Stability Condition for the Harmonic Oscillation

Inserting $v_0(\tau)$ as given by Eq. (2.9) into (2.21) leads to

$$\frac{d^2\eta}{d\tau^2} + (\theta_0 + 2\theta_{1s}\sin 2\tau + 2\theta_{1c}\cos 2\tau)\eta = 0$$

where
$$\theta_0 = c_1 - \delta^2 + \frac{3}{2}c_3(B^2 + r_1^2) \tag{2.22}$$

$$\theta_{1s} = \frac{3}{2}c_3 x_1 y_1 \qquad \theta_{1c} = \frac{3}{4}c_3[B^2 - (x_1^2 - y_1^2)]$$

We assume that a particular solution of Eq. (2.22) in the first unstable region is given by

$$\eta(\tau) = e^{\mu\tau}\phi(\tau) = e^{\mu\tau}\sin(\tau - \sigma_1) \tag{2.23}$$

Proceeding analogously as in Sec. 1.3b, stability condition $|\mu| < \delta$ leads to

$$\Delta_1(\delta) \equiv \begin{vmatrix} \theta_0 + \delta^2 - 1 - \theta_{1c} & \theta_{1s} - 2\delta \\ \theta_{1s} + 2\delta & \theta_0 + \delta^2 - 1 + \theta_{1c} \end{vmatrix} \equiv \frac{\partial(X_1, Y_1)}{\partial(x_1, y_1)} > 0 \tag{2.24}$$

(b) Stability Conditions for the Higher-Harmonic Oscillations

The conditions for stability of the solutions given by Eqs. (2.10) and (2.11) may also be derived by the same procedure as above. The results are:

Stability condition for solution (2.10):

$$\Delta_2(\delta) \equiv \frac{\partial(Z, X_2, Y_2)}{\partial(z, x_2, y_2)} > 0 \tag{2.25}$$

Stability condition for solution (2.11):

$$\Delta_3(\delta) \equiv \frac{\partial(X_1, Y_1, X_3, Y_3)}{\partial(x_1, y_1, x_3, y_3)} > 0 \tag{2.26}$$

The vertical tangency of the characteristic curves ($Bz$, $Br_1$, $Br_2$, and $Br_3$ relations) also occurs at the stability limit $\Delta_n(\delta) = 0$ (n = 1, 2, 3).

(c) Numerical Example

Putting $c_1 = 0$ and $c_3 = 1$ in Eq. (2.7) gives

$$\frac{d^2v}{d\tau^2} + k\frac{dv}{d\tau} + \frac{3}{2}B^2(1 + \cos 2\tau)v + v^3 = 0$$

By use of Eqs. (2.15), (2.17), and (2.18) the amplitude characteristics of Eqs. (2.9), (2.10), and (2.11) were calculated for $k = 0$ and 0.4. The result is plotted against B in Fig. 2.2. The dotted portions of the characteristic curves represent unstable states. It is to be mentioned that the portions of the B axis interposed between the end points of the characteristic curves are unstable. One sees in the figure that increasing B will bring about the excitation of higher-harmonic oscillations and that once the oscillation is started, it may be stopped by decreasing B to a value which is lower than before, thus exhibiting the phenomenon of hysteresis.

## 2.5 Numerical Analysis by Using a Digital Computer

In this section we shall seek the numerical solutions of Eq. (2.7) with the system parameters $k = 0.4$, $c_1 = 0$, and $c_3 = 1$, i.e.,

$$\frac{d^2v}{d\tau^2} + 0.4\frac{dv}{d\tau} + \frac{3}{2}B^2(1 + \cos 2\tau)v + v^3 = 0 \tag{2.27}$$

The same method as described in Sec. 1.6 is followed; therefore only the stable solutions are obtained.

Equation (2.27) is written as

$$\begin{aligned}\frac{dv}{d\tau} &= \dot{v}\\ \frac{d\dot{v}}{d\tau} &= -0.4\dot{v} - \frac{3}{2}B^2(1 + \cos 2\tau)v - v^3\end{aligned} \tag{2.28}$$

Since the right sides of Eqs. (2.28) are periodic functions in $\tau$ of period $\pi$, the mapping T from $\tau = n\pi$ to $(n + 1)\pi$, where $n = 0, 1, 2, \cdots$ is considered.

(a) Numerical Solution of the Harmonic Oscillation

Putting $B = 0.8$ in Eq. (2.27) gives

$$\frac{d^2v}{d\tau^2} + 0.4\frac{dv}{d\tau} + \frac{3}{2}(0.8)^2(1 + \cos 2\tau)v + v^3 = 0 \tag{2.29}$$

The numerical solution for Eq. (2.29) is*

$$\begin{aligned} v(\tau) = {} & 0.288 \cos \tau - 0.553 \sin \tau \\ & + 0.005 \cos 3\tau - 0.035 \sin 3\tau \\ & - 0.000 \cos 5\tau - 0.001 \sin 5\tau \\ & + \cdots \end{aligned} \tag{2.30}$$

The phase trajectory of Eq. (2.30) in the $v\dot{v}$ plane is shown in Fig. 2.3a. Figure 2.3b shows the waveforms of $v(\tau)$ converted from the trajectory of Fig. 2.3a. There are two kinds of waveform drawn by thick line and fine line. Their difference is only in sign; which one occurs depends on the choice of initial conditions (either at point 1 or 2) on the trajectory.

(b) Numerical Solution of the Second-Harmonic Oscillation

$$\frac{d^2v}{d\tau^2} + 0.4\frac{dv}{d\tau} + \frac{3}{2}(1.8)^2(1 + \cos 2\tau)v + v^3 = 0 \tag{2.31}$$

The numerical solution for Eq. (2.31) is

---

* From the form of Eq. (2.27) one readily sees that if $v(\tau)$ is a solution of Eq. (2.27) $-v(\tau)$ is also a solution.

$$
\begin{aligned}
v(\tau) = & -0.250 \\
& + 0.555 \cos 2\tau + 0.263 \sin 2\tau \\
& + 0.128 \cos 4\tau + 0.032 \sin 4\tau \\
& + 0.010 \cos 6\tau + 0.002 \sin 6\tau \\
& + 0.001 \cos 8\tau + 0.001 \sin 8\tau \\
& + \cdots
\end{aligned}
\tag{2.32}
$$

The phase trajectories and the waveforms of $v(\tau)$ are shown in Fig. 2.4a and b, respectively.

(c) Numerical Solution of the Third-Harmonic Oscillation

$$
\frac{d^2v}{d\tau^2} + 0.4\frac{dv}{d\tau} + \frac{3}{2}(2.8)^2(1 + \cos 2\tau)v + v^3 = 0 \tag{2.33}
$$

The numerical solution for Eq. (2.33) is

$$
\begin{aligned}
v(\tau) = & -0.065 \cos \tau + 0.376 \sin \tau \\
& + 0.162 \cos 3\tau - 0.338 \sin 3\tau \\
& + 0.046 \cos 5\tau - 0.170 \sin 5\tau \\
& + 0.006 \cos 7\tau - 0.027 \sin 7\tau \\
& + 0.000 \cos 9\tau - 0.002 \sin 9\tau \\
& + \cdots
\end{aligned}
\tag{2.34}
$$

Figure 2.5a and b shows the phase trajectory and the waveforms of $v(\tau)$, respectively.

The values of the coordinates of the stable fixed and periodic points are listed in Table 2.1. The values of the time increment h which is employed for finding the corresponding fixed and periodic points are also shown.

Table 2.1 Stable fixed and periodic points for Eq. (2.27) and the chosen step h.

| Value of B | Point | v | $\dot{v}$ | Value of h | Classification |
|---|---|---|---|---|---|
| 0.8 | Fig. 2.3a 1 | 0.2925 | -0.6621 | $\pi/30$ | Periodic point |
| | 2 | -0.2925 | +0.6621 | " | " |
| 1.8 | Fig. 2.4a 1 | 0.4430 | 0.6727 | $\pi/30$ | Fixed point |
| | 2 | -0.4430 | -0.6727 | " | " |
| 2.8 | Fig. 2.5a 1 | 0.1495 | -1.7041 | $\pi/60$ | Periodic point |
| | 2 | -0.1495 | +1.7041 | " | " |

## 2.6 Experimental Result

An experiment on the circuit of Fig. 2.1 has been performed [ 7, pp. 44-48]. The result is as follows.

The self-excitation of the fundamental and higher-harmonic oscillations was observed under varying E. As a result of the excitation of such a harmonic, the potential of the junction point of the two resonance circuits oscillates with respect to the neutral point of the applied voltage with the frequency of that harmonic. In Fig. 2.6, the anomalous neutral voltage $V_N$ (which is related to the flux $\phi$) is shown against the applied voltage.*

* The self-excited oscillation in the first unstable region (marked by I) has the same frequency as that of the applied voltage. See the waveform (a) in the figure. This phenomenon is known as the neutral inversion in electric transmission lines.

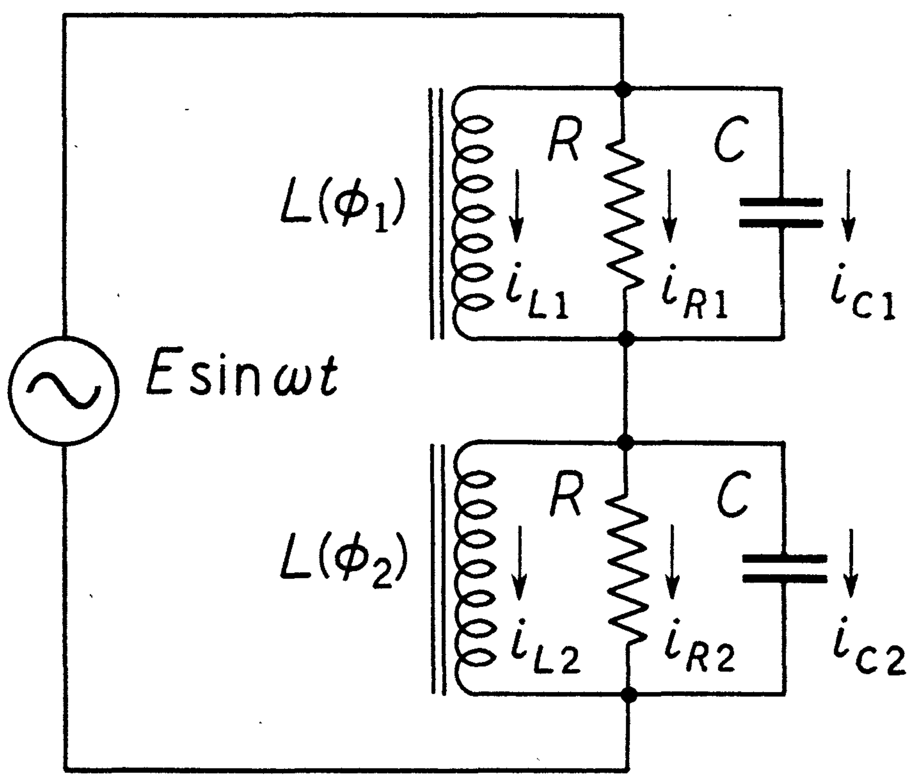


Fig. 2.1. Parallel-resonance circuit with nonlinear inductance.

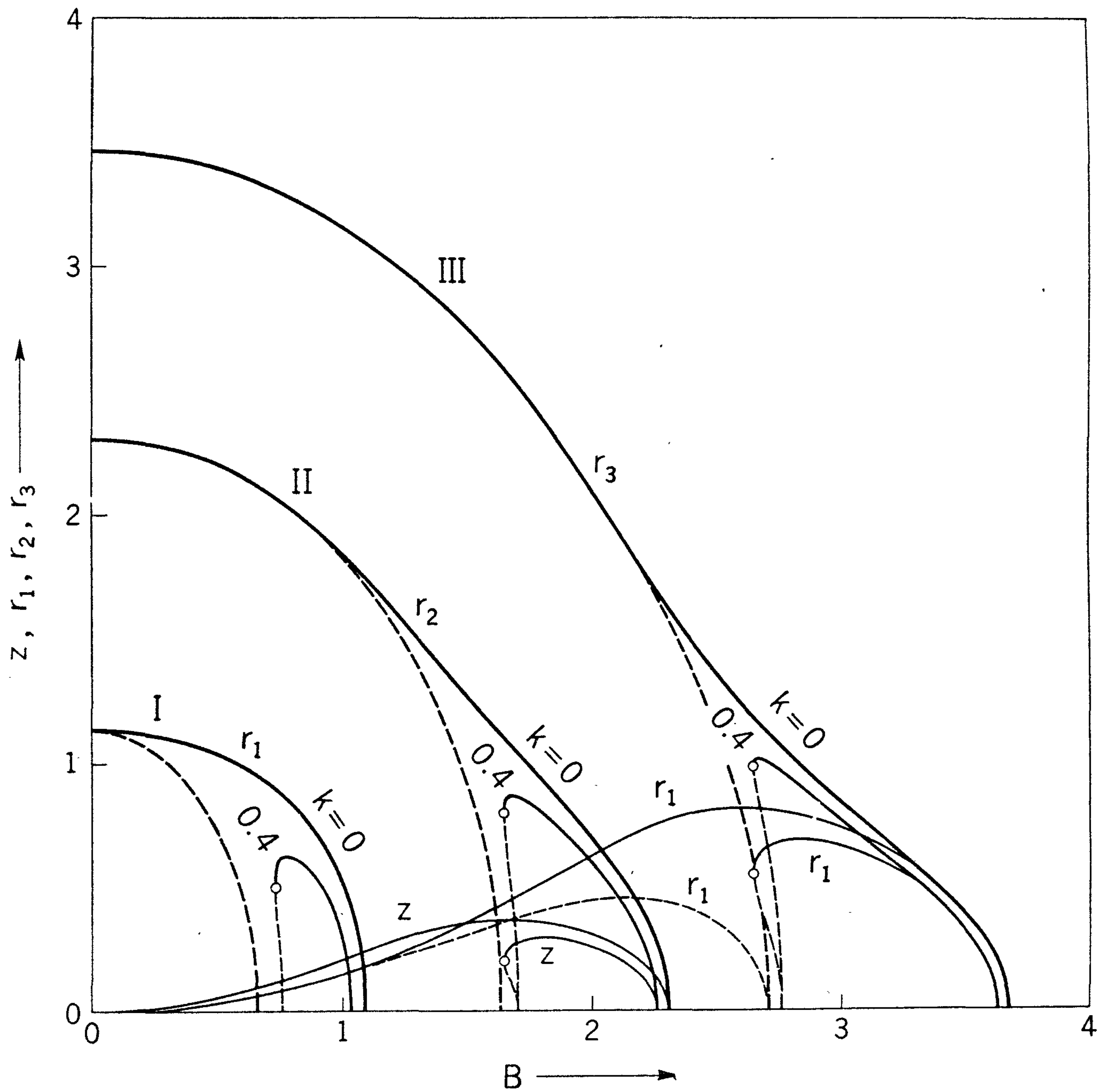


Fig. 2.2. Amplitude characteristics of the periodic solutions as given by Eqs. (2.9), (2.10), and (2.11).

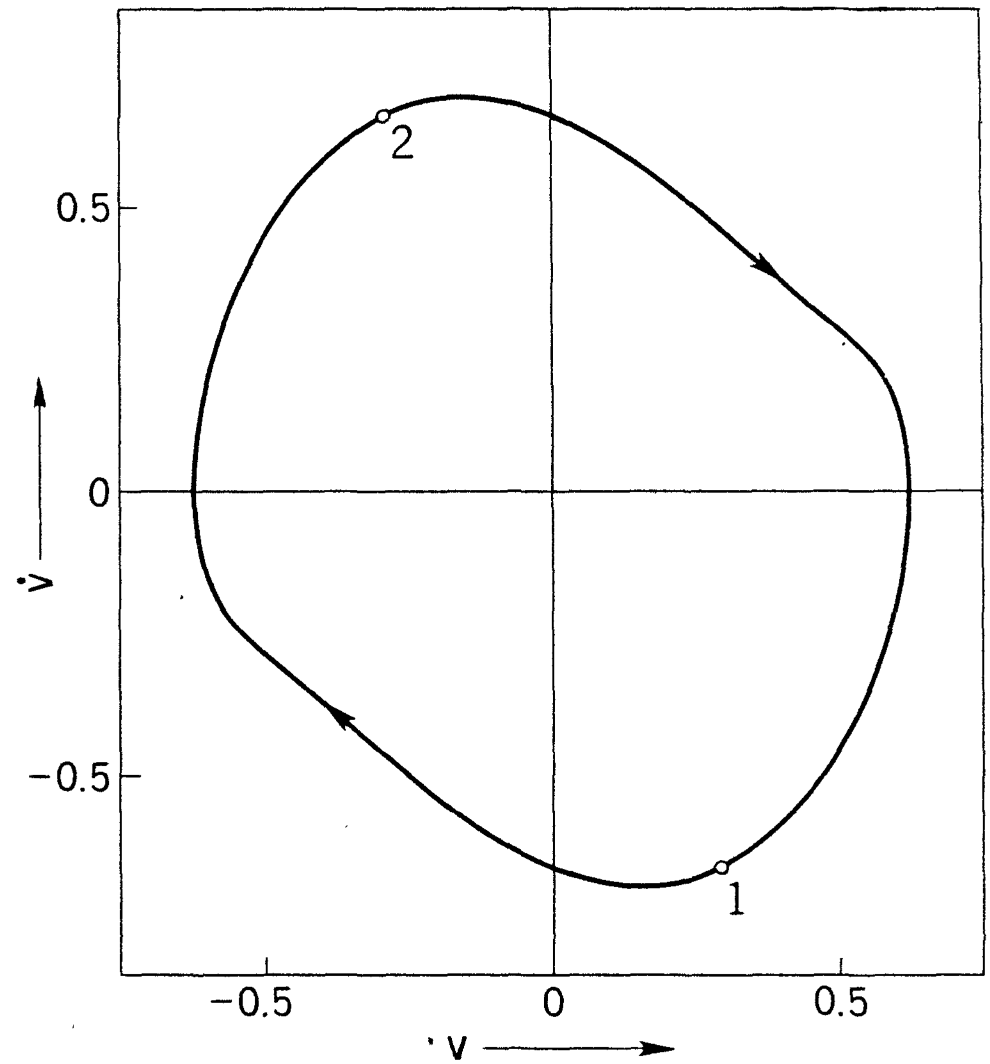


Fig. 2.3(a). Trajectory of the stable solutions for Eq. (2.29).

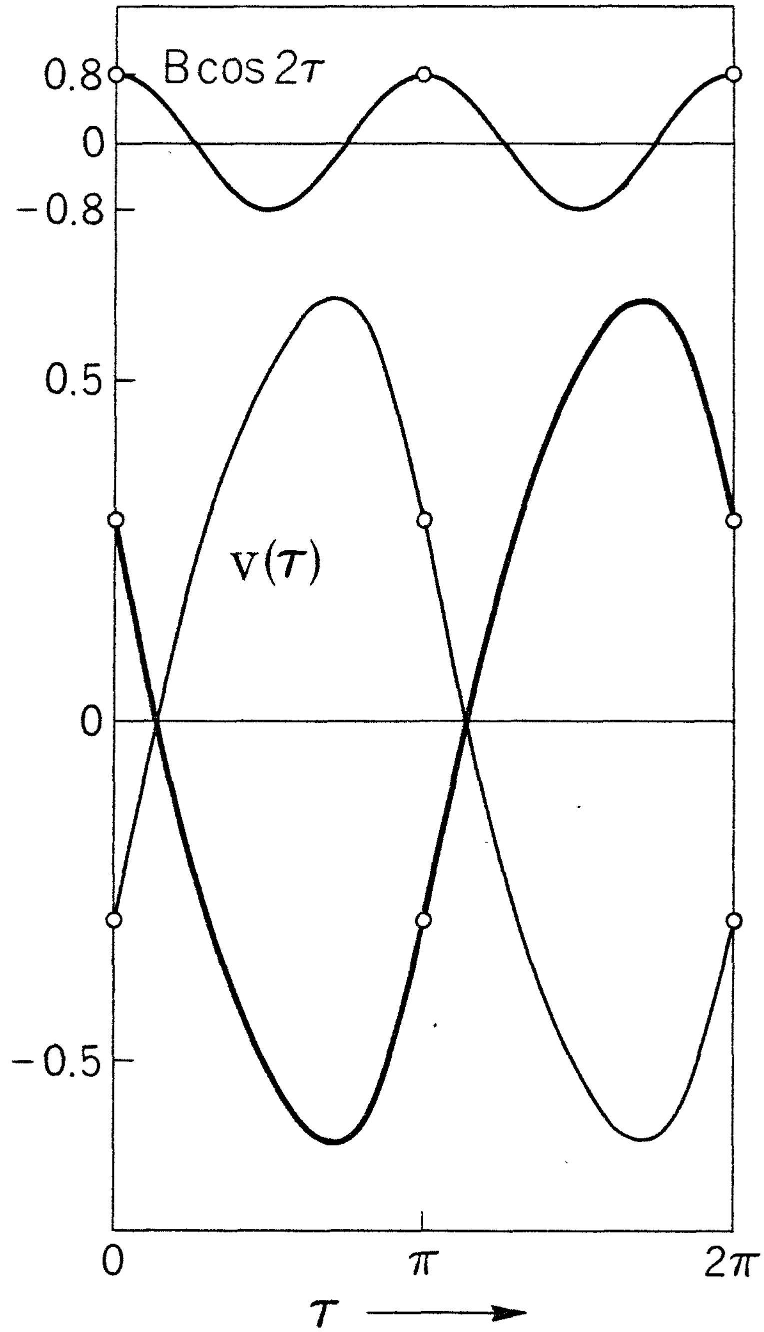


Fig. 2.3(b). Waveforms of $v(\tau)$ converted from the trajectory of Fig. 2.3a.

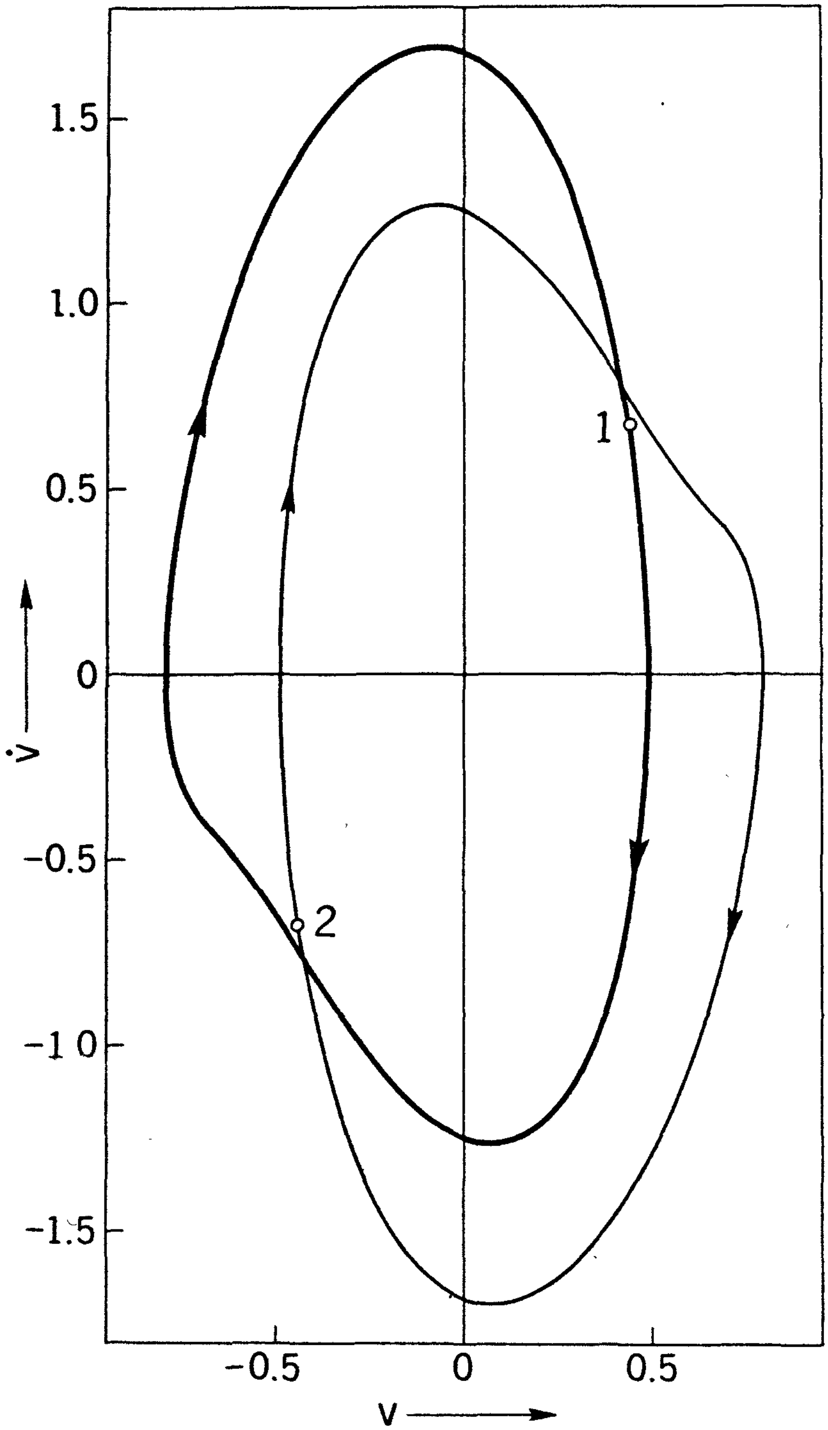


Fig. 2.4(a). Trajectories of the stable solutions for Eq. (2.31).

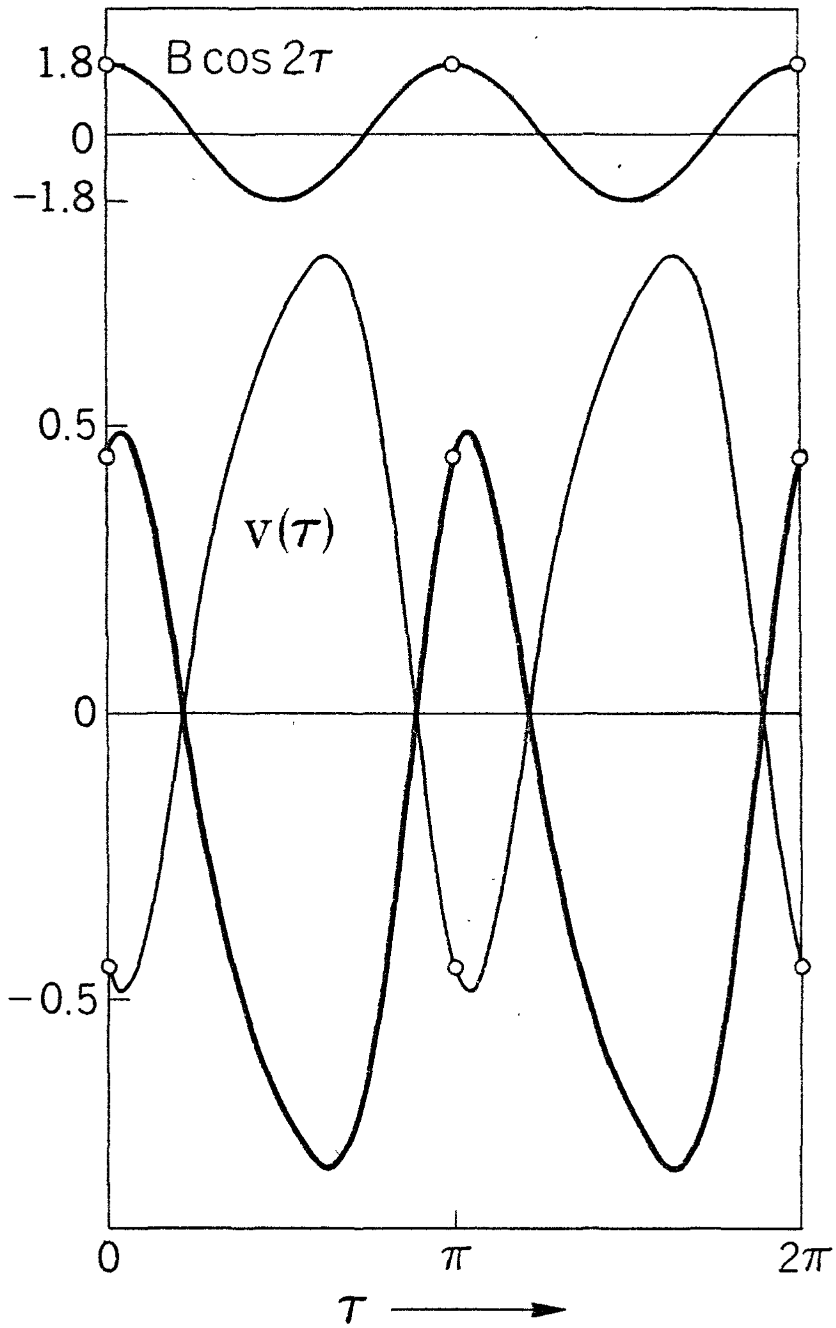


Fig. 2.4(b). Waveforms of v(τ) converted from the trajectories of Fig. 2.4a.

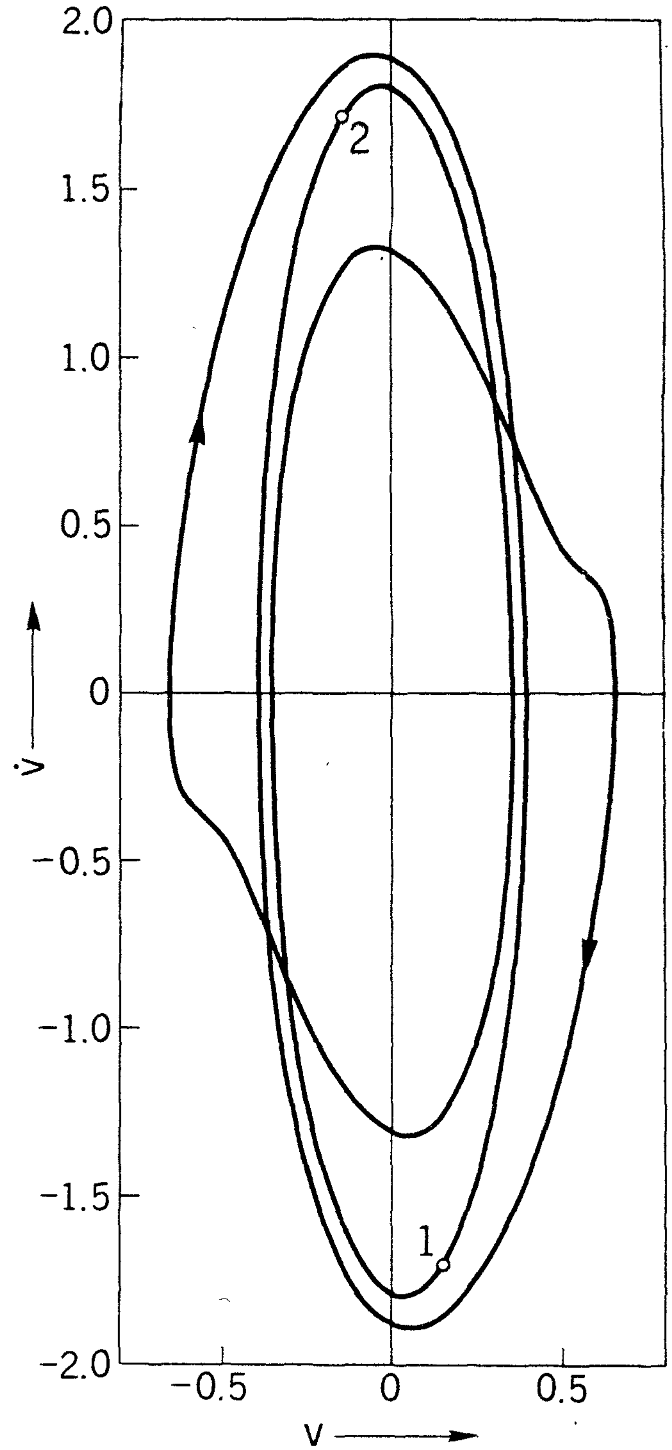


Fig. 2.5(a). Trajectory of the stable solutions for Eq. (2.33).

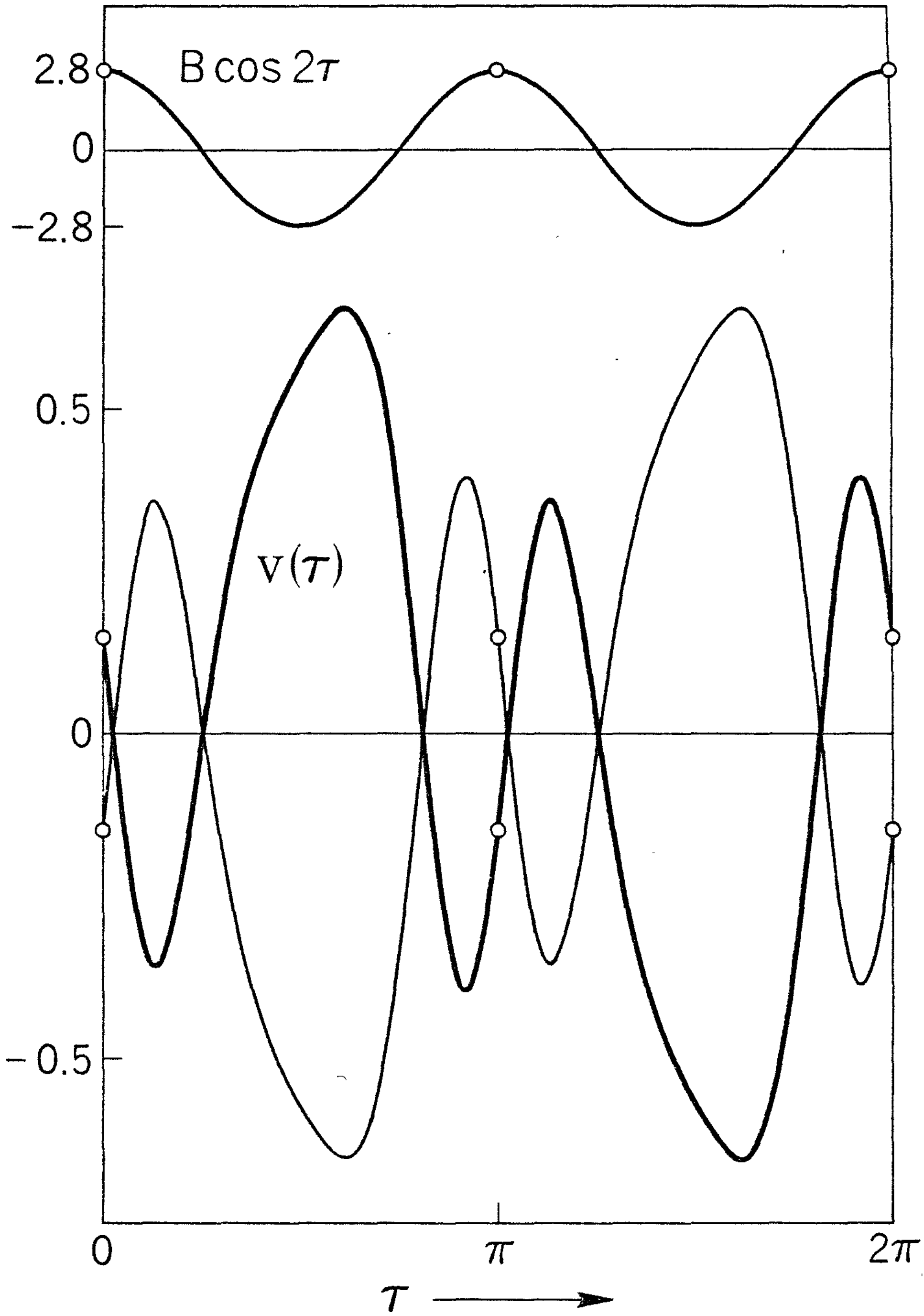


Fig. 2.5(b). Waveforms of v( τ ) converted from the trajectory of Fig. 2.5a.

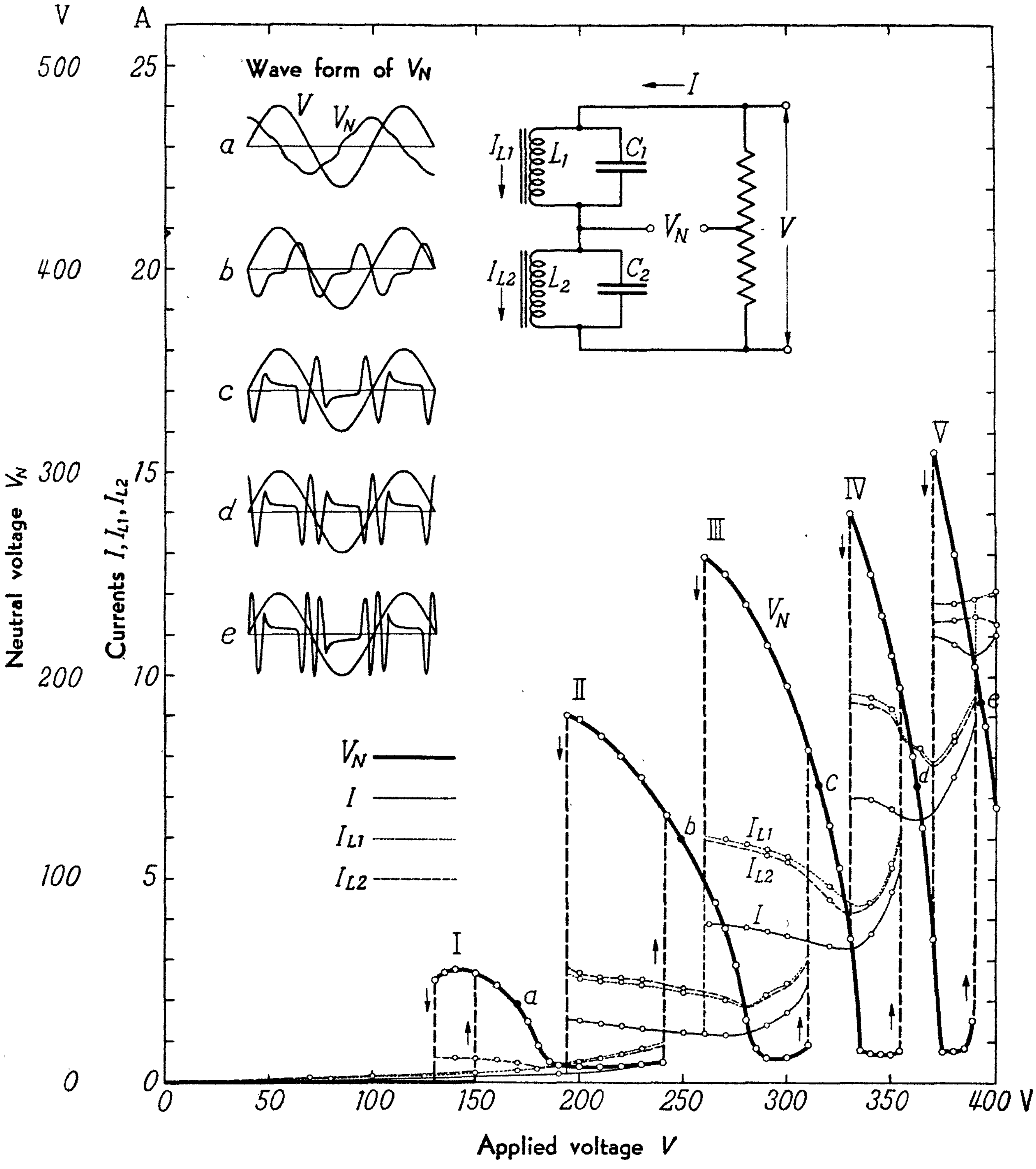


Fig. 2.6. Neutral instability caused by fundamental and higher-harmonic excitation.

# CHAPTER 3

# ALMOST PERIODIC OSCILLATIONS IN A SELF-OSCILLATORY SYSTEM WITH EXTERNAL FORCE

## 3.1 Introduction

In the preceding chapters we treated the cases in which the restoring force of the system was nonlinear. In this chapter we consider a case in which the nonlinearity appears in the damping of the system. This nonlinear damping results in the build up of an oscillation even in the absence of the external force; in other words, a self-excited oscillation occurs in this case.

When a periodic force is applied to a self-oscillatory system, the frequency of the self-excited oscillation, that is, the natural frequency of the system, falls in synchronism with the driving frequency, provided these two frequencies are not far different. This phenomenon of frequency entrainment may also occur when the ratio of the two frequencies is in the neighborhood of an integer (different from unity) or a fraction. Thus, if the amplitude and frequency of the external force are appropriately chosen, the natural frequency of the system is entrained by a frequency which is an integral multiple or submultiple of the driving frequency [12]. If the ratio of these two frequencies is not in the neighborhood of an integer or a fraction, one may expect the occurrence of an almost periodic oscillation [10, 14]. It is a salient feature of an almost periodic oscillation that the amplitude and phase of the oscillation vary slowly but periodically even in the steady state. However, the period of the amplitude variation is not an integral multiple of the period of the external force; the ratio of these two periods is in general incommensurable. Therefore, as a whole, there is no periodicity in the almost periodic oscillation.

First, we show the regions of entrainment; namely, if the amplitude and frequency of the external force are given in these regions, the entrainment occurs at the harmonic (fundamental), higher-harmonic, or subharmonic frequency of the external force. Second, we shall concentrate our attention to the almost periodic oscillations which occur when the external force is prescribed close to the boundary of the regions of entrainment and discuss the transition between entrained oscillations and almost periodic oscillations.

## 3.2 Entrainment of Frequency

We consider a system governed by the differential equation

$$\frac{d^2u}{dt^2} - \varepsilon(1 - u^2)\frac{du}{dt} + u = B\cos\nu t + B_0 \tag{3.1}$$

where $\varepsilon$ is a small positive constant, and $B\cos\nu t + B_0$ represents a forcing function containing a nonoscillatory component. Introducing a new variable defined by $v = u - B_0$, an alternative form of (3.1) may be written as

$$\frac{d^2v}{dt^2} - \mu(1 - \beta v - \gamma v^2)\frac{dv}{dt} + v = B\cos\nu t$$

$$\text{where} \qquad \mu = (1 - B_0^2)\varepsilon \qquad \beta = \frac{2B_0}{1 - B_0^2} \qquad \text{and} \qquad \gamma = \frac{1}{1 - B_0^2} \tag{3.2}$$

Since the system governed by Eq. (3.2) is of the self-excited type, $\mu$ must be positive, and therefore $B_0^2 < 1$. One sees further that $\mu$ is also a small quantity.

We shall, in this section, confine our attention to entrained oscillations. When $B = 0$, the natural frequency of the system (3.2) is nearly equal to unity. Therefore, when the driving frequency $\nu$ is in the neighborhood of unity, one may expect an entrained oscillation at the driving frequency $\nu$. This type of entrainment is referred to as harmonic entrainment, and the entrained harmonic oscillation $v(t)$ may be expressed approximately by

$$v(t) = b_1 \sin \nu t + b_2 \cos \nu t \tag{3.3}$$

On the other hand, when the driving frequency $\nu$ is far different from unity, one may expect the occurrence of higher-harmonic or subharmonic entrainment. In this case the entrained oscillation has a frequency which is an integral multiple or submultiple of the driving frequency $\nu$. An approximate solution for Eq. (3.2) may be expressed by

$$v(t) = \frac{B}{1 - \nu^2} \cos \nu t + b_1 \sin n\nu t + b_2 \cos n\nu t$$

where $\quad n = 2, 3, \cdots \quad$ for higher-harmonic oscillations $\quad$ (3.4)

$\quad n = 1/2, 1/3, \cdots \quad$ for subharmonic oscillations

The first term in the right side of Eq. (3.4) represents the forced oscillation at the driving frequency $\nu$. The second and third terms represent the entrained oscillation at the frequency $n\nu$ which is not far different from unity. Since $\mu$ is small, terms of frequency other than $\nu$ and $n\nu$ are ignored to this order of approximation.

The entrained oscillations and their stability were investigated in Ref. 12, where an example of the regions of entrainment at different frequencies was given. Namely, Fig. 3.1 shows such regions of entrainment for the following values of the system parameters:

$$\varepsilon = 0.2 \qquad \text{and} \qquad B_0 = 0.5$$

in Eq. (3.1). Consequently, the parameters in Eq. (3.2) are

$$\mu = 0.15 \qquad \beta = 4/3 \qquad \text{and} \qquad \gamma = 4/3$$

When the amplitude B and the frequency $\nu$ of the external force are given in the interior of these regions, the natural frequency of the system is entrained by the harmonic, higher-harmonic, or subharmonic frequency of the external force as indicated in the figure. One sees in Fig. 3.1 that the higher-harmonic or subharmonic entrainment occurs in a narrow range of the driving frequency $\nu$. On the other hand, the harmonic entrainment occurs at any driving frequency $\nu$ provided that the amplitude B of the external force is sufficiently large. In Fig. 3.1a, the boundary curve of the harmonic entrainment (drawn by dotted line in the figure) lies inside the region of the higher-harmonic entrainment. Since there is no abrupt change in the amplitudes of the harmonic and higher-harmonic components of the oscillations at the boundary of harmonic entrainment, this boundary curve has practically no singificance. In Fig. 3.1b, one sees that the continuity of the boundary curve of the harmonic entrainment is disturbed by the intrusion of the region of the 1/2-harmonic entrainment. The regions of the harmonic and 1/3-harmonic entrainments, on the other hand, have an overlapping area. This indicates that both the harmonic and 1/3-harmonic oscillations are sustained in this area common to the two regions, but only the 1/2-harmonic oscillation occurs in the region of 1/2-harmonic entrainment. When the external force is prescribed outside these regions, an almost periodic oscillation occurs.

In order to illustrate the phenomenon of frequency entrainment, some representative waveforms of v(t) obtained by using an analog computer are shown in Fig. 3.2. The block diagram of Fig. 3.3 shows an analog-computer setup for the solution of Eq. (3.2), in which the system parameters are set equal to the values as given above.* Table 3.1 shows the values of the amplitude B and the frequency $\nu$ of the external forces corresponding to the Fig. 3.2a to f, respectively. The points on the curves appear at the beginning of each cycle of the external force. These point marks are helpful for distinguishing between an entrained (periodic) oscillation and almost periodic (nonperiodic) oscillation.

Table 3.1. Amplitude and frequency of the external force in Fig. 3.2

| Fig. 3.2 | Amplitude B | Frequency $\nu$ |
|---|---|---|
| a | 0.1 | 0.996 |
| b | 0.5 | 0.499 |
| c | 0.5 | 0.332 |
| d | 2.0 | 1.99 |
| e | 2.0 | 2.97 |
| f | 0.55 | 0.700 |

* The integrating amplifiers in the block diagram integrates the input with respect to the machine time (in second), which is, in this particular case, 2 times the independent variable t.

### 3.3 Almost Periodic Oscillations Which Develop from Harmonic Oscillations

When the amplitude B and the frequency $\nu$ of the external force are prescribed outside the regions of entrainment, an almost periodic oscillation results. In the preceding section the solution of Eq. (3.2) was assumed, for the entrained oscillation, to take the form of Eq. (3.3) or (3.4). It would be natural to consider that, for the almost periodic oscillation, the coefficients $b_1$ and $b_2$ in Eqs. (3.3) and (3.4) are not constants but vary slowly with the time t. In this section we shall consider the almost periodic oscillation which develops from the harmonic oscillation and derive the relations which determine the time-varying amplitudes for the almost periodic oscillation.

#### (a) Derivation of the Fundamental Equations

From the above consideration one may assume that an almost periodic oscillation which develops from the harmonic oscillation is expressed by

$$v(t) = b_1(t) \sin \nu t + b_2(t) \cos \nu t \tag{3.5}$$

We now derive the relations which determine the time-varying coefficients, $b_1(t)$ and $b_2(t)$, in the above solution. Substituting Eq. (3.5) into (3.2) and equating the coefficients of the terms containing $\cos \nu t$ and $\sin \nu t$ separately to zero gives

$$\begin{aligned} \frac{dx_1}{d\tau} &= (1 - r_1^2)x_1 - \sigma_1 y_1 + \frac{B}{\mu\nu a_0} \equiv X_1(x_1, y_1) \\ \frac{dy_1}{d\tau} &= \sigma_1 x_1 + (1 - r_1^2)y_1 \equiv Y_1(x_1, y_1) \end{aligned} \tag{3.6}$$

where

$$\begin{aligned} &x_1 = \frac{b_1}{a_0} \qquad y_1 = \frac{b_2}{a_0} \qquad r_1^2 = x_1^2 + y_1^2 \\ &a_0 = \sqrt{\frac{4}{\gamma}} \qquad \tau = \frac{\mu}{2} t \qquad \sigma_1 = \frac{1 - \nu^2}{\mu\nu} \; : \text{ detuning} \end{aligned} \tag{3.7}$$

In the derivation of Eqs. (3.6) the following assumptions were made:
(1) $b_1(t)$ and $b_2(t)$ are slowly varying functions of t so that $d^2b_1/dt^2$ and $d^2b_2/dt^2$ may be neglected. (2) Since $\mu$ is a small quantity, $\mu\, db_1/dt$ and $\mu\, db_2/dt$ are also discarded.

The investigation of the solution of the nonautonomous system described by Eq. (3.2) is replaced by the study of Eqs. (3.6), in which $x_1$ and $y_1$ denote the normalized amplitudes of the forced oscillation. Equations (3.6) form an autonomous system of the first-order equations. The singular points of Eqs. (3.6) represent the harmonic oscillations of the original Eq. (3.2), and the limit cycles*, if exist, represent the almost periodic oscillations. Thus the entrained oscillation is obtained from Eqs. (3.6) by putting $dx_1/d\tau = 0$ and $dy_1/d\tau = 0$, i.e.,

$$X_1(x_{10}, y_{10}) = 0 \qquad\qquad Y_1(x_{10}, y_{10}) = 0 \tag{3.8}$$

where the subscript 0 is added to designate the equilibrium state. Eliminating $x_{10}$ and $y_{10}$ from Eqs. (3.8) gives

$$[(1 - r_{10}^2)^2 + \sigma_1^2]\, r_{10}^2 = \left(\frac{B}{\mu \nu a_0}\right)^2 \tag{3.9}$$

It will readily be seen that, when the amplitude B of the external force is zero, we obtain $r_{10}^2 = 1$ and $\sigma_1 = 0$, so that $a_0$ in Eqs. (3.7) represents the ultimate amplitude of the self-excited oscillation. The amplitudes $x_{10}$ and $y_{10}$, that is, the coordinates of the singular point of the system (3.6), are given by

---

* A closed trajectory towards which neighboring integral curves tend is called the limit cycle. Occurrences of this kind were first studied by Poincaré [23, p. 53].

$$x_{10} = -\frac{\mu\nu a_0}{B}(1 - r_{10}^2)r_{10}^2 \qquad y_{10} = \frac{\mu\nu a_0}{B}\sigma_1 r_{10}^2 \tag{3.10}$$

Equation (3.9) yields what we call the response curves for the harmonic oscillation as illustrated in Fig. 3.4. Each point on these curves yields the amplitude $r_{10}$ which is correlated with the frequency $\nu$ of a possible harmonic oscillation for a given value of the amplitude B.

(b) Stability of the Singular Point Correlated with the Periodic Solution

The stability of the singular point of the system (3.6) is correlated with the stability of the periodic solution of the original system (3.2). In order to investigate the stability of the equilibrium state, we consider sufficiently small variations $\xi$ and $\eta$ from the singular point defined by

$$x_1 = x_{10} + \xi \qquad y_1 = y_{10} + \eta \tag{3.11}$$

and determine whether these deviations approach zero or not with increase of the time $\tau$. Substituting Eqs. (3.11) into (3.6) and neglecting terms of higher degree than the first in $\xi$ and $\eta$ gives

$$\frac{d\xi}{d\tau} = a_1\xi + a_2\eta \qquad \frac{d\eta}{d\tau} = b_1\xi + b_2\eta$$

with

$$\begin{aligned} a_1 &= \left(\frac{\partial X_1}{\partial x_1}\right)_0 = 1 - r_{10}^2 - 2x_{10}^2 \\ a_2 &= \left(\frac{\partial X_1}{\partial y_1}\right)_0 = -\sigma_1 - 2x_{10}y_{10} \\ b_1 &= \left(\frac{\partial Y_1}{\partial x_1}\right)_0 = \sigma_1 - 2x_{10}y_{10} \\ b_2 &= \left(\frac{\partial Y_1}{\partial y_1}\right)_0 = 1 - r_{10}^2 - 2y_{10}^2 \end{aligned} \tag{3.12}$$

where $(\partial X_1/\partial x_1)_0$, ..., $(\partial Y_1/\partial y_1)_0$ stand for $\partial X_1/\partial x_1$, ..., $\partial Y_1/\partial y_1$ at $x_1 = x_{10}$, and $y_1 = y_{10}$. The characteristic equation of the system (3.12) is

$$\begin{vmatrix} a_1 - \lambda & a_2 \\ b_1 & b_2 - \lambda \end{vmatrix} = 0 \qquad (3.13)$$

or

$$\lambda^2 + p\lambda + q = 0$$

where

$$p = -(a_1 + b_2) = 2(2r_{10}^2 - 1) \qquad (3.14)$$

$$q = a_1 b_2 - a_2 b_1 = (1 - r_{10}^2)(1 - 3r_{10}^2) + \sigma_1^2$$

The variations $\xi$ and $\eta$ approach zero with the time $\tau$, provided that the real part of $\lambda$ is negative; in this case the corresponding periodic solution determined from Eqs. (3.10) and (3.5) is stable. This stability conditions is given by Routh-Hurwitz's criterion as [17]

$$p > 0 \qquad \text{and} \qquad q > 0 \qquad (3.15)$$

By making use of the stability conditions (3.15) the unstable portions of the response curves are shown dotted in Fig. 3.4. It is readily verified that the vertical tangencies of the response curves lie on the stability limit $q = 0$.

Let us take a glance at a discussion of the character of the integral curves in the neighborhood of the singular points of the system (3.6). For the singular point (3.10), the characteristic roots are given, by use of (3.14), as

$$\lambda_{1,2} = \frac{-p \pm \sqrt{p^2 - 4q}}{2} \qquad (3.16)$$

Poincaré [ 23, p. 14 ] has classified the types of singular points according to the character of the integral curves near the singular points, namely, according to the nature of the characteristic roots $\lambda$, as follows:

(1) The singularity is a nodal point, if the characteristic roots are both real and of the same sign, so that

$$p^2 - 4q \geq 0 \qquad \text{and} \qquad q > 0 \tag{3.17}$$

(2) The singularity is a saddle point, if the two roots are real but of opposite signs, so that

$$q < 0 \tag{3.18}$$

(3) The singularity is a focal point, if the two roots are cinjugate complex, so that

$$p^2 - 4q < 0 \tag{3.19}$$

If, in particular, both the roots are imaginary so that p = 0, the singularity is either a center or a focus.*

(c) Limit Cycle Correlated with an Almost Periodic Oscillation

As mentioned in Sec. 3.3a, an almost periodic oscillation which develops from the harmonic oscillation may be expressed by

$$v(t) = b_1(t) \sin \nu t + b_2(t) \cos \nu t \tag{3.20}$$

---

* Following the above classification, the type of a singularity will be definite when the characteristic roots $\lambda_1$ and $\lambda_2$ are neither zero nor pure imaginary. Such a singularity is called simple or of the first kind. However, we have also the singularity of the second kind for which the above conditions do not apply. The detailed discussion of such a singularity will be given in the following section.

where $b_1(t)$ and $b_2(t)$ are slowly varying functions of t. These time-varying amplitudes, or $x_1(\tau)$ and $y_1(\tau)$ in normalized form, are to be found from Eqs. (3.6). We consider the behavior of integral curves defined by Eqs. (3.6) in the $x_1y_1$ plane. It is known that, if the external force is given just outside the region of harmonic entrainment, Eqs. (3.6) have only one singularity which is unstable (see Fig. 3.4). It will also be seen that, for large values of $x_1$ and $y_1$, integral curves are directed towards the origin for increasing $\tau$. Hence the existence of a stable limit cycle may be concluded. We shall not go into the problem in which the detuning becomes so large that the natural frequency of the system is entrained by a higher-harmonic or subharmonic frequency (see Fig. 3.1). Even though the entrainment of such a type would not occur, an almost periodic oscillation should preferably be expressed in a different form than Eq. (3.20).

An example of the limit cycle is shown in Fig. 3.5a. The integral curves are drawn by making use of the isocline method. The system parameters in Eqs. (3.1) and (3.2) are the same as those in Sec. 3.2; the amplitude B and the frequency $\nu$ of the external force are prescribed just outside the region of harmonic entrainment (see Fig. 3.1b), i.e.,

$$B = 0.2 \qquad \text{and} \qquad \nu = 1.1$$

Through use of Eqs. (3.10), (3.14), and (3.19), the details of the singular point in Fig. 3.5a are readily known and are listed in Table 3.2. The period required for the representative point $(x_1(\tau),\ y_1(\tau))$ to complete one revolution along the limit cycle is 12.8 ··· times the period of the external force; hence the assumptions made in the derivation of Eqs. (3.6) are permissible.

Once the integral curves are obtained in the $x_1y_1$ plane, the time-response

Table 3.2. Singular point in Fig. 3.5a

| Singular point | $x_{10}$ | $y_{10}$ | $\lambda_1, \lambda_2$ | Classification |
|---|---|---|---|---|
| Fig. 3.5a | -0.245 | -0.400 | $0.561 \pm 1.254i$ | Unstable focus |

curve may be calculated by the following line integral:

$$T = \int \frac{ds}{\sqrt{X_1^2(x_1,y_1) + Y_1^2(x_1,y_1)}} \tag{3.21}$$

where $\qquad ds = \sqrt{(dx_1)^2 + (dy_1)^2}$ : line element on the integral curve

The waveform of the almost periodic oscillation obtained in this way is shown in Fig. 3.5b. The amplitude of the almost periodic oscillation varies periodically with large period. The points on the curves appear at the beginning of each cycle of the external force. One sees that in this case the phase of the almost periodic oscillation gradually lags the phase of the external force as t increases.*

---

* By using the relations (3.7), the solution (3.20) may be represented as

$$v(t) = a_0 r_1(t) \sin [\nu t + \theta(t)]$$

where $\qquad \theta(t) = \tan^{-1} y_1(t)/x_1(t)$

We see in Fig. 3.5a that the limit cycle contains the origin $x_1 = y_1 = 0$ in its interior and that the representative point moves in the clockwise direction. Therefore, the phase angle of the oscillation lags by $2\pi$ radians when the representative point makes one revolution along the closed trajectory.

(d) Transition between Entrained Oscillations and Almost Periodic Oscillations

We consider the behavior of integral curves of Eq. (3.6) particularly in the case where the amplitude B and the frequency $\nu$ of the external force are given near the boundary of harmonic entrainment. As mentioned in Sec. 3.3b, the boundary of harmonic entrainment is given by

$$q = (1 - r_{10}^2)(1 - 3r_{10}^2) + \sigma_1^2 = 0$$

or

$$p = 2(2r_{10}^2 - 1) = 0 \qquad (3.22)$$

The first equation applies in the case where the amplitude B and consequently the detuning $\sigma_1$ are comparatively small (see Fig. 3.4). Typical examples of integral curves in such a case are shown in Fig. 3.6a, b, and c. These figures show the integral curves under the conditions that B and $\nu$ of the external force are prescribed inside, on the boundary of, and outside the region of harmonic entrainment, respectively. As will be discussed in Sec. 3.4a, the coalescence of singular points occurs at the boundary of harmonic entrainment.

When the amplitude B and consequently the detuning $\sigma_1$ are large, the second equation of (3.22) applies. Typical examples of integral curves in such a case are shown in Fig. 3.7. At the boundary of harmonic entrainment the only singularity is a stable focus as will be verified in Sec. 3.4b. Slight increase in the detuning beyond the boundary will result in the occurrence of a stable limit cycle which is small in size, however. The limit cycle grows large as the detuning increases.

For intermediate values of B and $\sigma_1$, some complicated phenomena may occur [ 3, 5 ]. But we shall not enter this problem here, because such a region of external force is extremely narrow [cf. Chap. 4].

The difference in the behavior of integral curves between Figs. 3.6 and 3.7

is explained as follows: An almost periodic oscillation may be considered as a combination of two components, i.e., the free oscillation with the natural frequency of the system and the forced oscillation with the driving frequency. When the entrainment of frequency occurs, the situation in what follows may arise. If the amplitude B of the external force is small, the forced oscillation is not predominant. Since the detuning $\sigma_1$ is also small in this case, the free oscillation is entrained by the driving frequency (see Fig. 3.6). On the other hand, if B is large, the free oscillation is suppressed by the forced one (see Fig. 3.7).

## 3.4 Geometrical Discussion of Integral Curves at the Boundary of Harmonic Entrainment

We have considered the nature of singular points of Eqs. (3.6) in the preceding sections. As mentioned there, the types of singularities are determined once the roots (different from zero or pure imaginary) of the characteristic equation (3.13) are known. However, there still remain special cases to discuss in which the singular points are of higher order.

The following discussion is based on the autonomous equations (3.6) for critical values of B and $\nu$. And so the application of results, which will be obtained from them, to the oscillations governed by the nonautonomous equation (3.2) requires further examination, since the assumption is used to derive Eqs. (3.6).

### (a) Coalescence of Singular Points

Following the method of analysis due to Bendixson [2, pp. 58, 62, 74], we investigate the nature of singular point 2 in Fig. 3.6b. In this case the singularity lies on the boundary q = 0 in Fig. 3.4; its coordinates are, from Eqs. (3.10) and the first equation of (3.22), given by

$$x_{10} = -\frac{\mu\nu a_0}{9B}\left[1 + 3\sigma_1^2 - \sqrt{1 - 3\sigma_1^2}\right]$$
$$y_{10} = \frac{(1 - \nu^2)a_0}{3B}\left[2 + \sqrt{1 - 3\sigma_1^2}\right] \tag{3.23}$$

where the amplitude B and the frequency $\nu$ of the external force are related by*

$$\frac{2}{27}\left[1 + 9\sigma_1^2 - (1 - 3\sigma_1^2)^{3/2}\right] = \left(\frac{B}{\mu\nu a_0}\right)^2 \tag{3.24}$$

Transferring the origin to the singular point, i.e., putting

$$x_1 = x_{10} + \xi \qquad\qquad y_1 = y_{10} + \eta$$

we obtain, from Eqs. (3.6),

$$\frac{d\xi}{d\tau} = a_1\xi + a_2\eta + X_1(\xi, \eta)$$
$$\frac{d\eta}{d\tau} = b_1\xi + b_2\eta + Y_1(\xi, \eta) \tag{3.25}$$

where $\quad a_1 = a_2 = 0$

$$b_1 = \sigma_1 - 2x_{10}y_{10} \qquad\qquad b_2 = 1 - r_{10}^2 - 2y_{10}^2$$
$$X_1(\xi, \eta) = -3x_{10}\xi^2 - 2y_{10}\xi\eta - x_{10}\eta^2 - (\xi^2 + \eta^2)\xi \tag{3.26}$$
$$Y_1(\xi, \eta) = -y_{10}\xi^2 - 2x_{10}\xi\eta - 3y_{10}\eta^2 - (\xi^2 + \eta^2)\eta$$

---

* Relations (3.23) and (3.24) correspond to the upper boundary of the ellipse represented by the stability limit q = 0 in the $\sigma_1 r_{10}$ plane (see Fig. 3.4), since this portion turns to the boundary of entrainment on the $B\nu$ plane.

When $X_1(\xi, \eta)$ and $Y_1(\xi, \eta)$ are ignored, the characteristic equation of the system (3.25) is given by

$$\begin{vmatrix} a_1 - \lambda & a_2 \\ b_1 & b_2 - \lambda \end{vmatrix} = 0$$

from which we obtain

$$\lambda_1 = 0 \qquad\qquad \lambda_2 = b_2$$

Thus the singular point with which we are dealing is that of the second kind, and so we shall investigate the stability in what follows.

The tangents of the integral curves at the origin of the $\xi\eta$ plane are determined by (see Appendix I)

$$\xi(b_1\xi + b_2\eta) = 0 \tag{3.27}$$

We shall first show that there are two and only two branches of the integral curves which tend to the origin with the tangent $\xi = 0$. By making use of the transformation $\xi = \varphi\eta$, equations (3.25) lead to

$$\begin{aligned} \frac{d\varphi}{d\tau} &= -b_2\varphi - x_{10}\eta + X_2(\varphi, \eta) \\ \frac{d\eta}{d\tau} &= \qquad\qquad b_2\eta + Y_2(\varphi, \eta) \end{aligned} \tag{3.28}$$

where $X_2(\varphi, \eta)$ and $Y_2(\varphi, \eta)$ are the polynomials containing terms of higher degree than the first in $\varphi$, $\eta$. The characteristic equation becomes in this case

$$\begin{vmatrix} -b_2 - \lambda & -x_{10} \\ 0 & b_2 - \lambda \end{vmatrix} = 0$$

from which we obtain*

$$\lambda_{1,2} = \pm b_2$$

so that the singularity is a saddle point. Hence there are four branches of the integral curves tending to the origin in the $\varphi\eta$ plane, two of which are represented by $\eta = 0$, but these are reduced to the origin $\xi = \eta = 0$ of the $\xi\eta$ plane. We have, therefore, two and only two branches of the integral curves tending to the origin $\xi = \eta = 0$ with the tangent $\xi = 0$, one of them being situated above and the other under the $\xi$ axis.

Now we may conclude that all the other integral curves which tend to the origin have the tangent $\eta = -\frac{b_1}{b_2}\xi$. In order, therefore, to investigate them, we apply the transformation

$$\eta = (\psi - \frac{b_1}{b_2})\xi$$

to (3.25), and get

$$\xi^2 \frac{d\psi}{d\xi} = \frac{b_2\psi + \frac{Y_1(\xi,\psi)}{\xi}}{\frac{X_1(\xi,\psi)}{\xi^2}} - (\psi - \frac{b_1}{b_2})\xi \tag{3.29}$$

or

$$\xi^2 \frac{d\psi}{d\xi} = a\psi + b\xi + B_1(\xi,\psi)$$

where

$$a = \frac{-b_2^3}{b_1^2 x_{10} - 2b_1 b_2 y_{10} + 3b_2^2 x_{10}} \tag{3.30}$$

---

* When $q = 0$, the coefficient $b_2$ is given by

$$b_2 = 4(\frac{\mu\nu a_0}{B})^2 r_{10}^4(1 - r_{10}^2)(1 - 2r_{10}^2)$$

from this $b_2 < 0$ results at the upper boundary of $q = 0$.

$$b = \frac{(b_1^2 + b_2^2)(b_1x_{10} + b_2y_{10})}{b_2(b_1^2x_{10} - 2b_1b_2y_{10} + 3b_2^2x_{10})}$$

$B_1(\xi, \psi)$ being a series containing terms of higher degree than the first in $\xi$, $\psi$. This takes the form of Eq. (I.3) in Appendix I with m = 2 (an even number).* Hence, dividing the $\xi\psi$ plane into two regions along the $\psi$ axis, we see that all the integral curves tend to the origin on either side of the axis (which side it will be depending on the sign of a), and that, on the other side, one and only one branch of the integral curves tends to the origin, while all the others veer away from the origin. Therefore, in the end, we may conclude that the equilibrium state correlated with the singularity is semistable.

We shall further derive an approximate equation of the integral curves in the neighborhood of the singularity. By making use of the further transformation

$$p = \frac{1}{a}\xi \qquad\qquad q = a\psi + b\xi$$

equation (3.30) becomes

$$p^2 \frac{dq}{dp} = q + B_1'(p,q) \tag{3.31}$$

where $B_1'(p,q)$ contains terms of higher degree than the first in p, q, so that it may be neglected as compared with q, since we confine the discussion to the singular point and its vicinity alone. Integrating (3.31) under this condition, we have

$$q = C \cdot e^{-\frac{1}{p}} \tag{3.32}$$

C being a constant of integration, and, turning back to the original $\xi\eta$ rela-

---

* It is here assumed that $b_1^2x_{10} - 2b_1b_2y_{10} + 3b_2^2x_{10} \neq 0$.

tion, we finally obtain

$$\eta = \left(-\frac{b_1}{b_2} - \frac{b}{a}\xi + C\cdot e^{-\frac{a}{\xi}}\right)\xi \tag{3.33}$$

Numerical Example

In order to illustrate the foregoing analysis, we consider a case when the amplitude B and the frequency $\nu$ satisfy the following relations

$$\left(\frac{B}{\mu\nu a_0}\right)^2 = \frac{1}{10} \qquad q = 0$$

From this the following quantities are readily obtained;* i.e.,

$$B = 0.0842 \qquad \nu = 1.0243$$

$$x_{10} = -0.1675 \qquad y_{10} = -0.9570$$

$$b_1 = -0.6412 \qquad b_2 = -1.7756$$

$$a = 10.64 \qquad b = -6.894$$

Substituting these values into (3.33), we can draw the integral curves for several values of C. They are plotted in Fig. 3.8a. From equations (3.25), we see that a representative point moves on the integral curves in the direction of the arrows. Thus a point $(\xi(\tau), \eta(\tau))$ tends to the origin in the region $\xi > 0$, but leaves the origin in the other region $\xi < 0$. Hence, the singular point is semistable.

---

* Equations (3.6) are unchanged if $\sigma_1$ and $y_1$ are replaced by $-\sigma_1$ and $-y_1$, respectively. This implies that the phase-plane diagrams of the system (3.6) are symmetric about the $x_1$ axis each other if the external forces are prescribed by $B/\mu\nu\, a_0$, $\sigma_1$ and $B/\mu\nu\, a_0$, $-\sigma_1$. Hence we consider the right-hand boundary given by $\nu > 1$.

Now, in order to complete our discussion, we shall deal with the exceptional case in which

$$b_1^2 x_{10} - 2b_1 b_2 y_{10} + 3b_2^2 x_{10} = 0 \tag{3.34}$$

This takes place when the singularity is located at the points where the boundary $q = 0$ has vertical tangency. In this case we have

$$\left(\frac{B}{\mu \nu a_0}\right)^2 = \frac{8}{27} \qquad\qquad \sigma_1^2 = \frac{1}{3}$$

and the following values are readily obtained for $\sigma_1 = -1/\sqrt{3}$; i.e.,

$$x_{10} = -\frac{1}{\sqrt{6}} \qquad y_{10} = -\frac{1}{\sqrt{2}} \qquad r_{10}^2 = \frac{2}{3}$$

$$b_1 = -\frac{2}{\sqrt{3}} \qquad b_2 = -\frac{2}{3}$$

Substituting these values into Eq. (3.29), we have

$$\xi^2 \frac{d\psi}{d\xi} = \frac{-\frac{2}{3}\psi + 4\sqrt{2}\xi - \frac{16}{\sqrt{6}}\xi\psi + 4\sqrt{3}\xi^2 + \frac{3}{\sqrt{2}}\xi\psi^2 - 10\xi^2\psi + 3\sqrt{3}\xi^2\psi^2 - \xi^2\psi^3}{-4\xi + 2\sqrt{3}\xi\psi + \frac{1}{\sqrt{6}}\psi^2 - \xi\psi^2} - (\psi - \sqrt{3})\xi$$

However, this does not take the form of Eq. (3.30), and so, applying the further transformation $\psi = (\zeta + 6\sqrt{2})\xi$, we obtain

$$\xi^3 \frac{d\zeta}{d\xi} = \frac{1}{6}\zeta + 8\sqrt{3}\xi + B_2(\xi, \zeta) \tag{3.35}$$

where $B_2(\xi, \zeta)$ contains terms of higher degree than the first. This takes the form of Eq. (I.3) in Appendix I with $m = 3$ (odd) and $a = 1/6 > 0$, and so the singularity is a nodal point. In order to find the integral curves in the neighborhood of the singularity, we further put

$$p = \sqrt{6}\,\xi \qquad\qquad q = \frac{1}{6}\zeta + 8\sqrt{3}\,\xi$$

Equation (3.35) may then be written in the form

$$p^3 \frac{dq}{dp} = q + B_2'(p,q) \tag{3.36}$$

where $B_2'(p,q)$ contains terms of higher degree than the first. Hence, neglecting this, we integrate (3.36) and obtain

$$q = C\cdot e^{-\frac{1}{2p^2}}$$

C being a constant of integration, and in the $\xi\eta$ plane

$$\eta = (-\sqrt{3} + 6\sqrt{2}\,\xi - 48\sqrt{3}\,\xi^2 + C\xi\, e^{-\frac{1}{12\xi^2}})\,\xi \tag{3.37}$$

The integral curves are computed for several values of C, and plotted in Fig. 3.8b. From equations (3.25), we see that a representative point moves on the integral curves in the direction of the arrows. Thus a point $(\xi(\tau), \eta(\tau))$ from any initial condition tends ultimately to the origin. Hence, the singular point is stable.

(b) Existence of a Stable Focus

We investigate the nature of singular point in Fig. 3.7b. In this case the singularity lies on the boundary p = 0 in Fig. 3.4; its coordinates are, from Eqs. (3.10) and the second equation of (3.22), given by

$$x_{10} = -\frac{\mu\nu a_0}{4B} \qquad\qquad y_{10} = \frac{(1-\nu^2)a_0}{2B} \tag{3.38}$$

where the amplitude B and the frequency $\nu$ of the external force are related by*

* It is noted that $|\sigma_1| > 1/2$, $(B/\mu\nu a_0)^2 > 1/4$.

$$\frac{1}{2}\left(\frac{1}{4} + \sigma_1^2\right) = \left(\frac{B}{\mu\nu a_0}\right)^2 \tag{3.39}$$

Transferring the origin to the singular point, i.e., putting

$$x_1 = x_{10} + \xi \qquad y_1 = y_{10} + \eta$$

we obtain, from Eqs. (3.6),

$$\begin{aligned} \frac{d\xi}{d\tau} &= a_1\xi + a_2\eta + X_1(\xi, \eta) \\ \frac{d\eta}{d\tau} &= b_1\xi + b_2\eta + Y_1(\xi, \eta) \end{aligned} \tag{3.40}$$

where
$$a_1 = -\frac{1}{2} + \frac{a_0^2}{2A^2} \qquad a_2 = \left(1 - \frac{a_0^2}{A^2}\right)\sigma_1$$

$$b_1 = \left(3 - \frac{a_0^2}{A^2}\right)\sigma_1 \qquad b_2 = \frac{1}{2} - \frac{a_0^2}{2A^2}$$

$$A = \frac{B}{1 - \nu^2} \tag{3.41}$$

$$X_1(\xi, \eta) = -3x_{10}\xi^2 - 2y_{10}\xi\eta - x_{10}\eta^2 - (\xi^2 + \eta^2)\xi$$

$$Y_1(\xi, \eta) = -y_{10}\xi^2 - 2x_{10}\xi\eta - 3y_{10}\eta^2 - (\xi^2 + \eta^2)\eta$$

When $X_1(\xi, \eta)$ and $Y_1(\xi, \eta)$ are ignored, the characteristic equation of the system (3.40) is given by [cf. Eqs. (3.14)]

$$\lambda^2 + p\lambda + q = 0$$

Since $p^2 - 4q = 1 - 4\sigma_1^2 < 0$ and $p = 0$, the roots $\lambda$ are imaginary, so that the singularity is either a center or a focus (see Sec. 3.3b). Following the analysis due to Poincaré [22, 23], we shall investigate the type of singularity in what follows (see Appendix II).

Introducing new variables defined by

$$x = \sqrt{a_1 b_2 - a_2 b_1}\,(\xi + \eta)$$

$$y = (a_1 + b_1)\xi + (a_2 + b_2)\eta$$

we obtain, from Eqs. (3.40),

$$\frac{dx}{dz} = \quad y + X_2(x,y) \equiv X(x,y)$$

$$\frac{dy}{dz} = - x + Y_2(x,y) \equiv Y(x,y) \tag{3.42}$$

where $$z = \sqrt{a_1 b_2 - a_2 b_1}\cdot\tau = \sqrt{\sigma_1^2 - 1/4}\cdot\tau$$

and $X_2(x,y)$, $Y_2(x,y)$ are polynomials containing terms of degree higher than the first in x and y. Now let us consider a closed curve around the singularity as given by

$$F(x,y) = k$$

where k is a small positive constant. If the function F(x,y) could be constructed such that $\frac{\partial F}{\partial x} X + \frac{\partial F}{\partial y} Y = 0$, the singularity is a center; while, if $\frac{\partial F}{\partial x} X + \frac{\partial F}{\partial y} Y$ is either positive or negative in the neighborhood of the singularity, the singularity is a focus.

In Fig. 3.7b the external force is chosen such that B = 0.2 and $\nu$ = 1.0688, which are located on the boundary of harmonic entrainment. The other system parameters are the same as in Sec. 3.2. Then we obtain, from Eqs. (3.38),

$$x_{10} = - 0.3471 \qquad \text{and} \qquad y_{10} = - 0.6160$$

Following the procedure as described in Appendix II, we obtain

$$F(x,y) = F_2(x,y) + F_3(x,y) + F_4(x,y) = k$$

where $$F_2(x,y) = x^2 + y^2$$

$$F_3(x,y) = -1.26x^3 + 6.89x^2y - 0.33xy^2 + 6.50y^3$$

$$F_4(x,y) = -11.86x^4 - 12.87x^3y - 6.26xy^3 + 11.01y^4$$

In the neighborhood of the singularity we have

$$\frac{dF}{dz} = \frac{\partial F}{\partial x} X + \frac{\partial F}{\partial y} Y = -6.92(x^2 + y^2)^2 + \phi_5(x,y) < 0$$

where $\phi_5(x,y)$ is a polynomial containing terms of degree higher than the fourth in x and y. Hence the integral curves of Eqs. (3.42) cross the closed curve $F(x,y) = k$ from the exterior to the interior with increasing z. Therefore, we may conclude that, in the original $x_1y_1$ plane, the singularity $(x_{10},y_{10})$ is a stable focus.

## 3.5 Almost Periodic Oscillations Which Develop from Higher-Harmonic Oscillations

We shall, in this section, deal with the almost periodic oscillation which develops from the second- or third-harmonic entrainment.

### (a) Fundamental Equations

Almost periodic oscillations which develop from these higher-harmonic oscillations may be expressed by

$$v(t) = \frac{B}{1 - \nu^2} \cos \nu t + b_1(t) \sin n\nu t + b_2(t) \cos n\nu t \qquad n = 2 \text{ or } 3 \qquad (3.43)$$

where $b_1(t)$ and $b_2(t)$ are slowly varying functions of t. We here derive the relations which determine the time-varying coefficients, $b_1(t)$ and $b_2(t)$, in the above solutions.

Proceeding in the same manner as in Sec. 3.3a; namely, substituting Eq. (3.43) into (3.2) and equating the coefficients of the terms containing cos $n\nu t$ and sin $n\nu t$ separately to zero gives

$$\begin{aligned} \frac{dx_n}{d\tau} &= (D - r_n^2)x_n - \sigma_n y_n \equiv X_n(x_n, y_n) \\ \frac{dy_n}{d\tau} &= \sigma_n x_n + (D - r_n^2)y_n - F_n \equiv Y_n(x_n, y_n) \end{aligned} \tag{3.44}$$

where

$$\begin{aligned} & x_n = \frac{b_1}{a_0} \qquad y_n = \frac{b_2}{a_0} \qquad r_n^2 = x_n^2 + y_n^2 \\ & a_0 = \sqrt{\frac{4}{\gamma}} \qquad D = 1 - \frac{2A^2}{a_0^2} \qquad A = \frac{B}{1 - \nu^2} \\ & \tau = \frac{\mu}{2} t \qquad \sigma_n = \frac{1 - (n\nu)^2}{\mu n \nu} \quad \text{: detuning} \\ & F_2 = \frac{\beta}{4a_0} A^2 \qquad F_3 = \frac{\gamma}{12a_0} A^3 \end{aligned} \tag{3.45}$$

It is noted that the same assumptions as those mentioned in Sec. 3.3a must be made for the derivation of Eqs. (3.44). The entrained higher-harmonic oscillation is obtained from Eqs. (3.44) by putting $dx_n/d\tau = 0$ and $dy_n/d\tau = 0$. From these relations, we can readily find the amplitude characteristic for the higher-harmonic oscillations, i.e.,*

$$[(D - r_n^2)^2 + \sigma_n^2]\, r_n^2 = F_n^2 \tag{3.46}$$

---

* In order to avoid the troublesome notation, we hereafter omit the subscript 0 which designates the equilibrium state.

The amplitudes of the higher-harmonic component $x_n$ and $y_n$, that is, the coordinates of the singular point, are given by

$$x_n = \frac{\sigma_n r_n^2}{F_n} \qquad y_n = \frac{(D - r_n^2) r_n^2}{F_n} \tag{3.47}$$

Proceeding in the same manner as in Sec. 3.3b, the stability conditions for the singular point are as follows:

$$\begin{aligned} p_n &= 2(2r_n^2 - D) > 0 \\ q_n &= (D - r_n^2)(D - 3r_n^2) + \sigma_n^2 > 0 \end{aligned} \tag{3.48}$$

(b) Limit Cycles Correlated with Almost Periodic Oscillations

We consider the behavior of integral curves in the $x_n y_n$ plane defined by the Eqs. (3.44). It is known that, if the external force is given outside the regions of higher-harmonic entrainment, Eqs. (3.44) have only one unstable singularity.* It will also be seen that, for large values of $x_n$ and $y_n$, integral curves are directed toward the origin for increasing $\tau$. Therefore the existence of a stable limit cycle and hence of an almost periodic oscillation may be con-

---

* For nonzero values of D, equation (3.46) may be rewritten as

$$\left[\left(1 - \frac{r_n^2}{D}\right)^2 + \left(\frac{\sigma_n}{D}\right)^2\right] \frac{r_n^2}{D} = \frac{F_n^2}{D^3}$$

The above equation has the same form as Eq. (3.9). Therefore, if the quantities $r_{10}^2$, $\sigma_1$, and $(B/\mu\nu a_0)^2$ are replaced by $r_n^2/D$, $\sigma_n/D$ and $F_n^2/D^3$, respectively, the response curves of Fig. 3.4 also apply to the case of higher-harmonic oscillation. As we can verify shortly, the dotted portions of the response curves are also unstable for the higher-harmonic oscillation.

cluded.

Figure 3.9a shows an example of the limit cycle of Eqs. (3.44) for $n = 2$. In this case the corresponding almost periodic oscillation develops from the second-harmonic oscillation. The amplitude $B$ and the frequency $\nu$ of the external force are given by

$$B = 0.8 \qquad \text{and} \qquad \nu = 0.47$$

which are located just outside the region of the second-harmonic entrainment (see Fig. 3.1a). The other system parameters are the same as before. The period required for the representative point to complete one revolution along the limit cycle is 7.6 ... times the period of the external force. Figure 3.9b shows the waveform of the almost periodic oscillation represented by the limit cycle. In Fig. 3.10a is plotted the limit cycle of Eqs. (3.44) for $n = 3$; the corresponding almost periodic oscillation develops from the third-harmonic oscillation. The amplitude $B$ and the frequency $\nu$ of the external force are given by

$$B = 1.0 \qquad \text{and} \qquad \nu = 0.345$$

which are located just outside the region of the third-harmonic entrainment (see Fig. 3.1a). The period required for the representative point to complete one revolution along the limit cycle is 10.4 ... times the period of the external force. Figure 3.10b shows the waveform of the almost periodic oscillation represented by the limit cycle. The details of the singular points in Figs. 3.9a and 3.10a are readily known and are summed up in Table 3.3.

(c) Transition between Entrained Oscillations and Almost Periodic Oscillations

Introducing new variables defined by

$$x_n = \sqrt{D}\, y \qquad y_n = \sqrt{D}\, x \qquad r_n^2 = Dr^2$$

Table 3.3. Singular points in Figs. 3.9a and 3.10a

| Singular point | $x_n$ | $y_n$ | $\lambda_1, \lambda_2$ | Classification |
|---|---|---|---|---|
| Fig. 3.9a | 0.226 | 0.066 | $0.187 \pm 0.824i$ | Unstable focus |
| Fig. 3.10a | -0.195 | 0.043 | $0.061 \pm 0.457i$ | Unstable focus |

$$\sigma_n = D\,\sigma \qquad \tau = z/D \tag{3.49}$$

we obtain, from Eqs. (3.44),

$$\begin{aligned} \frac{dx}{dz} &= (1 - r^2)x - \sigma y + \frac{F_n}{D^{3/2}} \\ \frac{dy}{dz} &= \sigma x + (1 - r^2)y \end{aligned} \tag{3.50}$$

Equations (3.50) have the same form as (3.6). Hence the behavior of integral curves during the transition between entrained oscillations and almost periodic oscillations is analogous to that occurring between harmonic and almost periodic oscillations.

## 3.6 Almost Periodic Oscillations Which Develop from Subharmonic Oscillations

We shall, in this section, deal with the almost periodic oscillation which develops from the 1/2- or 1/3-harmonic entrainment.

### (a) Fundamental Equations

Almost periodic oscillations which develop from these subharmonic oscillations may be expressed by

$$v(t) = \frac{B}{1 - \nu^2} \cos \nu t + b_1(t) \sin n\nu t + b_2(t) \cos n\nu t$$
$$n = 1/2 \text{ or } 1/3 \tag{3.51}$$

where $b_1(t)$ and $b_2(t)$ are slowly varying functions of t. We here derive the relations which determine the time-varying coefficient, $b_1(t)$ and $b_2(t)$, in the above solutions.

Proceeding in the same manner as in Sec. 3.3a; namely, substituting Eq. (3.51) into (3.2) and equating the coefficients of the terms containing $\cos n\nu t$ and $\sin n\nu t$ separately to zero gives

$n = 1/2$:

$$\begin{aligned} \frac{dx_{1/2}}{d\tau} &= (D - r_{1/2}^2 + \tfrac{1}{2}\beta A)x_{1/2} - \sigma_{1/2}y_{1/2} \equiv X_{1/2}(x_{1/2}, y_{1/2}) \\ \frac{dy_{1/2}}{d\tau} &= \sigma_{1/2}x_{1/2} + (D - r_{1/2}^2 - \tfrac{1}{2}\beta A)y_{1/2} \equiv Y_{1/2}(x_{1/2}, y_{1/2}) \end{aligned} \tag{3.52}$$

$n = 1/3$:

$$\begin{aligned} \frac{dx_{1/3}}{d\tau} &= (D - r_{1/3}^2)x_{1/3} - \sigma_{1/3}y_{1/3} + \frac{A}{a_0}2x_{1/3}y_{1/3} \equiv X_{1/3}(x_{1/3}, y_{1/3}) \\ \frac{dy_{1/3}}{d\tau} &= \sigma_{1/3}x_{1/3} + (D - r_{1/3}^2)y_{1/3} + \frac{A}{a_0}(x_{1/3}^2 - y_{1/3}^2) \equiv Y_{1/3}(x_{1/3}, y_{1/3}) \end{aligned} \tag{3.53}$$

where

$$\begin{aligned} &x_n = \frac{b_1}{a_0} \qquad y_n = \frac{b_2}{a_0} \qquad r_n^2 = x_n^2 + y_n^2 \\ &a_0 = \sqrt{\frac{4}{\gamma}} \qquad D = 1 - \frac{2A^2}{a_0^2} \qquad A = \frac{B}{1 - \nu^2} \\ &\tau = \frac{\mu}{2}t \qquad \sigma_n = \frac{1 - (n\nu)^2}{\mu n\nu} \ \text{; detuning} \end{aligned} \tag{3.54}$$

It is noted that the same assumptions as those mentioned in Sec. 3.3a must be made for the derivation of Eqs. (3.52) and (3.53). The entrained subharmonic oscillation is obtained from Eqs. (3.52) or (3.53) by putting $dx_n/d\tau = 0$ and $dy_n/d\tau = 0$. From these relations, we can find the amplitude characteristics for the subharmonic oscillations, i.e.,

$n = 1/2$:

$$[(D - r_{1/2}^2)^2 + \sigma_{1/2}^2 - \tfrac{1}{4}\beta^2A^2]\, r_{1/2}^2 = 0 \tag{3.55}$$

$n = 1/3$: $\quad [(D - r_{1/3}^2)^2 + \sigma_{1/3}^2 - \frac{\gamma}{4} A^2 r_{1/3}^2]\, r_{1/3}^2 = 0 \qquad (3.56)$

From these relations, the amplitude $r_n$ of the subharmonic oscillation is found to be

$n = 1/2$: $\quad r_{1/2}^2 = 0 \qquad (3.57)$

or $\quad r_{1/2}^2 = D \pm \sqrt{\frac{\beta^2}{4} A^2 - \sigma_{1/2}^2} \qquad (3.58)$

$n = 1/3$: $\quad r_{1/3}^2 = 0 \qquad (3.59)$

or $\quad r_{1/3}^2 = (D + \frac{\gamma}{8} A^2) \pm \sqrt{(D + \frac{\gamma}{8} A^2)^2 - D^2 - \sigma_{1/3}^2} \qquad (3.60)$

When the amplitude $r_n$ is zero, no subharmonic response is obtained. Consequently, the periodic solution (3.51) has only the harmonic component $B/(1 - \nu^2)\cdot\cos \nu t$. The amplitude $r_n$ of the subharmonic oscillation may be obtained from Eq. (3.58) or (3.60) provided that the right sides of these equations are positive. One will notice from Eqs. (3.58) and (3.60) that the detuning $\sigma_n$ must be small enough when the entrainment at these subharmonic frequencies is expected (see Fig. 3.1b). The amplitudes of the subharmonic component $x_n$ and $y_n$, that is, the coordinates of the singular points, are given by

$n = 1/2$:

$$x_{1/2} = r_{1/2} \cos \theta_{1/2} \qquad r_{1/2} \cos(\theta_{1/2} + \pi)$$

$$y_{1/2} = r_{1/2} \sin \theta_{1/2} \qquad r_{1/2} \sin(\theta_{1/2} + \pi) \qquad (3.61)$$

where $\quad \cos 2\theta_{1/2} = \frac{-2(D - r_{1/2}^2)}{\beta A} \qquad \sin 2\theta_{1/2} = \frac{2\sigma_{1/2}}{\beta A}$

$n = 1/3$:

$$x_{1/3} = r_{1/3} \cos \theta_{1/3} \quad r_{1/3} \cos(\theta_{1/3} + \tfrac{2}{3}\pi) \quad r_{1/3} \cos(\theta_{1/3} + \tfrac{4}{3}\pi)$$

$$y_{1/3} = r_{1/3} \sin \theta_{1/3} \quad r_{1/3} \sin(\theta_{1/3} + \tfrac{2}{3}\pi) \quad r_{1/3} \sin(\theta_{1/3} + \tfrac{4}{3}\pi)$$

$$\text{where} \quad \cos 3\theta_{1/3} = \frac{-a_0 \sigma_{1/3}}{Ar_{1/3}} \qquad \sin 3\theta_{1/3} = \frac{-a_0(D - r_{1/3}^2)}{Ar_{1/3}} \tag{3.62}$$

Proceeding in the same manner as in Sec. 3.3b, the stability conditions for the singular points are as follows:

For $r_{1/2}^2 = 0$:

$$p_{1/2} = -2D > 0 \qquad q_{1/2} = D^2 - \tfrac{1}{4}\beta^2 A^2 + \sigma_{1/2}^2 > 0 \tag{3.63}$$

For $r_{1/2}^2 \neq 0$:

$$p_{1/2} = 2(2r_{1/2}^2 - D) > 0 \qquad q_{1/2} = 4r_{1/2}^2(r_{1/2}^2 - D) > 0 \tag{3.64}$$

For $r_{1/3}^2 = 0$:

$$p_{1/3} = -2D > 0 \qquad q_{1/3} = D^2 + \sigma_{1/3}^2 > 0 \tag{3.65}$$

For $r_{1/3}^2 \neq 0$:

$$p_{1/3} = 2(2r_{1/3}^2 - D) > 0 \qquad q_{1/3} = -6r_{1/3}^2(D + \tfrac{\gamma}{8} A^2 - r_{1/3}^2) > 0 \tag{3.66}$$

(b) Limit Cycle Correlated with Almost Periodic Oscillations

We consider the behavior of integral curves in the $x_n y_n$ plane defined by the Eqs. (3.52) or (3.53). Analogously as in the preceding sections, it may be concluded that, if the external force is given outside the regions of subharmonic entrainment, Eqs. (3.52) or (3.53) possess a limit cycle correlated with an almost periodic oscillation.

The graphical solution of Eqs. (3.52) or (3.53) may conveniently be obtained by introducing polar coordinates $x_n = r_n \cos \theta_n$, $y_n = r_n \sin \theta_n$. Thus we write, from Eqs. (3.52) and (3.53),

$$\frac{dr_{1/2}}{d\tau} = (D - r_{1/2}^2)r_{1/2} + \frac{\beta}{2} A r_{1/2} \cos 2\theta_{1/2} \equiv R_{1/2}(r_{1/2}, \theta_{1/2})$$
$$\frac{d\theta_{1/2}}{d\tau} = \sigma_{1/2} - \frac{\beta}{2} A \sin 2\theta_{1/2} \qquad\qquad \equiv \Theta_{1/2}(\theta_{1/2}) \tag{3.67}$$

and

$$\frac{dr_{1/3}}{d\tau} = (D - r_{1/3}^2)r_{1/3} + \frac{A}{a_0} r_{1/3}^2 \sin 3\theta_{1/3} \equiv R_{1/3}(r_{1/3}, \theta_{1/3})$$
$$\frac{d\ _{1/3}}{d\tau} = \sigma_{1/3} + \frac{A}{a_0} r_{1/3} \cos 3\theta_{1/3} \qquad\qquad \equiv \Theta_{1/3}(r_{1/3}, \theta_{1/3}) \tag{3.68}$$

Equations (3.67) are unchanged if $\theta_{1/2}$ is replaced by $\theta_{1/2} + \pi$, while Eqs. (3.68) are unchanged if $\theta_{1/3}$ is replaced by $\theta_{1/3} + \frac{2}{3}\pi$. This implies that phase-plane diagram of the system (3.67) is $\pi$ symmetric about the origin and that of (3.68) is $\frac{2}{3}\pi$ symmetric. Let $\phi_n$ be the angle with which the integral curve traverses the radius vector, then

$$\tan \phi_n = r_n \frac{d\theta_n}{dr_n} = r_n \frac{\Theta_n(r_n, \theta_n)}{R_n(r_n, \theta_n)} \qquad n = 1/2 \text{ or } 1/3 \tag{3.69}$$

The graphical construction of integral curves is much facilitated by drawing iso-$\phi$ curves instead of isoclines.

Figure 3.11a shows an example of the limit cycle of Eqs. (3.67). Some of the iso-$\phi$ curves are shown dotted in the figure. In this case the corresponding almost periodic oscillation develops from the 1/2-harmonic oscillation. The amplitude B and the frequency $\nu$ of the external force are given by

$$B = 4.0 \qquad \text{and} \qquad \nu = 2.15$$

which are located just outside the region of the 1/2-harmonic entrainment (see Fig. 3.1b). The other system parameters are the same as before. The period T required for the representative point to complete one revolution along the limit cycle is readily obtained from the second equation of (3.67), i.e.,

$$T = \int_0^{2\pi} \frac{d\,\theta_{1/2}}{|\sigma_{1/2}| - \frac{\beta}{2} A \sin 2\,\theta_{1/2}} = \frac{2\pi}{\sqrt{\sigma_{1/2}^2 - \frac{1}{4}\beta^2 A^2}} \tag{3.70}$$

It is worth noting that in this particular case the limit cycle is also obtained analytically by constructing a Liapunov function in what follows [15, pp. 74-82].

When the amplitude B and the frequency $\nu$ of the external force are given outside the region of the 1/2-harmonic entrainment, the system (3.52) has the only singular point which is unstable focus and is located at the origin $x_{1/2} = y_{1/2} = 0$ [cf. Eqs. (3.63)]. Hence the linear part of Eqs. (3.52), i.e.,

$$\begin{aligned} \frac{dx_{1/2}}{d\tau} &= (D + \tfrac{1}{2}\beta A)x_{1/2} - \sigma_{1/2} y_{1/2} \\ \frac{dy_{1/2}}{d\tau} &= \sigma_{1/2} x_{1/2} + (D - \tfrac{1}{2}\beta A) y_{1/2} \end{aligned} \tag{3.71}$$

has an asymptotically unstable singularity at the origin.

We try to determine a Liapunov function for the linear system (3.71) and assume a quadratic form

$$V(x_{1/2}, y_{1/2}) = ax_{1/2}^2 + 2bx_{1/2}y_{1/2} + cy_{1/2}^2 \tag{3.72}$$

The unknown coefficients a, b, and c will be determined in such a way that $dV/d\tau$ is a positive definite function of the form

$$\frac{dV}{d\tau} = 2(x_{1/2}^2 + y_{1/2}^2) \tag{3.73}$$

From Eqs. (3.71), (3.72) and (3.73), we obtain

$$a = \frac{1}{\Delta}\left[(D - \frac{1}{2}\beta A)D + \sigma_{1/2}^2\right]$$

$$b = -\frac{1}{\Delta}\frac{1}{2}\beta A\,\sigma_{1/2} \qquad (3.74)$$

$$c = \frac{1}{\Delta}\left[(D + \frac{1}{2}\beta A)D + \sigma_{1/2}^2\right]$$

where $$\Delta = (D^2 - \frac{1}{4}\beta^2 A^2 + \sigma_{1/2}^2)D$$

Then, using Eqs. (3.52), we obtain

$$\frac{dV}{d\tau} = \frac{\partial V}{\partial x_{1/2}}\cdot\frac{dx_{1/2}}{d\tau} + \frac{\partial V}{\partial y_{1/2}}\cdot\frac{dy_{1/2}}{d\tau} = 2r_{1/2}^2(1 - V)$$

so that the ellipse $V = 1$* represents a stable limit cycle to which neighboring integral curves tend asymptotically with increasing $\tau$. Using the values of the system parameters as mentioned above, we obtain, from Eq. (3.70), $T = 10.07 \cdots$ or equal to $45.9 \cdots$ times the period of the external force. An analytical expression for the limit cycle of Fig. 3.11a, derived from Eqs. (3.72) and (3.74), is

$$13.9\, x_{1/2}^2 - 17.9\, x_{1/2}y_{1/2} + 10.4\, y_{1/2}^2 = 1$$

The waveform of the almost periodic oscillation, calculated from the limit cycle, is shown in Fig. 3.11b.

Figure 3.12a shows an example of the limit cycle of Eqs. (3.68). The amplitude $B$ and the frequency $\nu$ of the external force are given by

$$B = 6.7 \qquad \text{and} \qquad \nu = 2.85$$

which are located just outside the region of 1/3-harmonic entrainment (see Fig.

---

* It is not difficult to show that $a > 0$, $c > 0$ and $ac - b^2 > 0$; hence $V$ is positive definite.

3.1b). The period required for the representative point to complete one revolution along the limit cycle is 67.1 ··· times the period of the external force. Figure 3.12b shows the waveform of the almost periodic oscillation represented by the limit cycle. The details of the singular points in Figs. 3.11a and 3.12a are readily known and are summed up in Table 3.4.

Table 3.4. Singular points in Figs. 3.11a and 3.12a

| Singular point | $x_n$ | $y_n$ | $\lambda_1, \lambda_2$ | Classification |
|---|---|---|---|---|
| Fig. 3.11a | 0 | 0 | $0.187 \pm 0.624i$ | Unstable focus |
| Fig. 3.12a | 0 | 0 | $0.410 \pm 0.684i$ | Unstable focus |

(c) Transition between Entrained Oscillations and Almost Periodic Oscillations

We shall investigate the behavior of integral curves of Eqs. (3.52) when the external force is given near the boundary of 1/2-harmonic entrainment. Three typical cases of integral curves are sketched in Fig. 3.13; namely, a, b, and c, are such cases that B and $\nu$ of the external force are prescribed inside, on the boundary of, and outside the region of 1/2-harmonic entrainment. Singularities 1 and 2 in Fig. 3.13a are stable nodes correlated with entrained oscillations. Singularities 3 and 4 are saddles which are intrinsically unstable. The origin is an unstable node. Therefore any integral curve will tend either to 1 or 2, depending on the location of the initial point from which the integral curve has started. In Fig. 3.13b two singular points coalesce so as to form a singularity of a higher order. Such singularities, 1 and 2, are of the node-saddle type. The representative point on the closed trajectory may stay for a moment at one of these singularities; but, when affected by a slight disturbance, the point will move to the other singularity in the direction of arrows. The limit cycle in Fig. 3.13c is correlated with an almost periodic oscillation.

Proceeding in the same manner as above, integral curves of Eqs. (3.53) are plotted in Fig. 3.14. The singularities are equidistant and equiangular about the origin. In Fig. 3.14a singularities 1, 2, and 3 are correlated with entrained oscillations of the 1/3-harmonic frequency, while singularities 4, 5, 6, and the origin are unstable. In Fig. 3.14b the coalescence of singular points occurs resulting in the node-saddle distribution of integral curves near the singularities. The limit cycle in Fig. 3.14c is correlated with an almost periodic oscillation.

## 3.7 Digital-Computer Analysis

In the preceding sections we investigated the almost periodic oscillations on the basis of the derived autonomous systems. In this section we examine these results by using the KDC-1 digital computer.

The method of analysis is similar to that we have used in Secs. 1.6 and 2.5; that is, the second-order differential equation (3.2) can be rewritten as the simultaneous equations of the first order

$$\begin{aligned} \frac{dv}{dt} &= \dot{v} \\ \frac{d\dot{v}}{dt} &= \mu\,(1 - \beta v - \gamma v^2)\dot{v} - v + B \cos \nu t \end{aligned} \qquad (3.75)$$

We consider the invariant curve [21, pp. 63-65] under the mapping in the $v\dot{v}$ plane; that is, the curve composed of the locus of the images. The mapping from $t = 2n\pi/\nu$ to $2(n + 1)\pi/\nu$, where $n = 0, 1, 2, \cdots$ is considered, since the right sides of Eqs. (3.75) are periodic functions in t of period $2\pi/\nu$.

When the amplitude B and frequency $\nu$ of the external force are prescribed outside the regions of entrainment, the point $P_n(v(2n\pi/\nu), \dot{v}(2n\pi/\nu))$ does not get to a stable fixed (or periodic) point, but moves permanently and generates a closed invariant curve, which corresponds to an almost periodic oscillation.* The state of closed invariant curve is analogous to limit cycle in the xy plane.

We show some examples of closed invariant curves of Eq. (3.75) for several combinations of B and $\nu$, and compare the results with those obtained in the preceding sections.

(a) Almost Periodic Oscillation Which Develops from Harmonic Entrainment

We consider the case when the amplitude B and frequency $\nu$ of the external force are prescribed just outside the region of harmonic entrainment.

A numerical analysis of the system (3.75) was carried out for the external force as given by

$$B = 0.2 \qquad \text{and} \qquad \nu = 1.1$$

which are the same as those we have used in Fig. 3.5. The system parameters in Eqs. (3.75) are the same as those in the preceding sections; i.e.,

$$\mu = 0.15 \qquad \beta = 4/3 \qquad \text{and} \qquad \gamma = 4/3$$

After a long period of time t, a point $P_n(v(2n\pi/\nu), \dot{v}(2n\pi/\nu))$ moves along the closed invariant curve as illustrated in Fig. 3.15. The small circles on the curves represent an example of the time intervals which are $2\pi/\nu$ or equal to

---

* Strictly speaking we cannot see with mathematical rigor that an almost periodic oscillation is whether a periodic oscillation with large period or a nonperiodic oscillation. At this point, however, we regard an almost periodic oscillation as a nonperiodic oscillation.

one period of the external force. The period required for the point $P_n$ to complete one revolution along the closed invariant curve is 11.4 ··· times the period of the external force. In performing the numerical integration of Eqs. (3.75), we used the Runge-Kutta-Gill's method (with the step h equal to $\pi/12\nu$).

The closed curve converted from the limit cycle of Fig. 3.5a is also shown (by dotted line) in the figure. It is obtained by the following relations [cf. Eq. (3.20)].

$$v = a_0 y_1 \qquad \dot{v} = a_0\left(\nu x_1 + \frac{dy_1}{dt}\right) \doteqdot a_0 \nu x_1 \tag{3.76}$$

One sees in the figure that these two closed curves show fairly good accordance; thus, the expression (3.20) for the almost periodic oscillation is considered to be legitimate.

(b) Almost Periodic Oscillations Which Develop from Higher-Harmonic Entrainment

Figures 3.16 and 3.17 show the closed invariant curves of Eqs. (3.75) with the external forces as given by

$$B = 0.8 \qquad \text{and} \qquad \nu = 0.47 \qquad \text{for Fig. 3.16}$$

$$B = 1.0 \qquad \text{and} \qquad \nu = 0.345 \qquad \text{for Fig. 3.17}$$

which correspond to Figs. 3.9a and 3.10a, respectively. The system parameters are the same as before. The periods required for the point $P_n$ to complete one revolution along the closed invariant curves of Figs. 3.15 and 3.16 are 9.9 ··· and 8.1 ··· times the period of the external force, respectively. Closed curves converted from the limit cycles of Figs. 3.9a and 3.10a are also shown by dotted lines. They are obtained by the following relations [cf. Eq. (3.43)].

$$\begin{aligned} &v = A + a_0 y_n \qquad \dot{v} = a_0\left(n\nu x_n + \frac{dy_n}{dt}\right) \doteqdot a_0 n \nu x_n \\ &\text{where} \qquad A = B/(1 - \nu^2) \qquad \text{and} \qquad n = 2 \text{ or } 3 \end{aligned} \tag{3.77}$$

One sees in the figures that in both cases there are considerable discrepancies between the full and dotted lines.

(c) Almost Periodic Oscillations Which Develop from Subharmonic Entrainment

Figures 3.18 and 3.19 show the closed invariant curves of Eqs. (3.75) with the external forces as given by

$$B = 4.0 \qquad \text{and} \qquad \nu = 2.15 \qquad \text{for Fig. 3.18}$$

$$B = 6.7 \qquad \text{and} \qquad \nu = 2.85 \qquad \text{for Fig. 3.19}$$

which correspond to Figs. 3.11a and 3.12a, respectively. The system parameters are the same as before. The small circles on the curves indicate the courses of the successive mapping: that is, initial point (marked by the number 0 in the figure) is transferred in turn to the points marked by the natural number in succession. Thus the time intervals between two successive points on the closed invariant curves are the integral multiples of the period of the external force; i.e., $4\pi/\nu$ and $6\pi/\nu$ for Figs. 3.18 and 3.19, respectively. The periods required for the point $P_n$ to complete one revolution along the closed invariant curves of Figs. 3.18 and 3.19 are about 41 and 72 times the period of the external force, respectively. Closed curves converted from the limit cycles of Fig. 3.11a and 3.12a are also shown by dotted lines. They are obtained by the following relations [cf. Eq. (3.51)].

$$v = A + a_0 y_n \qquad \dot{v} = a_0\left(n\nu x_n + \frac{dy_n}{dt}\right) \fallingdotseq a_0 n\nu x_n \tag{3.78}$$

where $\quad A = B/(1 - \nu^2) \qquad \text{and} \qquad n = 1/2 \text{ or } 1/3$

One sees in the figures that in both cases two closed curves (drawn by full and dotted lines) show fairly good accordance.

## 3.8 Concluding Remarks

Almost periodic oscillations which occur in a self-oscillatory system under a periodic force have been investigated by making use of the method of variation of parameters which assume the slowly varying amplitude and phase of the oscillation. When the amplitude and frequency of the external force are prescribed close to the regions of harmonic and subharmonic entrainment, this approximate method furnishes a fairly good description of the almost periodic oscillation. But when the external force is given close to the regions of higher-harmonic entrainment, this method brings less satisfactory results as we saw in Sec. 3.7b. This fact results from the form of approximate solution as given by Eq. (3.43). If we consider higher-harmonic components moreover, results will be improved. However, this method becomes practically inapplicable, since the analysis is compelled to resort to the graphical solution in a higher-dimensional state space. In addition when the external force is given just between but not near the regions of entrainment, the analysis does not account for very well, because the assumption that the amplitude and phase of the oscillation vary slowly does not hold. The method of combination oscillations which consist of two simple harmonic components, one with the natural frequency of the system and the other with the driving frequency [24, pp. 163-171], is useful under such situation.

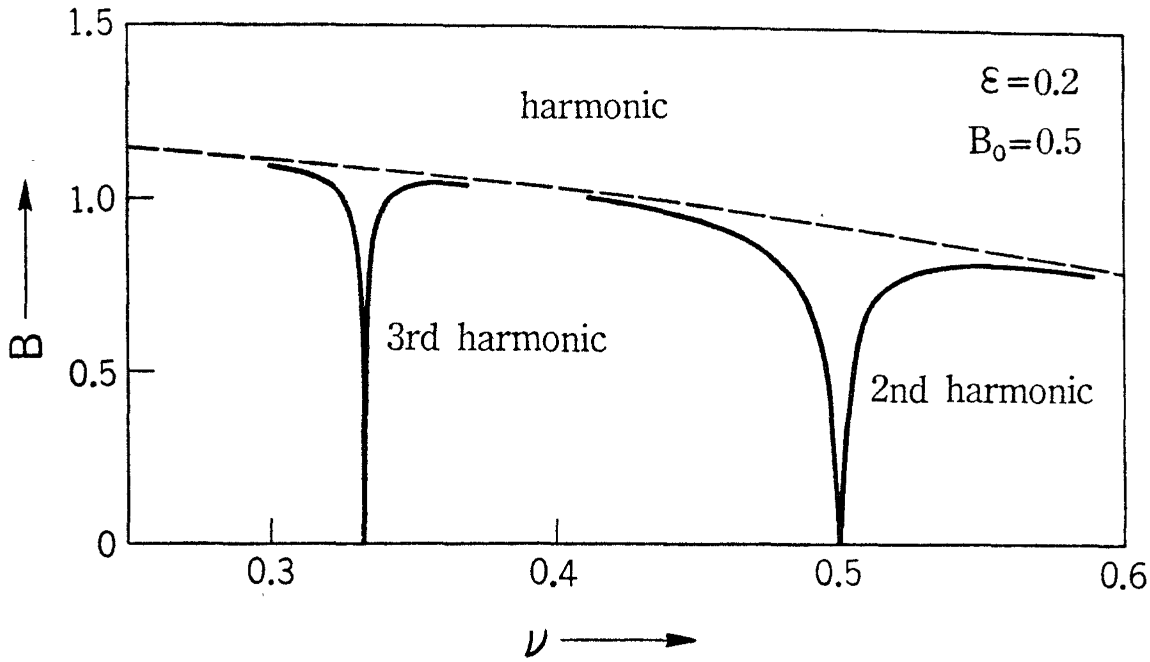


(a) Harmonic and higher-harmonic entrainments.

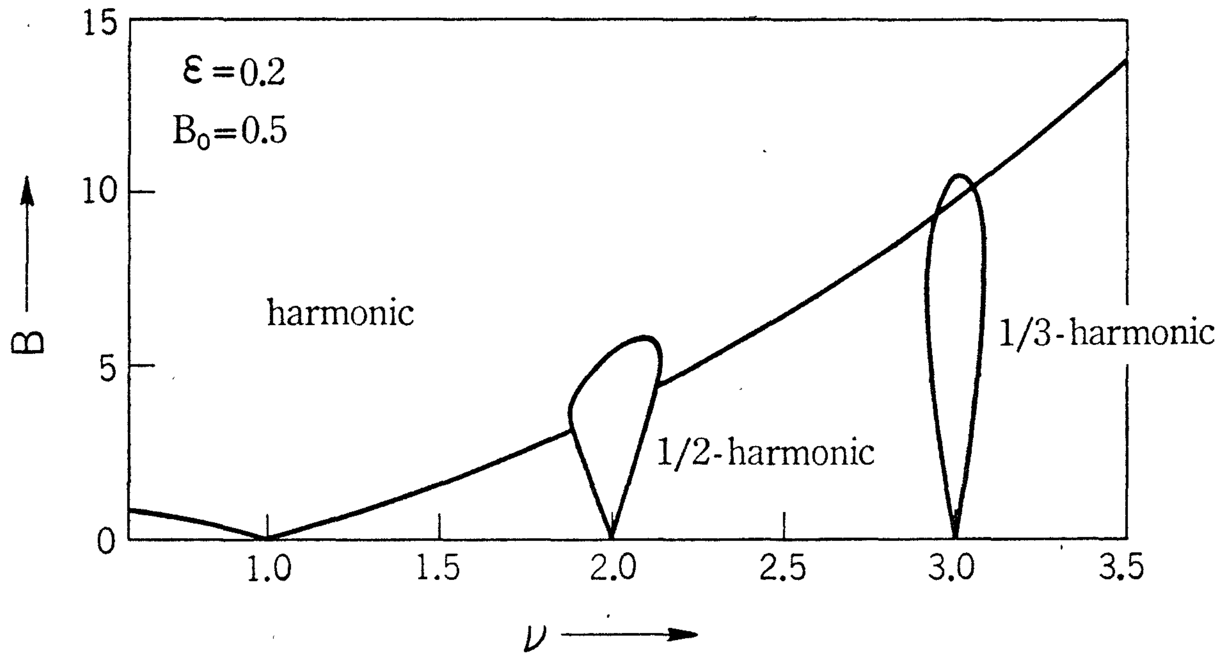


(b) Harmonic and subharmonic entrainments.

Fig. 3.1. Regions of frequency entrainment.

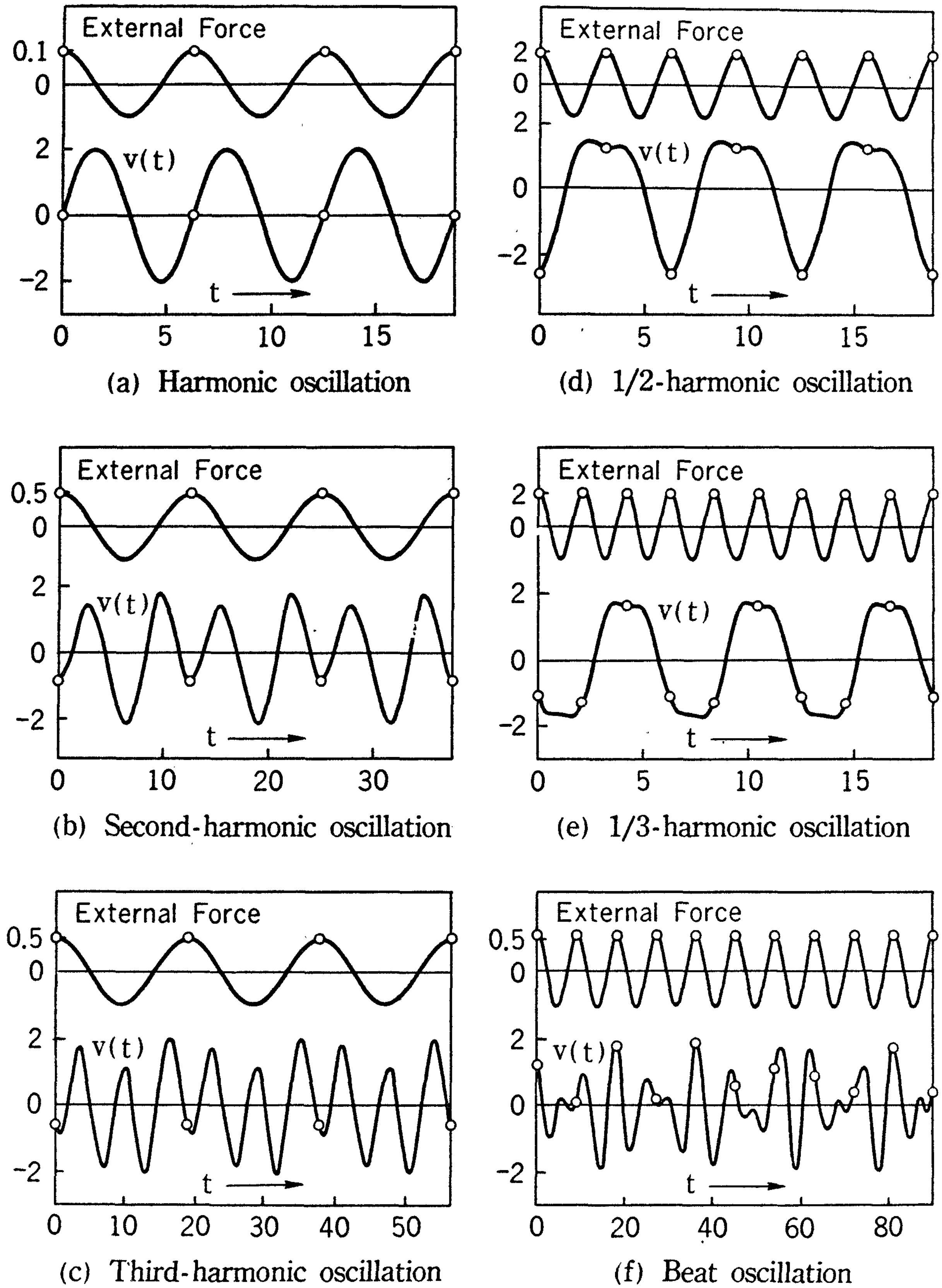


Fig. 3.2. Waveforms of the oscillations in the system described by Eq. (3.2) (obtained by analog-computer analysis).

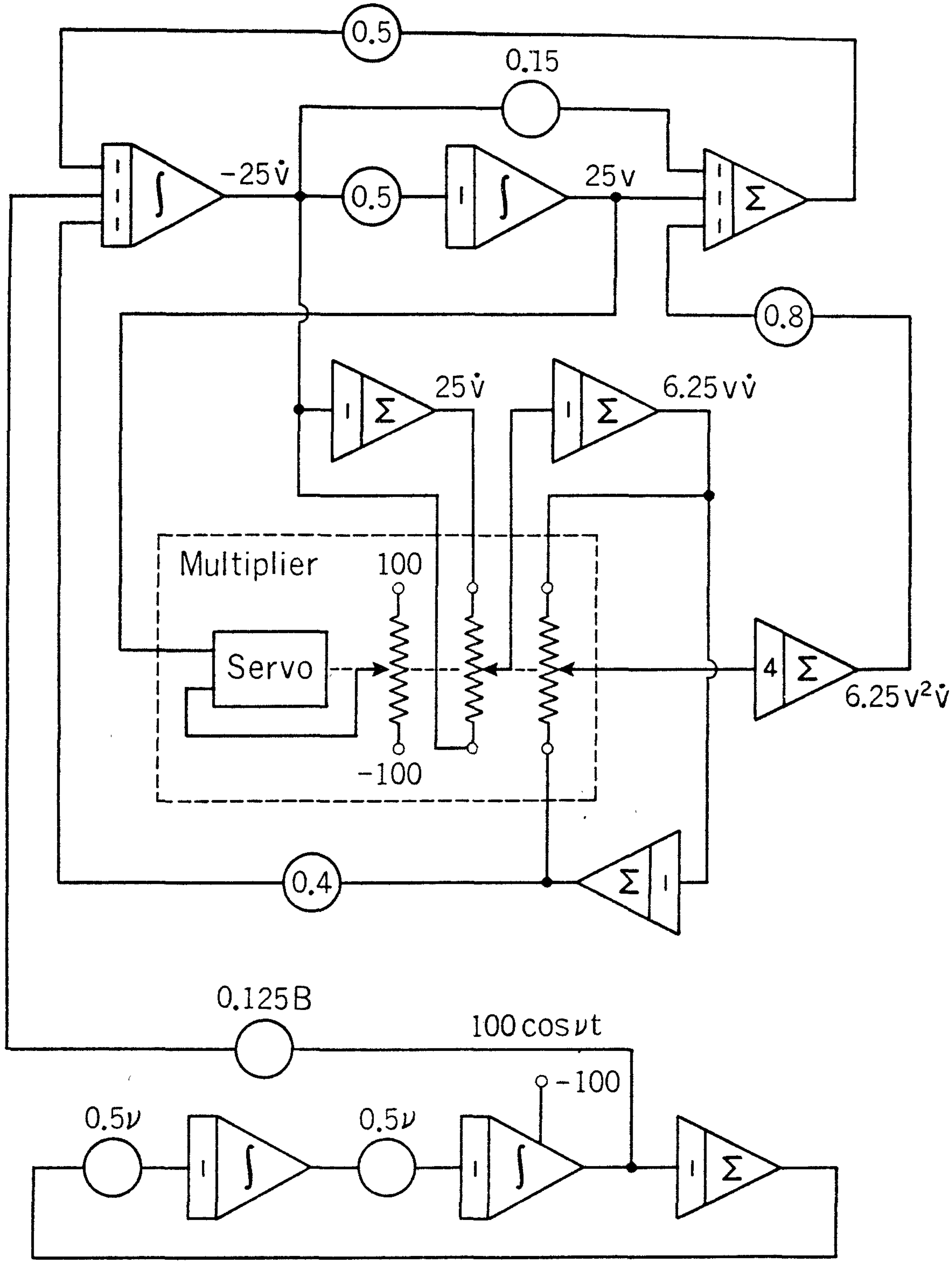


Fig. 3.3. Computer block diagram for Eq. (3.2).

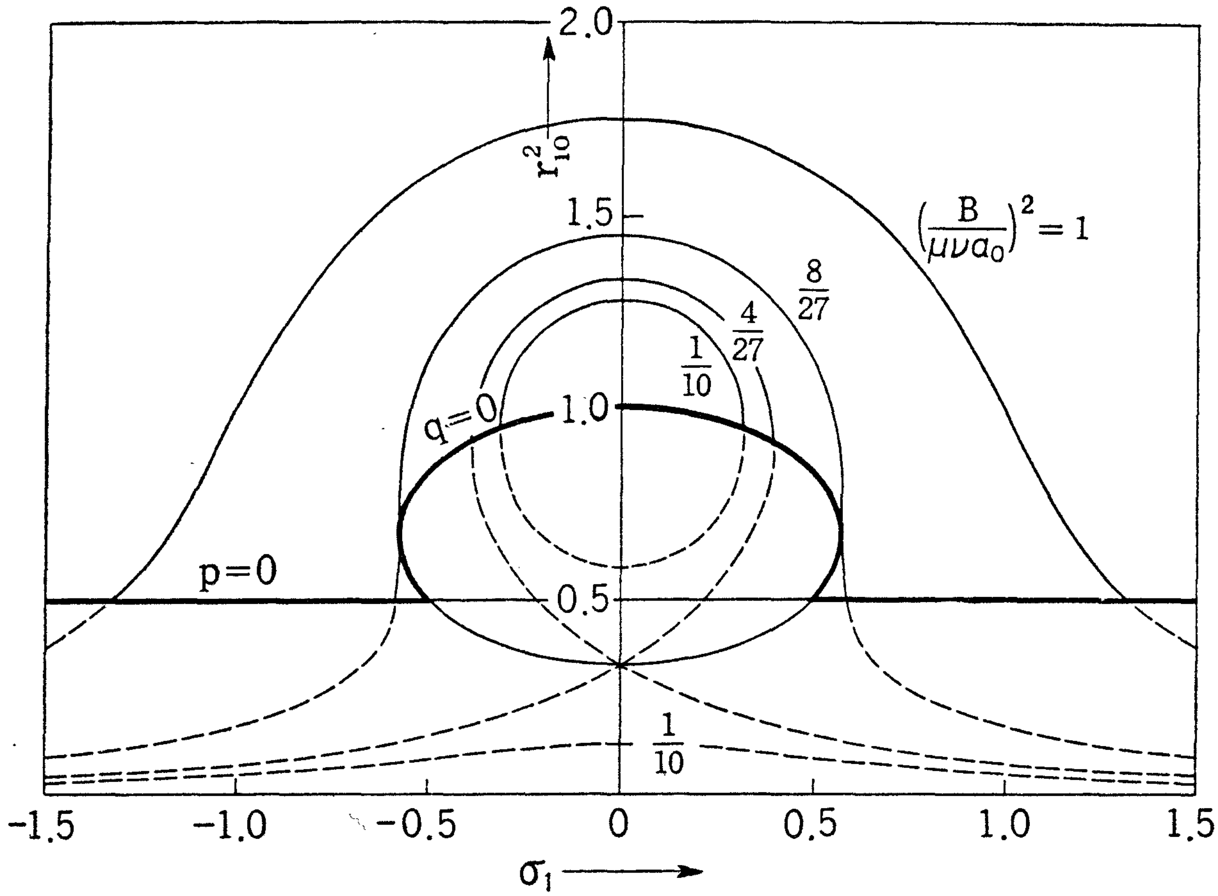


Fig. 3.4. Normalized response curves for the harmonic oscillation.

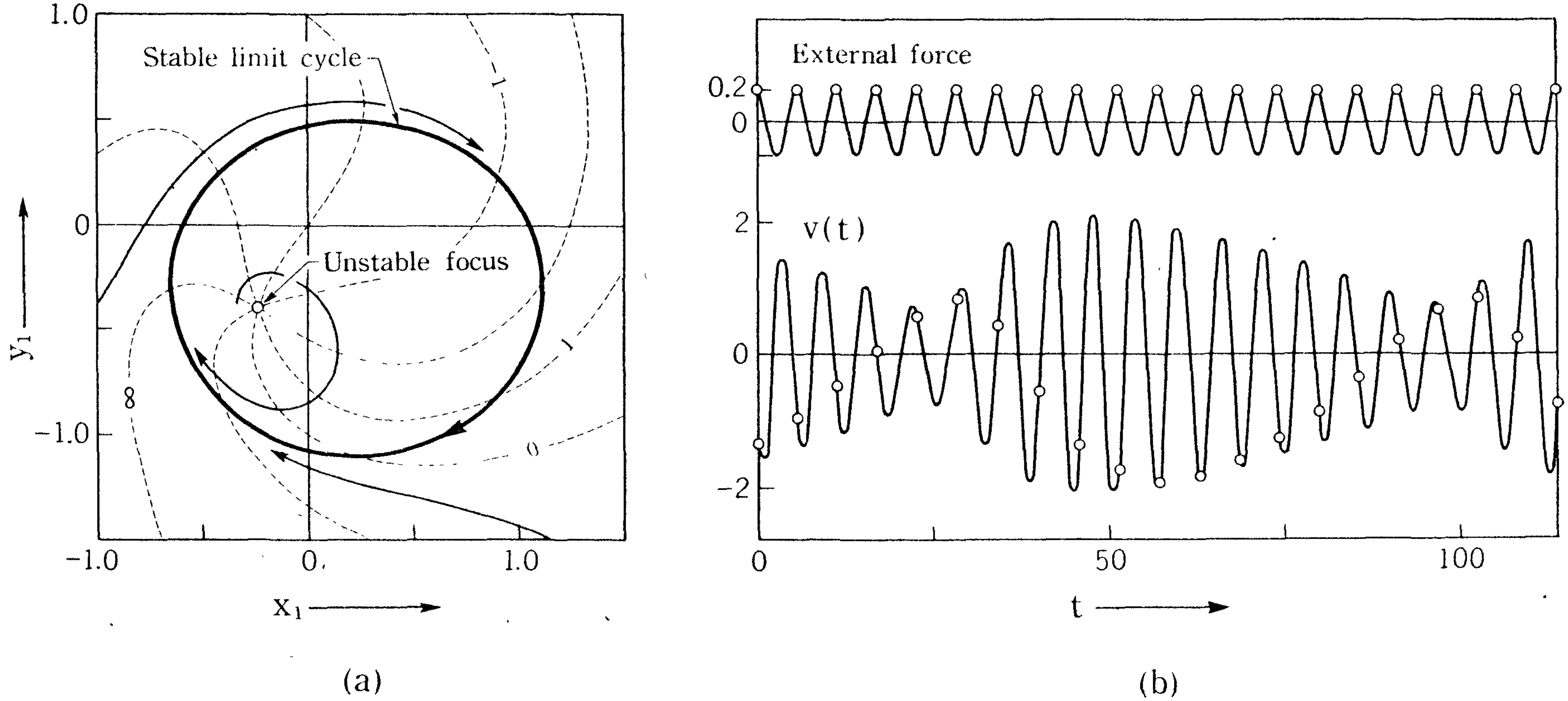


Fig. 3.5. Almost periodic oscillation which develops from the harmonic oscillation. (a) Limit cycle representing the almost periodic oscillation. (b) Waveform of the almost periodic oscillation.

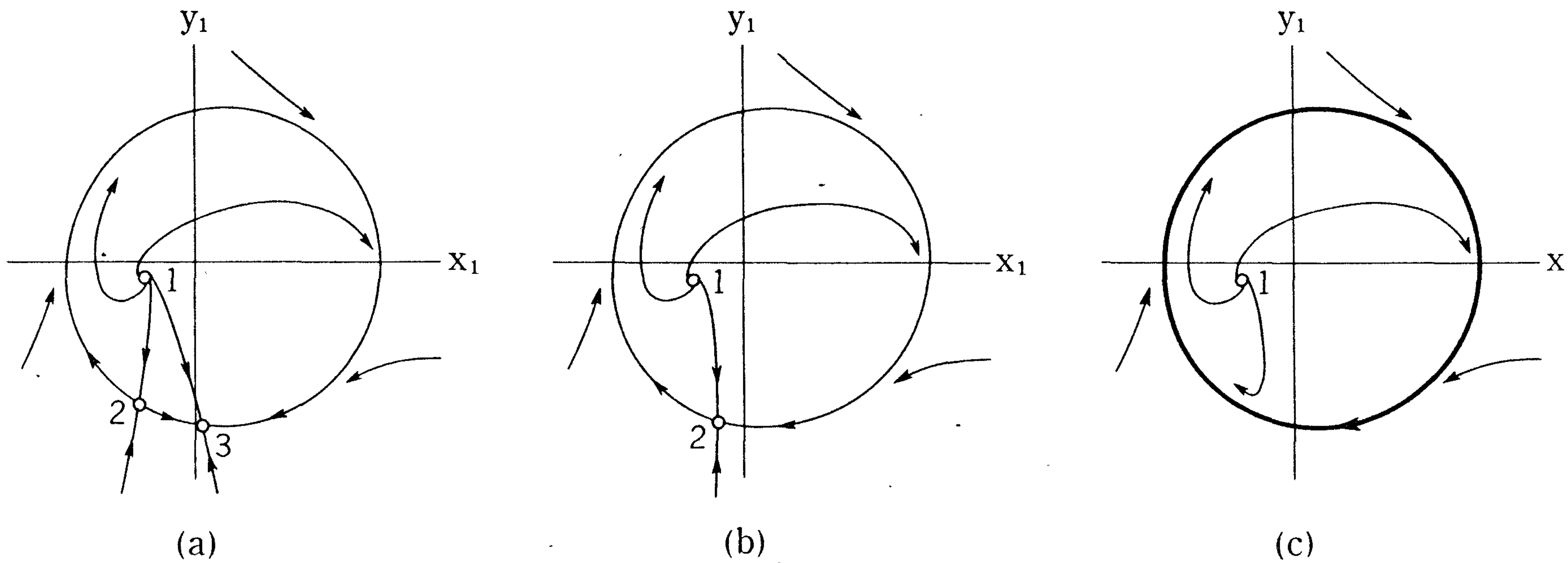


Fig. 3.6. Transition between entrained oscillation and almost periodic oscillation for small detuning. (a) Singularities representing the harmonic oscillations. (b) Coalescence of singularities at the boundary of entrainment. (c) Limit cycle representing the almost periodic oscillation.

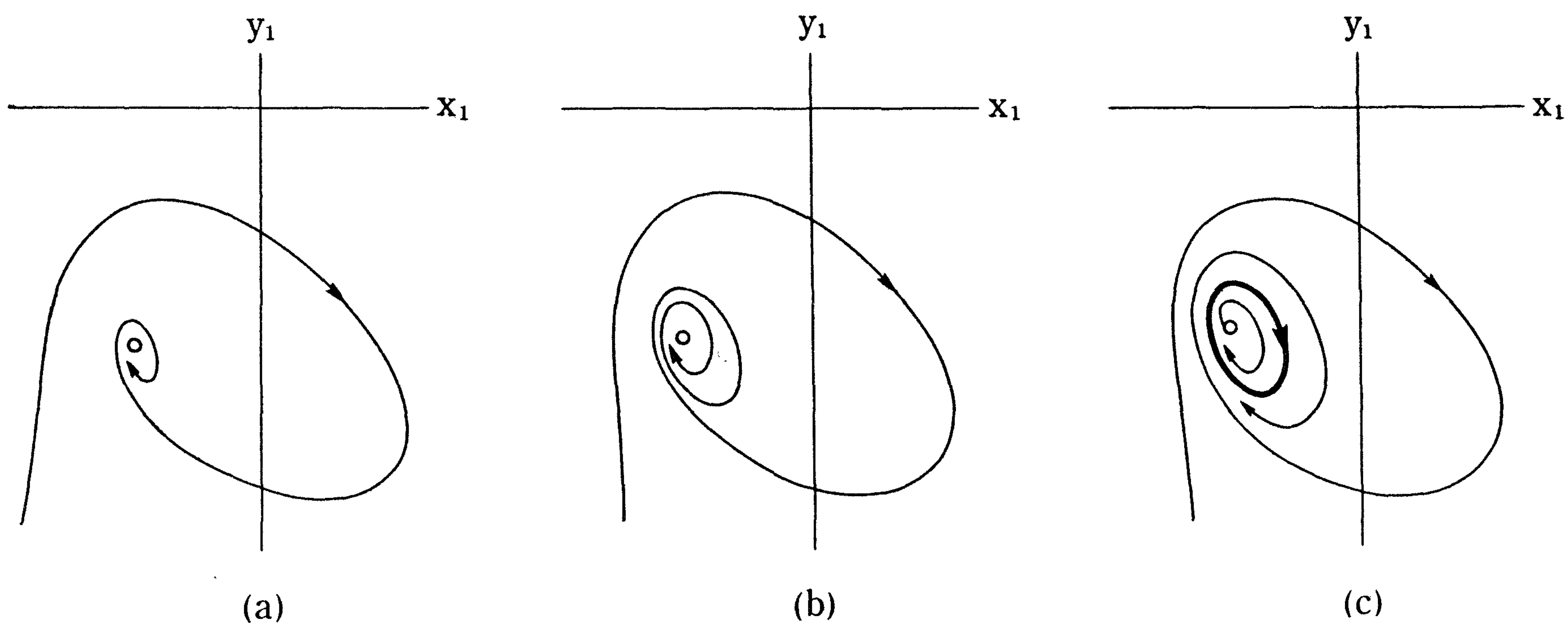


Fig. 3.7. Transition between entrained oscillation and almost periodic oscillation for large detuning. (a) Singularity representing the harmonic oscillation. (b) Singularity of the focus type at the boundary of entrainment. (c) Limit cycle representing the almost periodic oscillation.

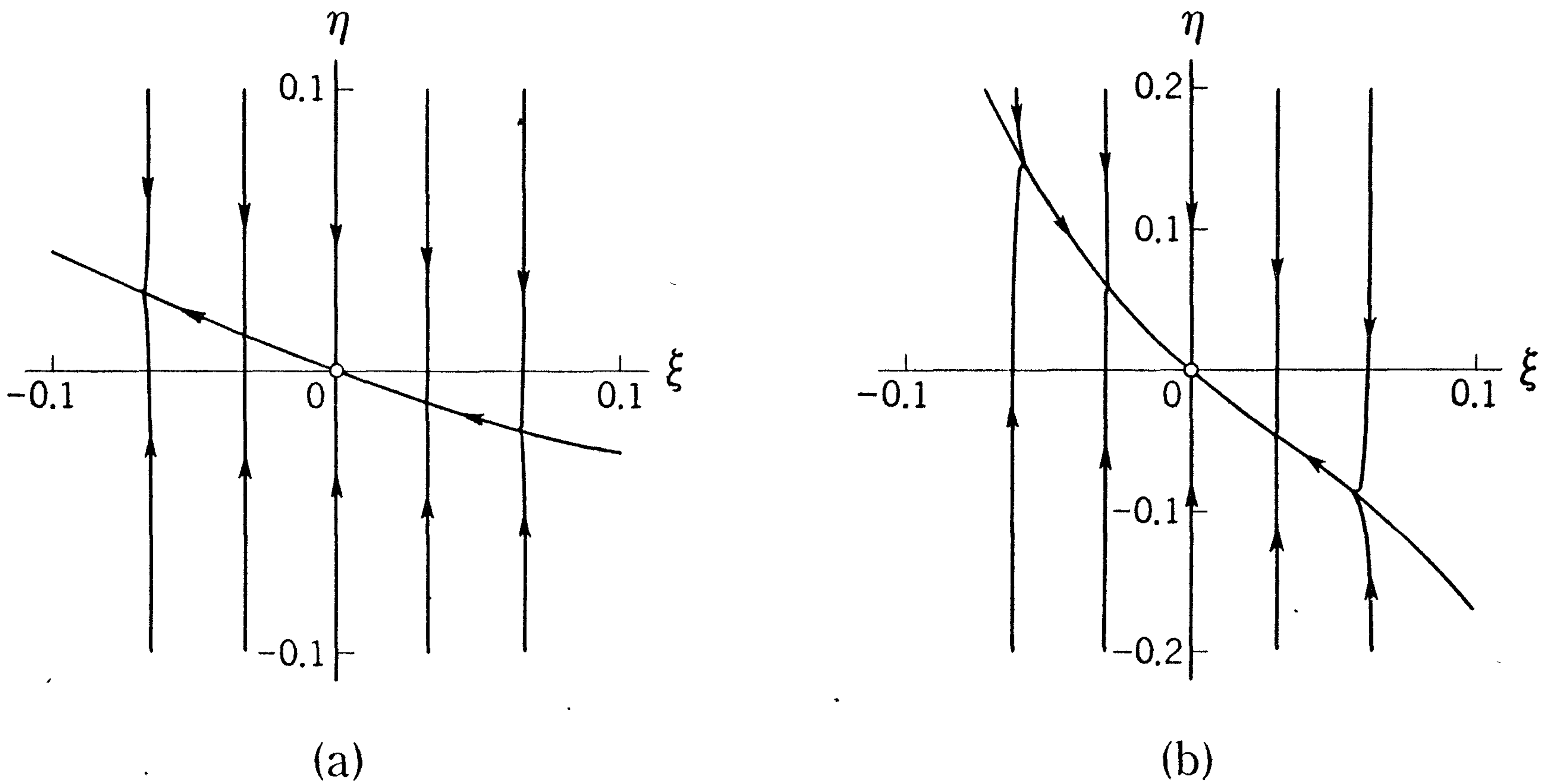


Fig. 3.8. Coalescence of singular points at the boundary of harmonic entrainment. (a) Node-saddle distribution of integral curves near the singularity. (b) Nodal distribution of integral curves near the singularity.

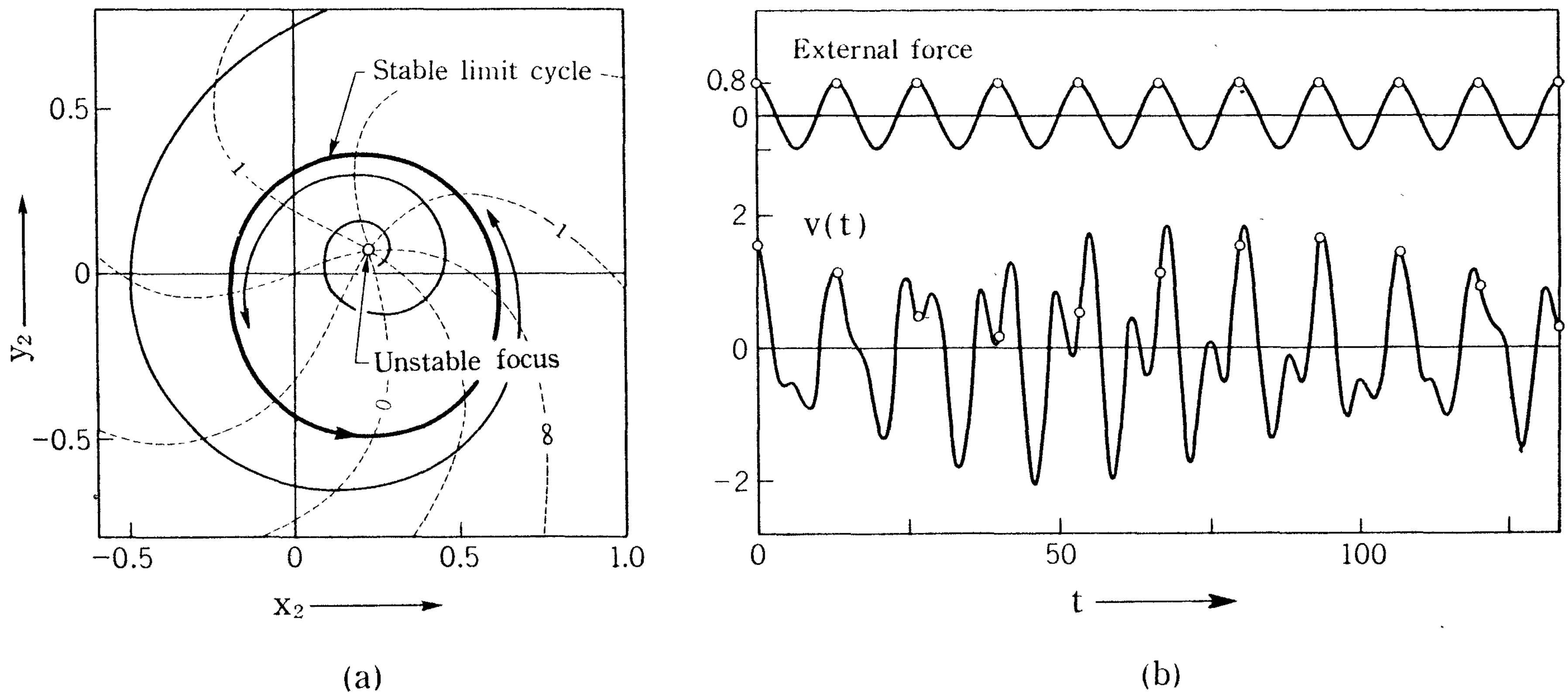


Fig. 3.9. Almost periodic oscillation which develops from the second-harmonic oscillation. (a) Limit cycle representing the almost periodic oscillation. (b) Waveform of the almost periodic oscillation.

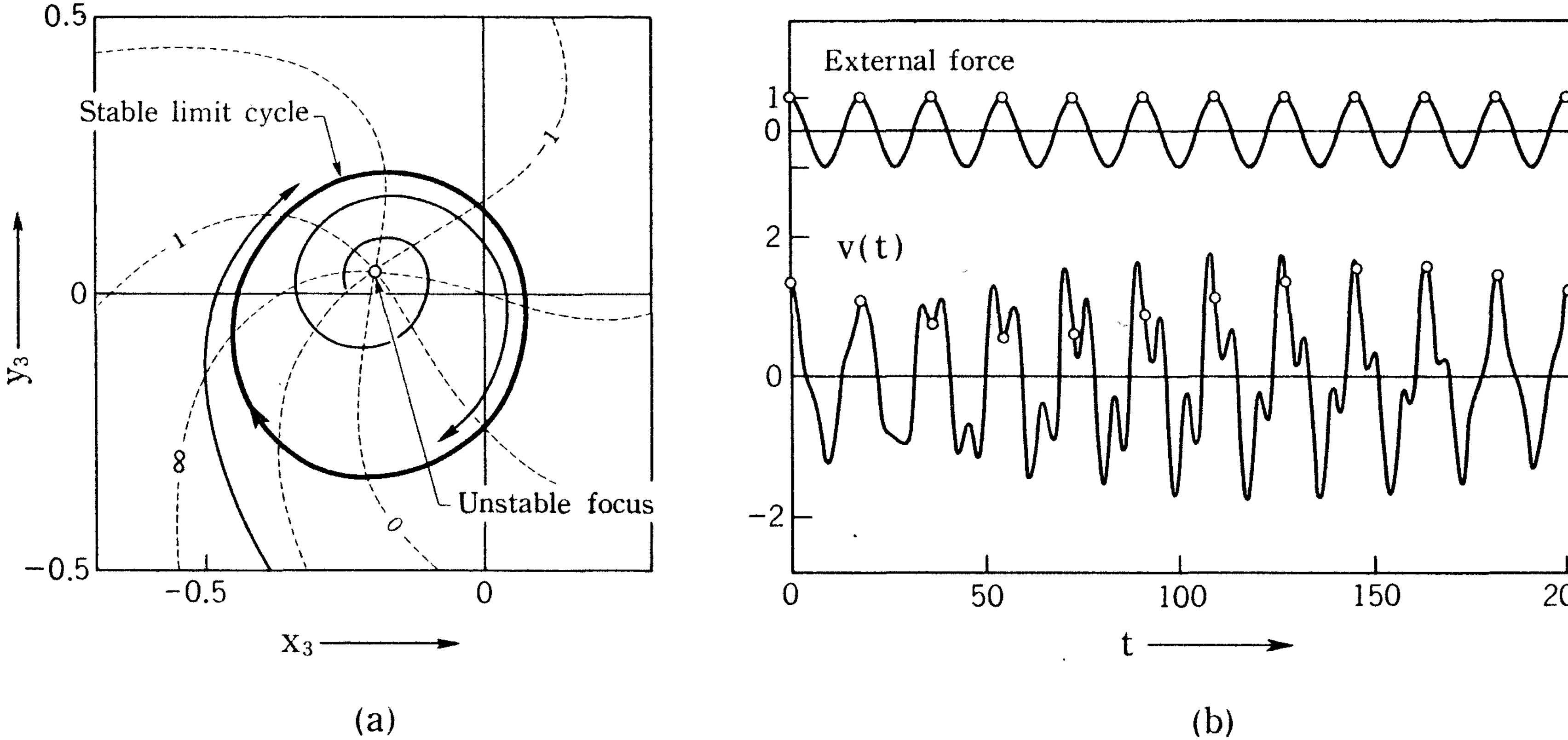


Fig. 3.10. Almost periodic oscillation which develops from the third-harmonic oscillation. (a) Limit cycle representing the almost periodic oscillation. (b) Waveform of the almost periodic oscillation.

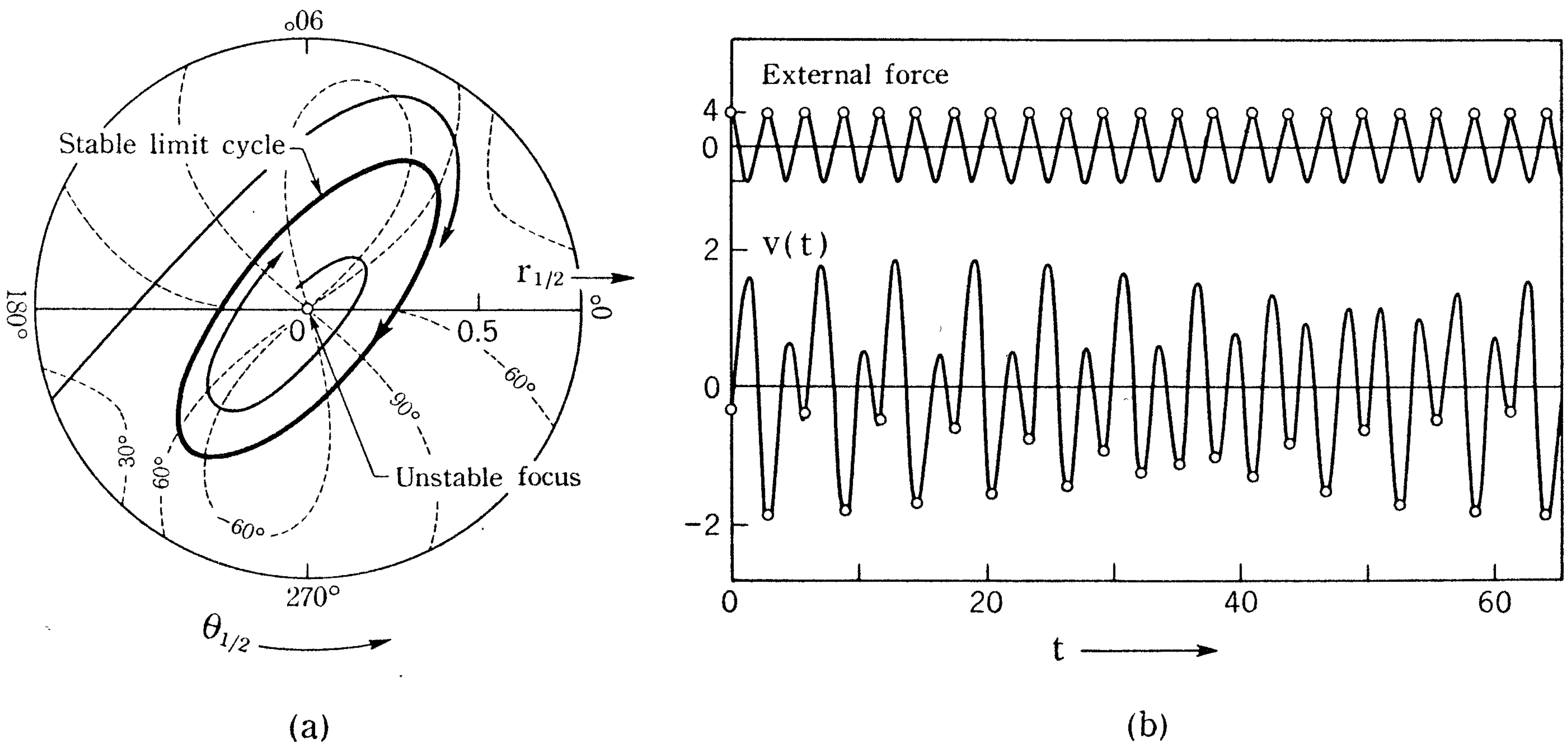


Fig. 3.11. Almost periodic oscillation which develops from the subharmonic oscillation of order 1/2. (a) Limit cycle representing the almost periodic oscillation. (b) Waveform of the almost periodic oscillation.

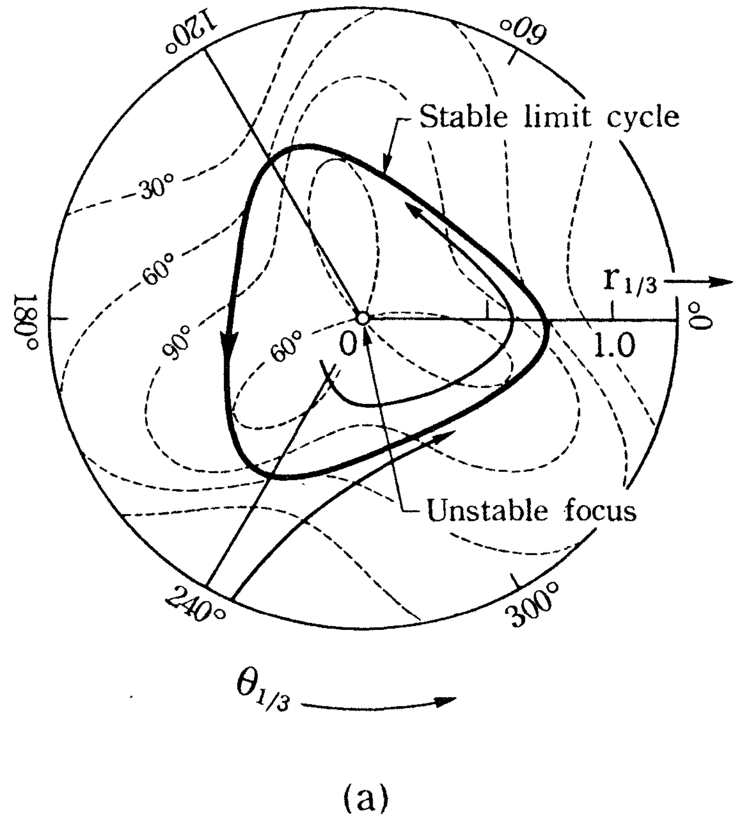


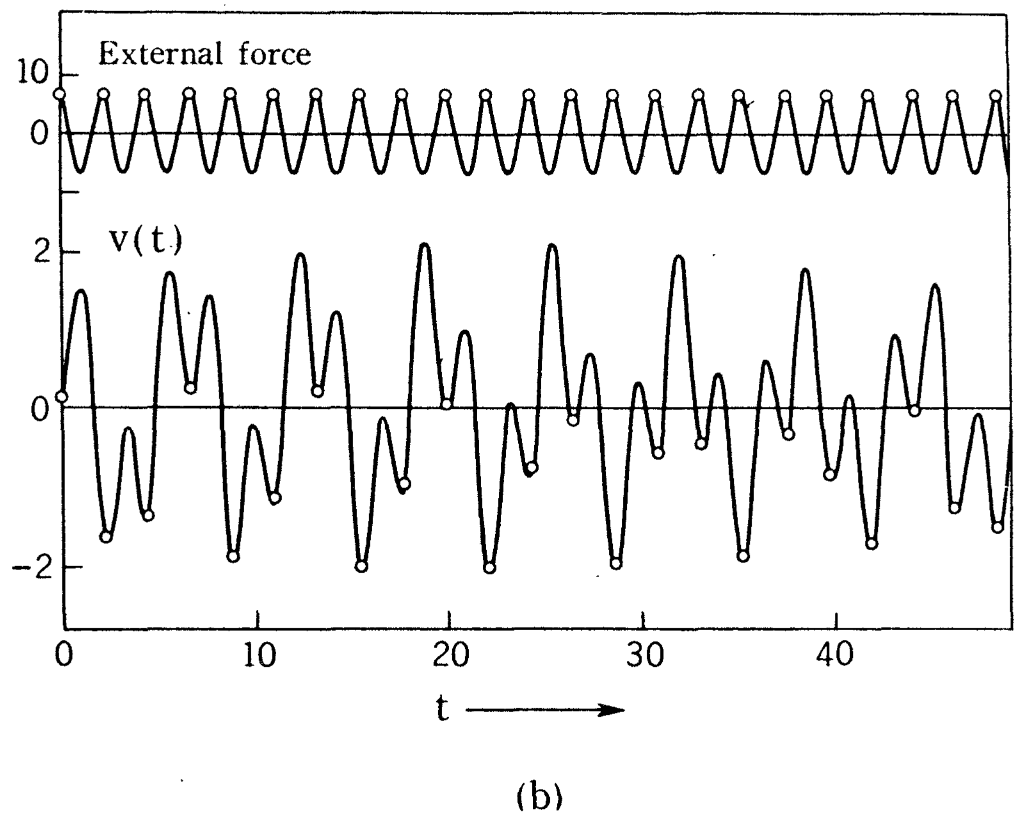


Fig. 3.12. Almost periodic oscillation which develops from the subharmonic oscillation of order 1/3. (a) Limit cycle representing the almost periodic oscillation. (b) Waveform of the almost periodic oscillation.

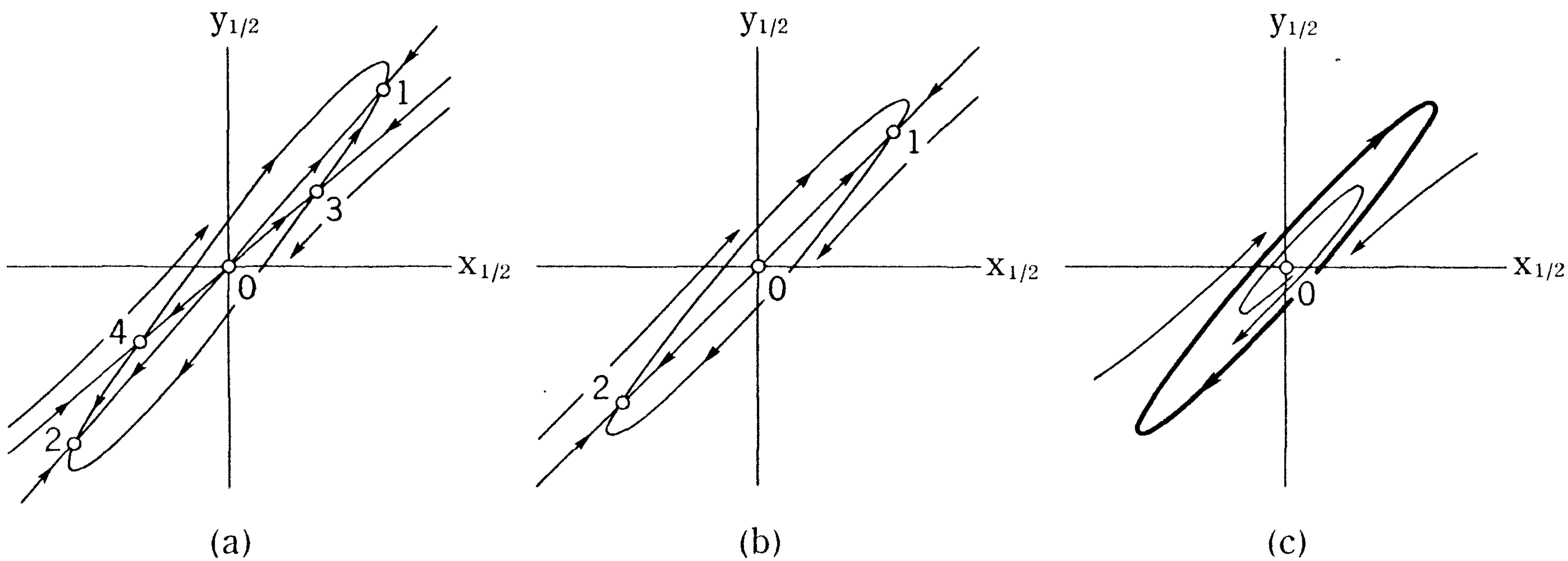


Fig. 3.13. Transition between entrained oscillation and almost periodic oscillation. (a) Singularities representing the subharmonic oscillations of order 1/2. (b) Coalescence of singularities at the boundary of entrainment. (c) Limit cycle representing the almost periodic oscillation.

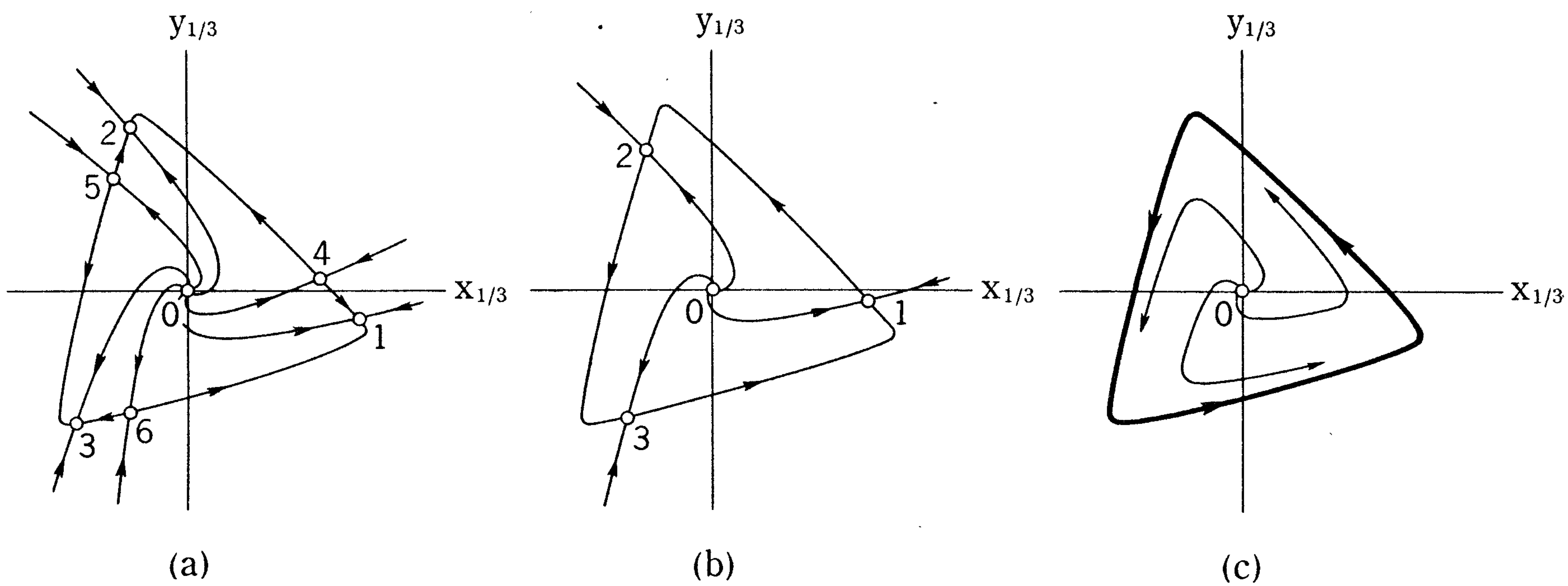


Fig. 3.14. Transition between entrained oscillation and almost periodic oscillation. (a) Singularities representing the subharmonic oscillations of order 1/3. (b) Coalescence of singularities at the boundary of entrainment. (c) Limit cycle representing the almost periodic oscillation.

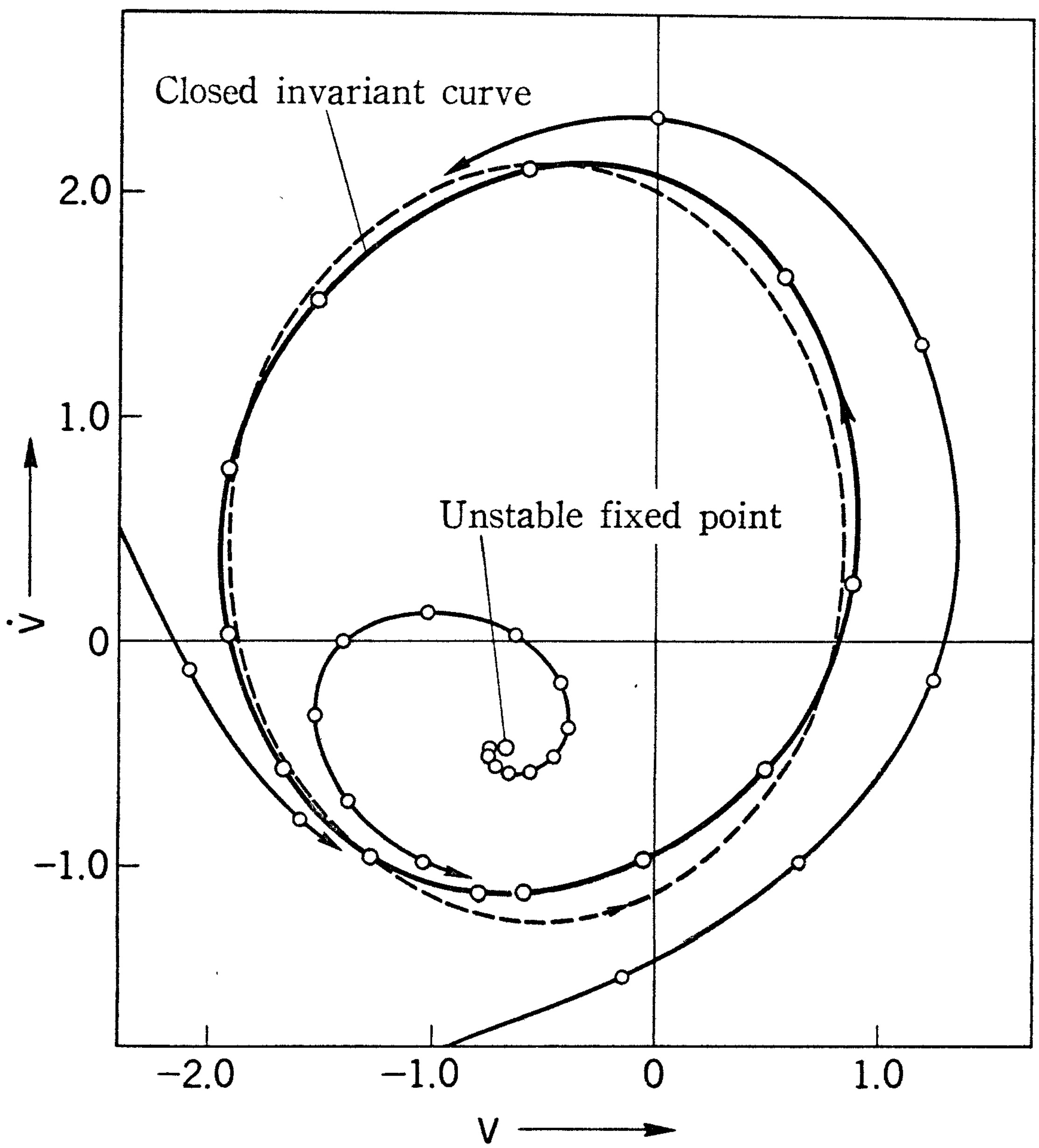


Fig. 3.13. The loci of image points and closed invariant curve.

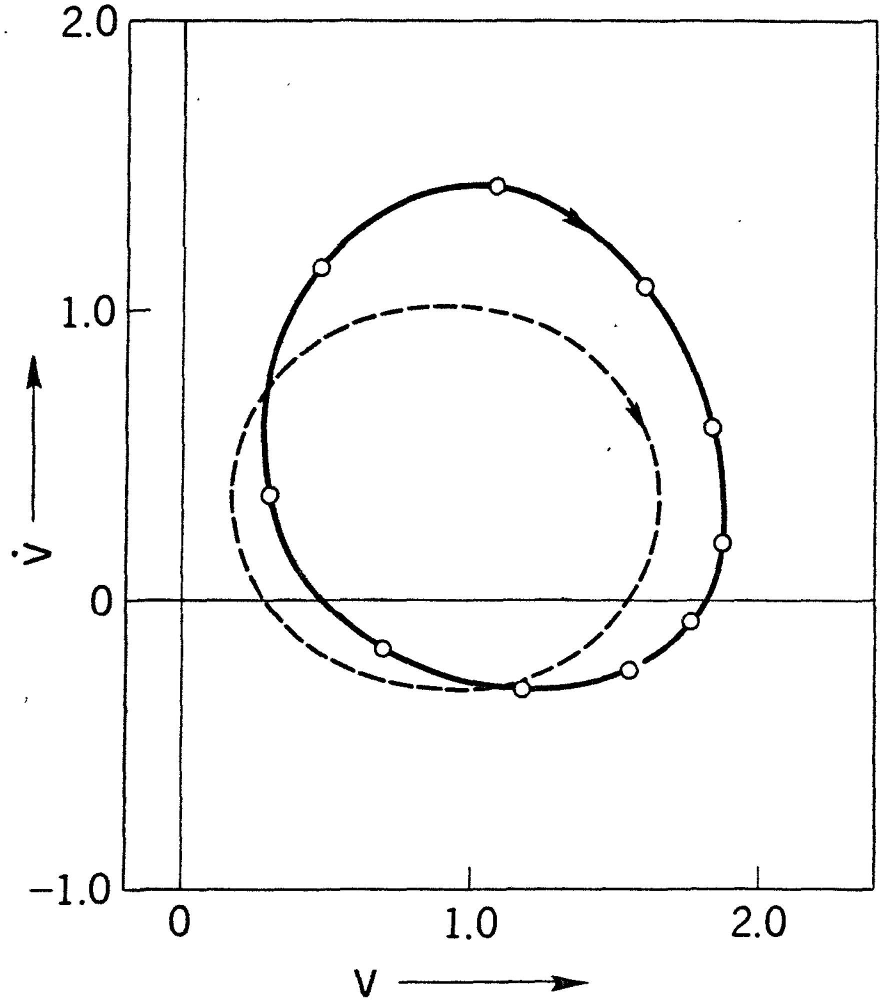


Fig. 3.16. Closed invariant curve of Eqs. (3.75) in the case where B = 0.8 and $\nu$ = 0.47.

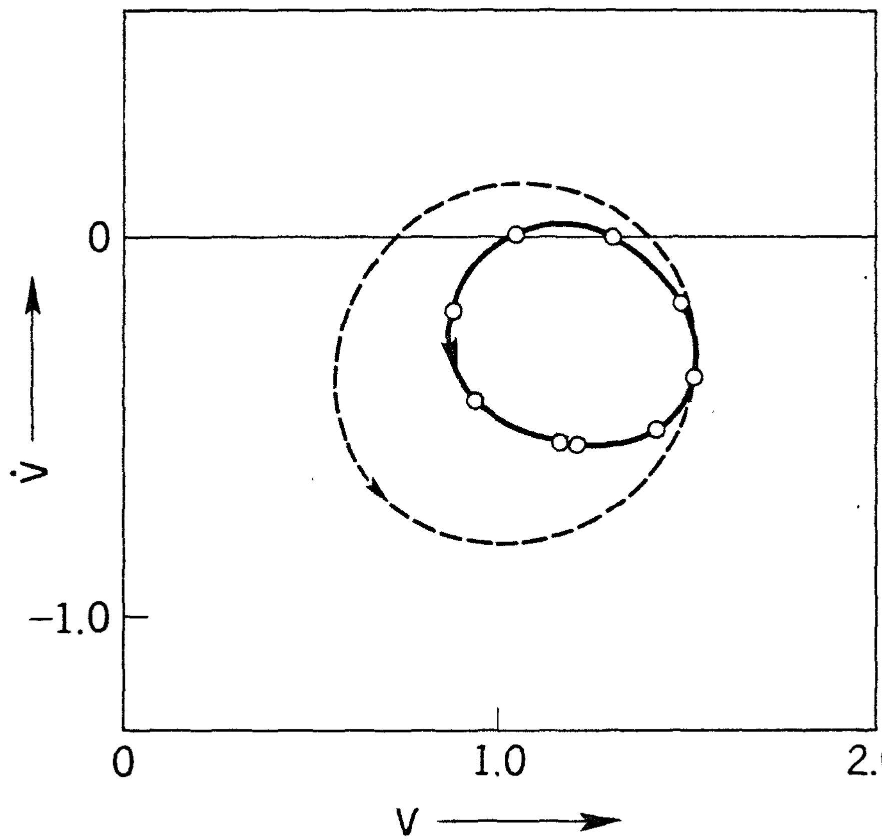


Fig. 3.17. Closed invariant curve of Eqs. (3.75) in the case where B = 1.0 and $\nu$ = 0.345.

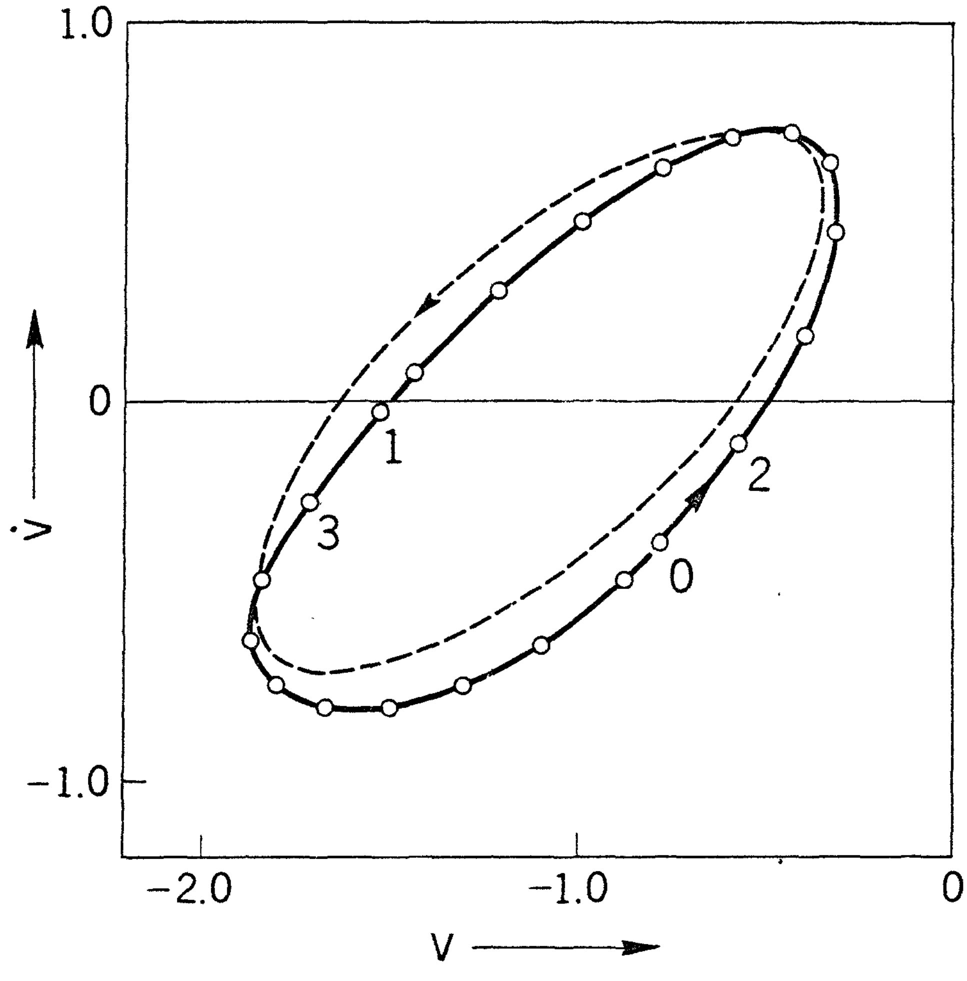


Fig. 3.18. Closed invariant curve of Eqs. (3.75) in the case where B = 4.0 and $\nu$ = 2.15.

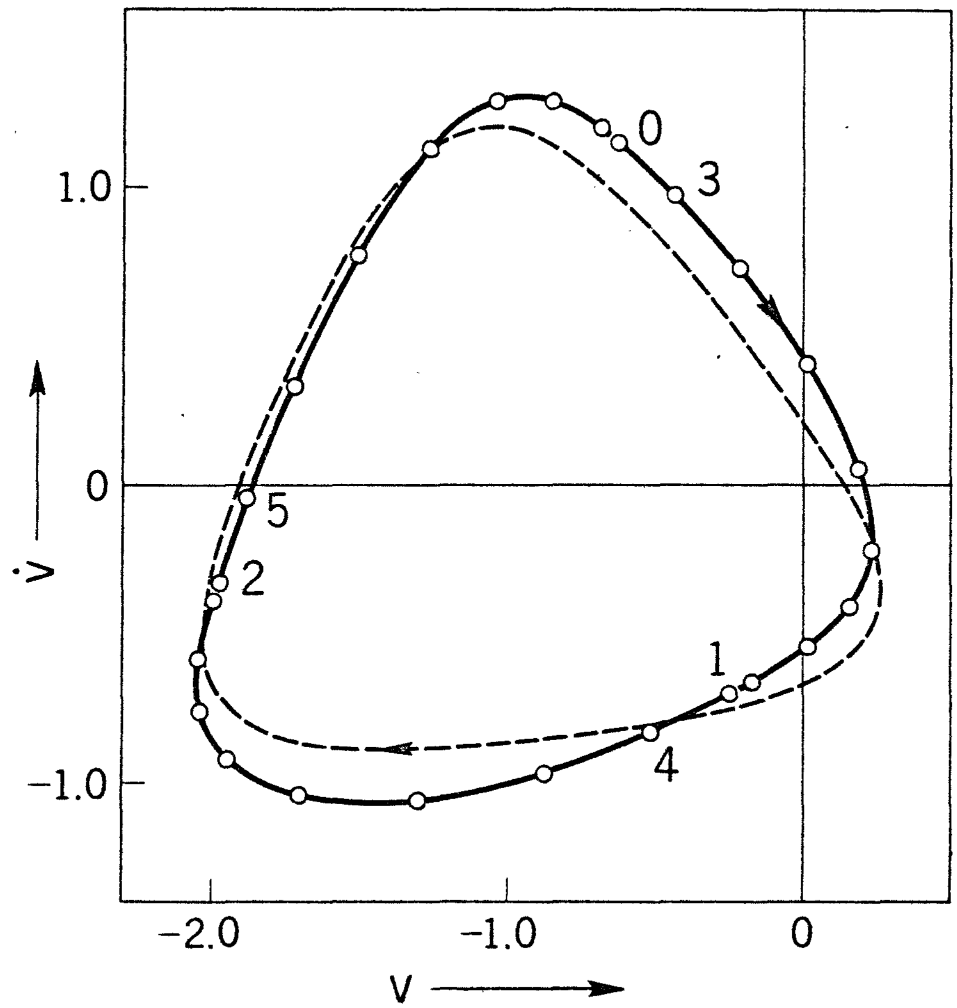


Fig. 3.19. Closed invariant curve of Eqs. (3.75) in the case where B = 6.7 and $\nu$ = 2.85.

## CHAPTER 4

## SELF-OSCILLATORY SYSTEM WITH NONLINEAR RESTORING FORCE

### 4.1 Introduction

In the preceding chapter we treated the problem in which the damping of the system was nonlinear. In this chapter we consider a problem in which both the damping and the restoring force are nonlinear; that is, a system governed by the differential equation

$$\frac{d^2v}{dt^2} - \mu\,(1 - \gamma v^2)\,\frac{dv}{dt} + v^3 = B \cos \nu t \tag{4.1}$$

where $\mu$ is a small positive constant and $\gamma$ is positive also and $B \cos \nu t$ represents a forcing function.

In the preceding analysis we overlooked the case where both the entrained and almost periodic oscillations occur even for the same values of the external forces, since such a range of the external forces is extremely narrow. On the other hand in the system described by Eq. (4.1) the response curves are skewed by the nonlinear restoring force as one will see later. From this standpoint it may be conjectured that such a range of the external forces becomes broader than that of before. Therefore we consider a particular case in which two types of steady-state responses occur depending only on different values of the initial conditions. Special attention is directed toward the transition between entrained oscillations and almost periodic oscillations which occurs under such circumstances. The method of analysis is much the same as we have used in the foregoing chapter.

## 4.2 Harmonic Oscillations

We shall, in this section, deal with the harmonic entrainment and the transition between entrained and almost periodic oscillations.

### (a) Fundamental Equations

When no external force is applied to the system, a free oscillation is self-excited. To find the ultimate amplitude and frequency of the oscillation, we put, to a first approximation,

$$v(t) = a_0 \cos \omega_0 t \tag{4.2}$$

and substitute this into Eq. (4.1) with $B = 0$. Then, equating the coefficients of the terms containing $\sin \omega_0 t$ and $\cos \omega_0 t$ separately to zero, we obtain

$$a_0^2 = \frac{4}{\gamma} \qquad \omega_0^2 = \frac{3}{4} a_0^2 = \frac{3}{\gamma} \tag{4.3}$$

We see that the natural frequency $\omega_0$ of the system is proportional to the amplitude $a_0$ of the free oscillation. These results due to the presence of nonlinear restoring force.

When the external force with the frequency $\nu$ being nearly equal to $\omega_0$ is present, the entrained harmonic oscillation or the almost periodic oscillation which develops from harmonic entrainment occurs depending on the value of B. Hence we assume the approximate solution of the form

$$v(t) = b_1(t) \sin \nu t + b_2(t) \cos \nu t \tag{4.4}$$

where $b_1(t)$, $b_2(t)$ become constants for entrained oscillations and slowly varying functions of the time t for almost periodic oscillations.

Proceeding analogously as in Sec. 3.3a, we shall derive the relations which determine the time-varying coefficients, $b_1(t)$ and $b_2(t)$, in the above solution. Thus we substitute Eq. (4.4) into (4.1) and equate the coefficients of the terms containing $\cos \nu t$ and $\sin \nu t$ separately to zero. The result is

$$\begin{aligned} \frac{dx_1}{d\tau} &= (1 - r_1^2)x_1 - \sigma_1 y_1 + \frac{B}{\mu\nu a_0} \equiv X_1(x_1,y_1) \\ \frac{dy_1}{d\tau} &= \sigma_1 x_1 + (1 - r_1^2)y_1 \equiv Y_1(x_1,y_1) \end{aligned} \tag{4.5}$$

where

$$\begin{aligned} &x_1 = \frac{b_1}{a_0} \qquad y_1 = \frac{b_2}{a_0} \qquad r_1^2 = x_1^2 + y_1^2 \\ &a_0 = \sqrt{\frac{4}{\gamma}} \qquad \omega_0 = \sqrt{\frac{3}{\gamma}} \qquad \tau = \frac{\mu}{2} t \\ &\sigma_1 = \frac{\omega_0^2 r_1^2 - \nu^2}{\mu\nu} \; : \; \text{detuning} \end{aligned} \tag{4.6}$$

It should, however, be remembered that the same assumptions as those mentioned in Sec. 3.3a must be made for the derivation of Eqs. (4.5). Those equations have the same form as Eqs. (3.6), but it should be noted that the definition of the detuning $\sigma_1$ differs from that of in Eqs. (3.7). In this case, the detuning is a function of both the amplitude $r_1$ and the driving frequency $\nu$. This is a reasonable result since the natural frequency of the system is modified to $\omega_0 r_1$. Equations (4.5) serve as fundamental equations in studying almost periodic oscillations as well as entrained oscillations. The entrained harmonic oscillation is obtained by putting $dx_1/d\tau = 0$ and $dy_1/d\tau = 0$, i.e.,

$$X_1(x_1,y_1) = 0 \qquad Y_1(x_1,y_1) = 0 \tag{4.7}$$

Eliminating $x_1$ and $y_1$ from the above equations gives

$$[(1 - r_1^2)^2 + \sigma_1^2]\, r_1^2 = \left(\frac{B}{\mu\nu a_0}\right)^2 \tag{4.8}$$

The amplitudes $x_1$ and $y_1$, that is, the coordinates of the singular point, are given by

$$x_1 = -\frac{\mu\nu a_0}{B}(1 - r_1^2)r_1^2 \qquad y_1 = \frac{\mu\nu a_0}{B}\sigma_1 r_1^2 \tag{4.9}$$

Figure 4.1 shows the response curves as given by the Eq. (4.8) for the following values of the system parameters:

$$\mu = 0.2 \qquad \text{and} \qquad \gamma = 8$$

One sees that the response curves in the case of nonlinear restoring force could be thought of as arising from those for the linear case (see Fig. 3.4) by bending the latter to the right.

(b) Stability of the Singular Point Correlated with the Periodic Solution

Proceeding analogously as in Sec. 3.3b, we investigate the stability of the equilibrium state by considering the behavior of sufficiently small variations $\xi$ and $\eta$ from the singular point and determine whether these deviations approach zero or not with increase of $\tau$. The character of the integral curves near the singular point is to be determined by the following equations:

$$\frac{d\xi}{d\tau} = a_1\xi + a_2\eta \qquad \frac{d\eta}{d\tau} = b_1\xi + b_2\eta$$

with

$$\begin{aligned} a_1 &= \left(\frac{\partial X_1}{\partial x_1}\right)_0 = 1 - r_1^2 - 2x_1^2 - 2\frac{\omega_0^2}{\mu\nu}x_1y_1 \\ a_2 &= \left(\frac{\partial X_1}{\partial y_1}\right)_0 = -2x_1y_1 - \sigma_1 - 2\frac{\omega_0^2}{\mu\nu}y_1^2 \\ b_1 &= \left(\frac{\partial Y_1}{\partial x_1}\right)_0 = -2x_1y_1 + \sigma_1 + 2\frac{\omega_0^2}{\mu\nu}x_1^2 \\ b_2 &= \left(\frac{\partial Y_1}{\partial y_1}\right)_0 = 1 - r_1^2 - 2y_1^2 + 2\frac{\omega_0^2}{\mu\nu}x_1y_1 \end{aligned} \tag{4.10}$$

where $(\partial X_1/\partial x_1)_0$, ..., $(\partial Y_1/\partial y_1)_0$ stand for $\partial X_1/\partial x_1$, ..., $\partial Y_1/\partial y_1$ at the singular point. By making use of the Routh-Hurwitz's criterion, the conditions for stability of the singular point are given by

$$
\begin{aligned}
p &= -(a_1 + b_2) = 2(2r_1^2 - 1) > 0 \\
q &= a_1 b_2 - a_2 b_1 = (1 - r_1^2)(1 - 3r_1^2) + \sigma_1^2 + 2\,\frac{\omega_0^2}{\mu\nu}\,\sigma_1 r_1^2 > 0
\end{aligned}
\tag{4.11}
$$

The stability limits $p = 0$ and $q = 0$ are also shown in Fig. 4.1. Hence the dotted-line portions of the response curves are unstable. It is readily verified that the vertical tangencies of the response curves lie on the stability limit $q = 0$.

(c) Region of Harmonic Entrainment

From the results obtained in the preceding section, the region of harmonic entrainment is obtained on the $B\nu$ plane as illustrated in Fig. 4.2. On this plane each point $(\nu, B)$ represents a particular patterns of integral curves (i.e., the phase portrait) of Eqs. (4.5) on the $x_1 y_1$ plane. The number and character of the singularities is prescribed by the location of the point $(\nu, B)$. The boundary curve $BD\omega_0EA$ corresponds to the upper boundary of $q = 0$ in Fig. 4.1, and ACGB to the lower boundary of $q = 0$. For points on these boundaries, phase portrait has a higher-order singularity corresponding to a point on the stability limit $q = 0$ (cf. Sec. 3.4a). The boundary curve HDCF corresponds to the boundary of $p = 0$. It touches the curve BGA at the point C and $B\omega_0$ at D. The points C and D correspond to the intersection of $q = 0$ with $p = 0$ in Fig. 4.1. For points on the curve CD, the singularity on $p = 0$ is a saddle point within $q < 0$, and hence, this boundary curve has practically no significance. On the other hand, for points on the curves HD and CF, the singularity on $p = 0$ is a higher-order singularity representing the transition between a stable and unstable focus (cf. Sec. 3.4b).

From the above explanation, we see that when B and $\nu$ are in the region represented by the curvilinear triangle $\omega_0 AB$, Eqs. (4.5) have three singularities, one of which is a saddle point. Outside this region, there are only one stable or unstable singularity according as above or below the boundaries HG and EF. Hence in the regions represented by the curvilinear triangles ACE and BDG there are three singularities, one of which is a saddle point and the remaining two are the stable singularities in the region ACE and the unstable singularities in BDG. The region above the line $HD\omega_0 EF$ (drawn by thick line in the figure), therefore, becomes the region of harmonic entrainment since there are at least one stable singularity in the phase portrait.

(d) Example of the Phase Portrait

From the result above obtained, we see that if B and $\nu$ of the external force are prescribed outside the region of harmonic entrainment, Eqs. (4.5) have only unstable singularity. It will also be seen that, for large values of $x_1$ and $y_1$, the representative point on the integral curve will cross the family of concentric circles centered at the origin from the outside to the inside as $\tau$ increases. Hence the existence of a stable limit cycle in the $x_1 y_1$ plane may be concluded, which corresponds to an almost periodic oscillation. However, even if B and $\nu$ are given inside the region of harmonic entrainment, Eqs. (4.5) can possess a stable limit cycle in addition to a stable singular point for particular values of B and $\nu$.

Figure 4.3 shows an example of phase portrait of such a case. The amplitude B and the frequency $\nu$ of the external force are given by

$$B = 0.35 \qquad \text{and} \qquad \nu = 1$$

Table 4.1. Singular Points in Fig. 4.3

| Singular point | $x_1$ | $y_1$ | $\lambda_1, \lambda_2$ | $\mu_1, \mu_2$* | Classification |
|---|---|---|---|---|---|
| 1 | -0.086 | -0.546 | $0.39 \pm 3.80i$ | | Unstable focus |
| 2 | 0.536 | -1.212 | 0.87, -5.89 | 2.80, 0.09 | Saddle (unstable) |
| 3 | 1.571 | -0.255 | -1.11, -7.02 | 4.77,-2.54 | Stable node |

*$\mu_1, \mu_2$ are the tangential directions of the integral curves at the singular points.

which are located in the region of harmonic entrainment (see Fig. 4.2). The other system parameters are the same as in Sec. 4.2a. The details of the singularities in Fig. 4.3 are readily known and are listed in Table 4.1. We see in the figure a stable limit cycle which encircles the unstable focus 1. One of the integral curves (drawn by thick line in the figure) that contains the saddle point 2, that is, the separatrix, divides the whole plane into two regions, in one of which all integral curves tend to the limit cycle, while in the other to the nodal point 3. Thus both the almost periodic and entrained oscillations may occur in this system, which one it will be depending on the initial condition.

(e) Transition between Entrained Oscillations and Almost Periodic Oscillations

In the preceding section we showed the case in which both the entrained and the almost periodic oscillations occur depending only on different values of the initial conditions. Here we consider the transition between entrained oscillations and almost periodic oscillations which occurs under such circumstances.

Figure 4.4 shows an example of the amplitude characteristic (B vs. $r_1^2$) when

$\nu$ is kept constant (= 0.9). By making use of the stability conditions (4.11) we classified the singular points along the amplitude characteristic illustrated in Fig. 4.4. The results are listed in Table 4.2.

Table 4.2. Classification of singular points along the amplitude characteristic of Fig. 4.4

| Interval | p | q | $p^2 - 4q$ | Classification |
|---|---|---|---|---|
| oa | - | + | - | Unstable foci |
| ab | + | + | - | Stable foci |
| bc | + | + | + | Stable nodes |
| cd | + | - | + | Saddles (unstable) |
| de | + | + | + | Stable nodes |
| ef | + | + | - | Stable foci |

The occurrence and extinction of a limit cycle, as B varies along this characteristic, will most easily be understood by plotting the phase portraits of Eqs. (4.5) for various values of B. The results are shown in Fig. 4.5. When B is given below $B_1$ of Fig. 4.4, a limit cycle exists which encircles an unstable focal point. This state is shown in Fig. 4.5a. Coalescence of singularities appears at $B = B_1$. Further increase in B results in the separation of this higher-order singular point into two simple singular points, that is, the coexistence of a stable limit cycle and a stable node. When $B = B_2$, there exists a closed integral curve starting from the saddle point and coming back to the same point. The limit cycle disappears when B is increased beyond $B_2$. However, when B reaches $B_3$ the integral curves show the same behavior as in Fig. 4.5d.

A limit cycle appears once more for $B_3 < B < B_4$ and shrinks up to a stable focus at $B = B_4$ (cf. Sec. 3.4b). For values of B between $B_4$ and $B_5$, there exist two types of stable singularities, correlated with the resonant and non-resonant oscillations, but there is no limit cycle. The coalescence of singularities occurs at $B = B_5$ and then this higher-order singularity disappears. Hence it is concluded that an almost periodic oscillation occurs for $B < B_2$ and $B_3 < B < B_4$, a resonant oscillation for $B_1 < B$, and a nonresonant oscillation for $B_4 < B < B_5$.

Here we introduce the mean-square amplitude of the almost periodic oscillation defind by

$$\bar{r}_1^2 = \frac{1}{T}\oint_C r_1^2 d\tau \tag{4.12}$$

where C is an integration path being taken round the limit cycle and T is a period for the representative point $(x_1(\tau), y_1(\tau))$ to complete one revolution along the limit cycle. This mean-square amplitudes $\bar{r}_1^2$ of the almost periodic oscillation are plotted by chain lines in Fig. 4.6. The arrows in the figure show the transition of these oscillations. Thus we see that between $B_1$ and $B_2$ there exists hysteresis and at $B_3$ and $B_5$ jump phenomena take place from the lower to the higher branch.

It should also be mentioned that, for other values of the external forces, the situation may somewhat be different from that mentioned above. Under certain conditions (for example, for different values of $\nu$), an almost periodic oscillation occurs for any values of B below $B_4$, that is, chain lines are connected, or only for values below $B_1$ and between $B_3$ and $B_4$. In the latter case no hysteresis between $B_1$ and $B_2$ results, since the coalescence of singularities appears on the limit cycle (cf. Fig. 3.5b).

In this section we investigated the right hand transitional region as given by $\nu > \omega_0$, but for certain values of B and $\nu$, particularly in the neighborhood of the curvilinear triangle BGD in Fig. 4.2, some complicated phenomena may occur [6]. However, we shall not enter into this problem here, because such a region of the external forces is extremely narrow (cf. Chap. 5).

(f) Analog-Computer Analysis

In the preceding sections two types of steady-state responses and the transition between these were investigated on the basis of the derived autonomous system (4.5). In this section we examine these results by using an analog computer.

The solution of the original differential equation (4.1), i.e.,

$$\frac{d^2v}{dt^2} - \mu\,(1 - \gamma\,v^2)\,\frac{dv}{dt} + v^3 = B\cos\nu t$$

are sought for various combinations of B and $\nu$. The system parameters are the same as in Sec. 4.2a, i.e.,

$$\mu = 0.2 \qquad \text{and} \qquad \gamma = 8$$

The region of harmonic entrainment thus obtained is shown in Fig. 4.7. The lines in the figure show the boundaries of entrainment, or boundaries of different types of oscillations. The hatching area indicates the presence of an almost periodic oscillation in addition to an entrained oscillation. The other domains of the different types of oscillations are the same as already explained in Fig. 4.2 and should be self-explanatory. The result concerning hysteresis (cf. Fig. 4.6) is also confirmed.

4.3 Subharmonic Oscillations of Order 1/3

(a) Fundamental Equations

When the external force with the frequency $\nu$ being nearly equal to $3\omega_0$ is present, the entrained oscillation or the almost periodic oscillation which develops from 1/3-harmonic entrainment occurs depending on the value of B. We assume the approximate solution of the form

$$v(t) = A\cos\nu t + b_1(t)\sin\frac{1}{3}\nu t + b_2(t)\cos\frac{1}{3}\nu t \tag{4.13}$$

with

$$A = a_0 w = \frac{B}{\omega_0^2 w^2 - \nu^2}$$

where $b_1(t)$, $b_2(t)$ become constants for entrained oscillations and slowly varying functions of the time t for almost periodic oscillations.*

Proceeding analogously as before, we shall derive the relations which determine these time-varying coefficients, $b_1(t)$ and $b_2(t)$, in the above solutions. Thus we substitute the first equation of (4.13) into (4.1) and equate the coefficients of the terms containing $\cos\frac{1}{3}\nu t$ and $\sin\frac{1}{3}\nu t$ separately to zero. The result is

$$\begin{aligned}\frac{dx_{1/3}}{d\tau} &= (D - r_{1/3}^2)x_{1/3} - (\sigma_{1/3} + 6kw^2)y_{1/3}\\ &\quad + 3kw(x_{1/3}^2 - y_{1/3}^2) + 2wx_{1/3}y_{1/3} \equiv X_{1/3}(x_{1/3}, y_{1/3})\\ \frac{dy_{1/3}}{d} &= (\sigma_{1/3} + 6kw^2)x_{1/3} + (D - r_{1/3}^2)y_{1/3}\\ &\quad + w(x_{1/3}^2 - y_{1/3}^2) - 6kwx_{1/3}y_{1/3} \equiv Y_{1/3}(x_{1/3}, y_{1/3})\end{aligned} \tag{4.14}$$

where $\qquad x_{1/3} = \frac{b_1}{a_0} \qquad y_{1/3} = \frac{b_2}{a_0} \qquad r_{1/3}^2 = x_{1/3}^2 + y_{1/3}^2$

---

* The amplitude of the harmonic component in Eq. (4.13) is given by Eqs. (4.8) and (4.9), and this will be investigated in Sec. 4.3c.

$$a_0 = \sqrt{\frac{4}{\gamma}} \qquad \omega_0 = \sqrt{\frac{3}{\gamma}} \qquad \tau = \frac{\mu}{2} t$$

$$k = \frac{\omega_0^2}{\mu\nu} \qquad D = 1 - 2w^2 \qquad a_0 w = \frac{B}{\omega_0^2 w^2 - \nu^2} \tag{4.15}$$

$$\sigma_{1/3} = \frac{\omega_0^2 r_{1/3}^2 - (\nu/3)^2}{\mu\,(\nu/3)} \quad : \quad \text{detuning}$$

It should, however, be remembered that the same assumptions as those mentioned in Sec. 3.3a must be made for the derivation of Eqs. (4.14). The entrained 1/3-harmonic oscillation is obtained from Eqs. (4.14) by putting $dx_{1/3}/d\tau = 0$ and $dy_{1/3}/d\tau = 0$. From these relations, we can find the amplitude characteristic for the 1/3-harmonic oscillation, i.e.,

$$[(D - r_{1/3}^2)^2 + (\sigma_{1/3} + 6kw^2)^2 - (1 + 9k^2)w^2 r_{1/3}^2]\, r_{1/3}^2 = 0 \tag{4.16}$$

From the above relation, the amplitude of the 1/3-harmonic oscillation is found to be

$$r_{1/3}^2 = 0 \tag{4.17}$$

or

$$r_{1/3}^2 = D + \frac{1}{2}(1 + 9k^2)w^2 \pm \sqrt{[D + \frac{1}{2}(1 + 9k^2)w^2]^2 - D^2 - (\sigma_{1/3} + 6kw^2)^2} \tag{4.18}$$

When the amplitude $r_{1/3}$ is zero, no subharmonic response is obtained. Consequently, the approximate solution (4.13) has only the harmonic component. The amplitudes of the 1/3-harmonic component $x_{1/3}$ and $y_{1/3}$, that is, the coördinates of the singular points, are

$$x_{1/3} = r_{1/3}\cos\theta_{1/3} \qquad r_{1/3}\cos(\theta_{1/3} + \tfrac{2}{3}\pi) \qquad r_{1/3}\cos(\theta_{1/3} + \tfrac{4}{3}\pi)$$

$$y_{1/3} = r_{1/3}\sin\theta_{1/3} \qquad r_{1/3}\sin(\theta_{1/3} + \tfrac{2}{3}\pi) \qquad r_{1/3}\sin(\theta_{1/3} + \tfrac{4}{3}\pi)$$

where

$$\cos 3\theta_{1/3} = \frac{-3k(D - r_{1/3}^2) - (\sigma_{1/3} + 6kw^2)}{(1 + 9k^2)wr_{1/3}} \tag{4.19}$$

$$\sin 3\theta_{1/3} = \frac{3k(\sigma_{1/3} + 6kw^2) - (D - r_{1/3}^2)}{(1 + 9k^2)wr_{1/3}}$$

Proceeding analogously as before, the stability conditions for the singular points are as follows:

For $r_{1/3}^2 = 0$:

$$p_{1/3} = -2D > 0 \qquad q_{1/3} = D^2 + (\sigma_{1/3} + 6kw^2)^2 > 0 \tag{4.20}$$

For $r_{1/3}^2 \neq 0$:

$$p_{1/3} = 2(2r_{1/3}^2 - D) > 0$$

$$\begin{aligned} q_{1/3} = {} & (D - r_{1/3}^2)(D - 7r_{1/3}^2) + (\sigma_{1/3} + 6kw^2)^2 \\ & + 18k(\sigma_{1/3} + 6kw^2)r_{1/3}^2 - 4(1 + 9k^2)w^2r_{1/3}^2 > 0 \end{aligned} \tag{4.21}$$

(b) Region of 1/3-Harmonic Entrainment

From the above results, the region of 1/3-harmonic entrainment is obtained on the B$\nu$ plane as illustrated in Fig. 4.8. The system parameters are the same as those in the preceding sections. One sees that the region of 1/3-harmonic entrainment becomes broader than that of the linear case (see Fig. 3.1b). In the figure the boundary curve of the harmonic entrainment as given by $D = 0$ [see Eqs. (4.20)] is also shown.

The number and character of the singularities of the system (4.14) is prescribed by the location of the point $(\nu, B)$. When the amplitude B and frequency $\nu$ of the external force are given inside the region of 1/3-harmonic entrainment, Eqs. (4.14) have six singularities, which are non vanishing and are correlated with the subharmonic oscillations of order 1/3. The three of which are stable and the remainders are unstable singularities. It must also be mentioned that the origin is always the singular point of Eqs. (4.14), which is correlated with the harmonic oscillation [see Eq. (4.17)]. The boundary curve $D = 0$ decides the stability of this singularity. Therefore, in the area common to two regions (harmonic and 1/3-harmonic entrainments), two types of entrained oscillations are sustained.

(c) Remarks on the Approximation in the Analysis of Sec. 4.3(b)

When the frequency $\nu$ is in the region where the subharmonic entrainment occurs, the condition $\sigma_1^2 \gg (1 - r_1^2)^2$ is satisfied. Under this condition we neglect the amplitude $x_1$ as compared with $y_1$ in Eqs. (4.9), and we obtain the approximation, by using the notation w for $r_1$, from Eq. (4.8)

$$a_0^2 w^2 \doteqdot \left(\frac{B}{\omega_0^2 w^2 - \nu^2}\right)^2 = A^2 \tag{4.22}$$

which is consistent with the assumption made for the amplitude of the forced oscillation in Eq. (4.13). Using the relation (4.22), the first condition of Eqs. (4.11) may readily be written as

$$D \equiv 1 - \frac{2A^2}{a_0^2} < 0 \tag{4.23}$$

It is clear that the second condition of Eqs. (4.11) is satisfied for large detuning $\sigma_1$. Therefore, Eq. (4.23) is the only condition for stability of the harmonic oscillation.

(d) Example of the Phase Portrait

As we saw in Sec. 4.2d, where the phase portrait has a stable limit cycle as well as a stable singular point. However, in the system given by Eqs. (4.14), the similar situation may arise. We shall show in what follows an example of such a case.

Let us consider a case in which the external force is given by

$$B = 2.5 \qquad \text{and} \qquad \nu = 2.4$$

which are located in the region of 1/3-harmonic entrainment but outside the region of harmonic entrainment (see Fig. 4.8). By using these values in Eqs. (4.14), the phase portrait is plotted in Fig. 4.9. In the figure we see seven singular points, which are determined directly from Eqs. (4.17) and (4.19), and are shown in Table 4.3.

Table 4.3. Singular points in Fig. 4.9

| Singular point | $x_{1/3}$ | $y_{1/3}$ | $\lambda_1, \lambda_2$ | $\mu_1, \mu_2$* | Classification |
|---|---|---|---|---|---|
| 0 | 0 | 0 | $0.206 \pm 2.139i$ | — | Unstable focus |
| 1 | 0.137 | 1.235 | $-2.882 \pm 4.643i$ | — | Stable focus |
| 2 | -1.138 | -0.499 | $-2.882 \pm 4.643i$ | — | Stable focus |
| 3 | 1.001 | -0.736 | $-2.882 \pm 4.643i$ | — | Stable focus |
| 4 | 0.503 | 0.456 | 2.484, -3.914 | -0.060, 18.77 | Saddle (unstable) |
| 5 | -0.646 | 0.207 | 2.484, -3.914 | -1.998, 0.508 | Saddle (unstable) |
| 6 | 0.143 | -0.663 | 2.484, -3.914 | 1.516, -0.651 | Saddle (unstable) |

* $\mu_1, \mu_2$ are the tangential directions of the integral curves at the singular points.

In Fig. 4.9 we see that the three stable singular points 1, 2, and 3 are correlated with the 1/3-harmonic oscillation, and that they are equidistant from the origin, the angular distance between any two of these singular points being equal to $\frac{2}{3}\pi$ radians. The same properties are also applied to the singular points 4, 5, and 6, which are saddle points. A stable limit cycle which encircles the origin (unstable focus) exists, which is correlated with the almost periodic oscillation. The separatrices (drawn by thick lines in the figure) that contain the saddle points 3, 4, or 5 divide the whole plane into four regions, in one of which containing the origin all integral curves tend to the limit cycle, whereas in the others either to the singular point 1, 2, or 3. Thus both the almost periodic and entrained oscillations may occur in this case, which one it will be depending on the initial condition.

(e) Transition between Entrained Oscillations and Almost Periodic Oscillations

In the present section we shall investigate the appearance and disappearance of limit cycle around the origin when the external force is varied beyond the boundary of harmonic entrainment.

It will easily be seen from the stability conditions (4.20) that the origin is a focus for all values of the external forces under consideration. Then, the system (4.14) assumes the form, by introducing $(\xi, \eta)$ for $(x_{1/3}, y_{1/3})$,

$$\frac{d\xi}{d\tau} = a\xi - b\eta + X_2(\xi, \eta)$$

$$\frac{d\eta}{d\tau} = b\xi + a\eta + Y_2(\xi, \eta)$$

where $$a = D = 1 - 2w^2 \qquad b = \frac{2\omega_0^2 w^2 - (\nu/3)^2}{\mu(\nu/3)} \tag{4.24}$$

$$X_2(\xi, \eta) = 3kw(\xi^2 - \eta^2) + 2w\xi\eta - (\xi + 3k\eta)(\xi^2 + \eta^2)$$

$$Y_2(\xi, \eta) = w(\xi^2 - \eta^2) - 6kw\xi\eta + (3k\xi - \eta)(\xi^2 + \eta^2)$$

We see in the above equations that a, b, and the coefficients of $X_2$ and $Y_2$ are determined once the external force is given. Since a is the real part of the characteristic roots and becomes zero when $w^2 = \frac{1}{2}$, the focal point (the origin) is stable or unstable according as $w^2 > \frac{1}{2}$ or $w^2 < \frac{1}{2}$. Hence we regard w as a parameter.

Passing to polar coordinates $\zeta, \varphi$ given by $\xi = \zeta \cos \varphi$, $\eta = \zeta \sin \varphi$, Eqs. (4.24) are transferred as

$$\frac{d\zeta}{d\varphi} = \frac{a\zeta + w(3k \cos 3\varphi + \sin 3\varphi)\zeta^2 - \zeta^3}{b + w(\cos 3\varphi - 3k \sin 3\varphi)\zeta + 3k\zeta^2} \tag{4.25}$$

Since the origin is a focus, the integral curve starting from $\zeta = \zeta_0$, $\varphi = 0$ will pass completely round the origin, provided $\zeta_0$ is sufficiently small. We now follow the standard procedure due to Poincaré [1, pp. 215-224], to obtain a solution of this equation for small values of $\zeta$.

We write the Eq. (4.25)

$$\frac{d\zeta}{d\varphi} = \frac{A_1\zeta + A_2\zeta^2 + A_3\zeta^3}{B_1 + B_2\zeta + B_3\zeta^2} \tag{4.26}$$

where $A_i$ and $B_i$ (i = 1, 2, 3) are given in the previous equation. We see that $A_2$ and $B_2$ are the functions of $3\varphi$ and the others are constants determined by the external force. This implies that integral curves of Eq. (4.26) are $\frac{2}{3}\pi$ symmetric about the origin.

We expand the denominator of Eq. (4.26) in ascending powers of $\zeta$ to give

$$\frac{d\zeta}{d\varphi} = K_1\zeta + K_2\zeta^2 + K_3\zeta^3 + \cdots$$

where $$K_1 = \frac{A_1}{B_1}$$

$$K_2 = \frac{A_2B_1 - A_1B_2}{B_1^2}$$

$$K_3 = \frac{A_3B_1^2 - A_2B_1B_2 - A_1B_1B_3 + A_1B_2^2}{B_1^3} \tag{4.27}$$

$$\cdots\cdots$$

Let $\zeta = f(\varphi, \zeta_0, w)$ be the solution of the above equation such that $\zeta = \zeta_0$ when $\varphi = 0$; that is,

$$\zeta_0 = f(0, \zeta_0, w) \tag{4.28}$$

This solution may be expanded in powers of $\zeta_0$, if $\zeta_0$ is sufficiently small, in the form*

$$\zeta = u_1(\varphi, w)\zeta_0 + u_2(\varphi, w)\zeta_0^2 + u_3(\varphi, w)\zeta_0^3 + \cdots \tag{4.29}$$

By substituting Eq. (4.29) into (4.27) and equating the coefficients of like powers of $\zeta_0$, then we obtain a set of differential equations

$$\frac{du_1}{d\varphi} - K_1u_1 = 0$$

$$\frac{du_2}{d\varphi} - K_1u_2 = K_2u_1^2$$

$$\frac{du_3}{d\varphi} - K_1u_3 = 2K_2u_1u_2 + K_3u_1^3 \tag{4.30}$$

$$\cdots\cdots$$

* Since $\zeta = 0$ is a solution of Eq. (4.27), we must have $f \equiv 0$ for $\zeta_0 = 0$, and so the series has no constant term.

In view of the relation (4.28) we have

$$u_1(0, w) = 1 \qquad u_i(0, w) = 0 \qquad (i = 2, 3, \ldots) \tag{4.31}$$

The differential equations (4.30) together with the initial conditions (4.31) enable us to determine $u_1$, $u_2$, $\cdots$ in succession. Thus the solutions of Eqs. (4.30) with the initial conditions (4.31) are

$$\begin{aligned} u_1(\varphi, w) &= \exp[\int_0^{\varphi} K_1 d\varphi] = \exp[\tfrac{a}{b}\varphi] \\ u_2(\varphi, w) &= u_1 \int_0^{\varphi} K_2 u_1 d\varphi \\ u_3(\varphi, w) &= \frac{u_2^2}{u_1} + u_1 \int_0^{\varphi} K_3 u_1^2 d\varphi \\ &\cdots\cdots \end{aligned} \tag{4.32}$$

The necessary and sufficient condition for the existence of the small limit cycle around the focus at the origin cutting the $\zeta$ axis at the point $\zeta = \zeta_0$, $\varphi = 0$ is that

$$\zeta(\tfrac{2}{3}\pi) - \zeta_0 = f(\tfrac{2}{3}\pi, \zeta_0, w) - \zeta_0 \equiv \zeta_0 \Phi(\zeta_0, w^2) = 0 \tag{4.33}$$

or rejecting $\zeta_0 = 0$

$$\begin{aligned} &\Phi(\zeta_0, W) \equiv \alpha_1(W) + \alpha_2(W)\zeta_0 + \alpha_3(W)\zeta_0^2 + \cdots = 0 \\ \text{where} \qquad & W = w^2 \\ &\alpha_1(W) = u_1(\tfrac{2}{3}\pi, w) - 1 = \exp[\tfrac{2a}{3b}\pi] - 1 \\ &\alpha_i(W) = u_i(\tfrac{2}{3}\pi, w) \qquad (i = 2, 3, \cdots) \end{aligned} \tag{4.34}$$

This equation establishes a relation between $W$ and $\zeta_0$, and we readily see that the curve $\Phi(\zeta_0, W) = 0$ passes the point $W_0(W = \frac{1}{2}, \zeta_0 = 0)$ on the $W\zeta_0$ plane.

We will then consider the behavior of the curve at $W_0$. Here we notice from Eqs. (4.32) and (4.34) that the following four relations are satisfied at $W_0$: i.e.,

$$\alpha_1(\tfrac{1}{2}) = 0 \qquad \alpha_1'(\tfrac{1}{2}) = -\frac{4\pi}{3b}$$
$$\alpha_2(\tfrac{1}{2}) = 0 \qquad \alpha_3(\tfrac{1}{2}) = -\frac{2\pi}{3b} \tag{4.35}$$

where the prime over a quantity refer to a differentiation with respect to $W$. The slope of the tangent at any point of the curve $\Phi = 0$ is the value of $d\zeta_0/dW = -(\Phi_W/\Phi_{\zeta_0})$. At the point $W_0$ this expression is infinite, as one will easily see from the first and the second members of Eqs. (4.35). Hence the tangent at $W_0$ is vertical. To find out whether the arc coming to $W_0$ rises to the right or to the left of the tangent, we must examine $W_0$ for a maximum or minimum of $W$ as a function of $\zeta_0$. By differentiating Eq. (4.34) and by using the relations (4.35) we have

$$\left(\frac{d^2W}{d\zeta_0^2}\right)_{W_0} = \frac{-2\alpha_3(\frac{1}{2})}{\alpha_1'(\frac{1}{2})} = -1 < 0 \tag{4.36}$$

From the above result we see that $W$ has a maximum value at $W_0$, and the arc of $\Phi = 0$ comes to $W_0$ from the left of the tangent as in Fig. 4.10. Hence limit cycles may exist only for $W < \frac{1}{2}$ and are necessarily stable. The region $W > \frac{1}{2}$ is free of limit cycles. Thus as $W$ increases, the focus, unstable below $W_0$, becomes stable and the stable limit cycle shrinks up to the focus when $W_0$ is passed.

The limit cycle of Fig. 4.9 shrinks up to the origin as B increases and passes the boundary $D = 0$, and the phase portrait has the stable singularities representing both the harmonic and the 1/3-harmonic entrainment. Further increase in B comes to extinction of the singularities representing the 1/3-harmonic responses through the coalescence of singular points at the boundary of 1/3-harmonic entrainment, and only the origin is left which represents the harmonic entrainment. When B is decreased from Fig. 4.9 the limit cycle grows large and passes through the saddle points and then disappears. But for other values of $\nu$ the limit cycle is existent for all values of B below $D = 0$. At the lower boundary of 1/3-harmonic entrainment ($\nu > 3\omega_0$) the hysteresis phenomenon, similar to those between $B_1$ and $B_2$ (see Figs. 4.6 and 4.7), may occur. This types of transitions are comfirmed by analog-computer analysis.

## 4.4 Concluding Remarks

Various types of oscillations in the system described by Eq. (4.1) have been investigated on the basis of the derived autonomous systems. In particular we were mainly concerned with the transition which occurs in the right hand regions ($\nu > \omega_0$ or $\nu > 3\omega_0$) on the $B\nu$ plane. It may be conjectured that the general features of the transition in the case of linear restoring force — particularly in the neighborhood of $(B/\mu\nu a_0)^2 = 8/27$ and $|\sigma_1| = 1/2$ (see Fig. 3.4) or $\nu \fallingdotseq 3$ and the boundary of harmonic entrainment (see Fig. 3.1b) — are, to some extent, similar to those obtained in this chapter.

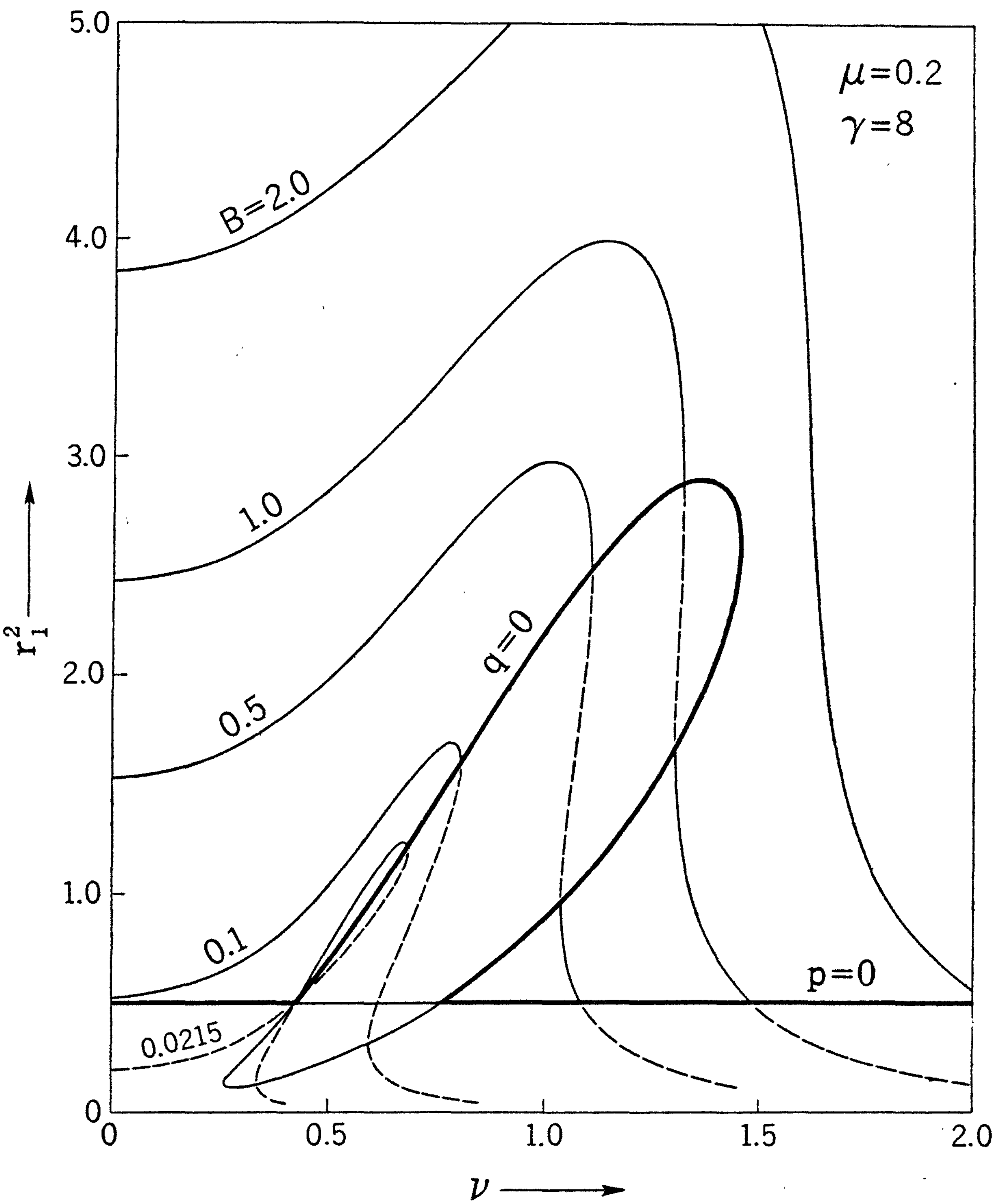


Fig. 4.1. Normalized response curves for the harmonic oscillation in the system described by Eq. (4.1).

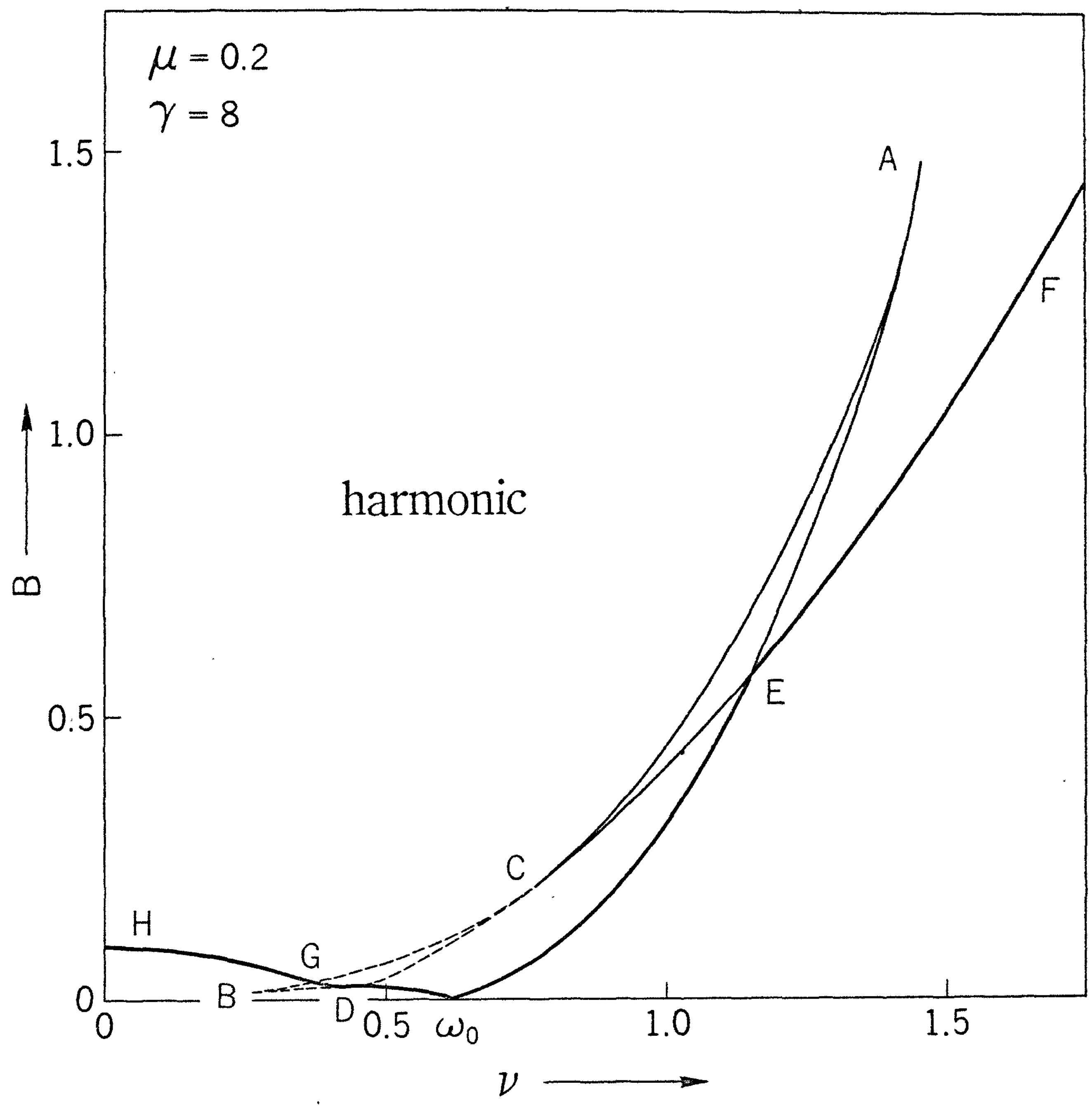


Fig. 4.2.. Region of harmonic entrainment.

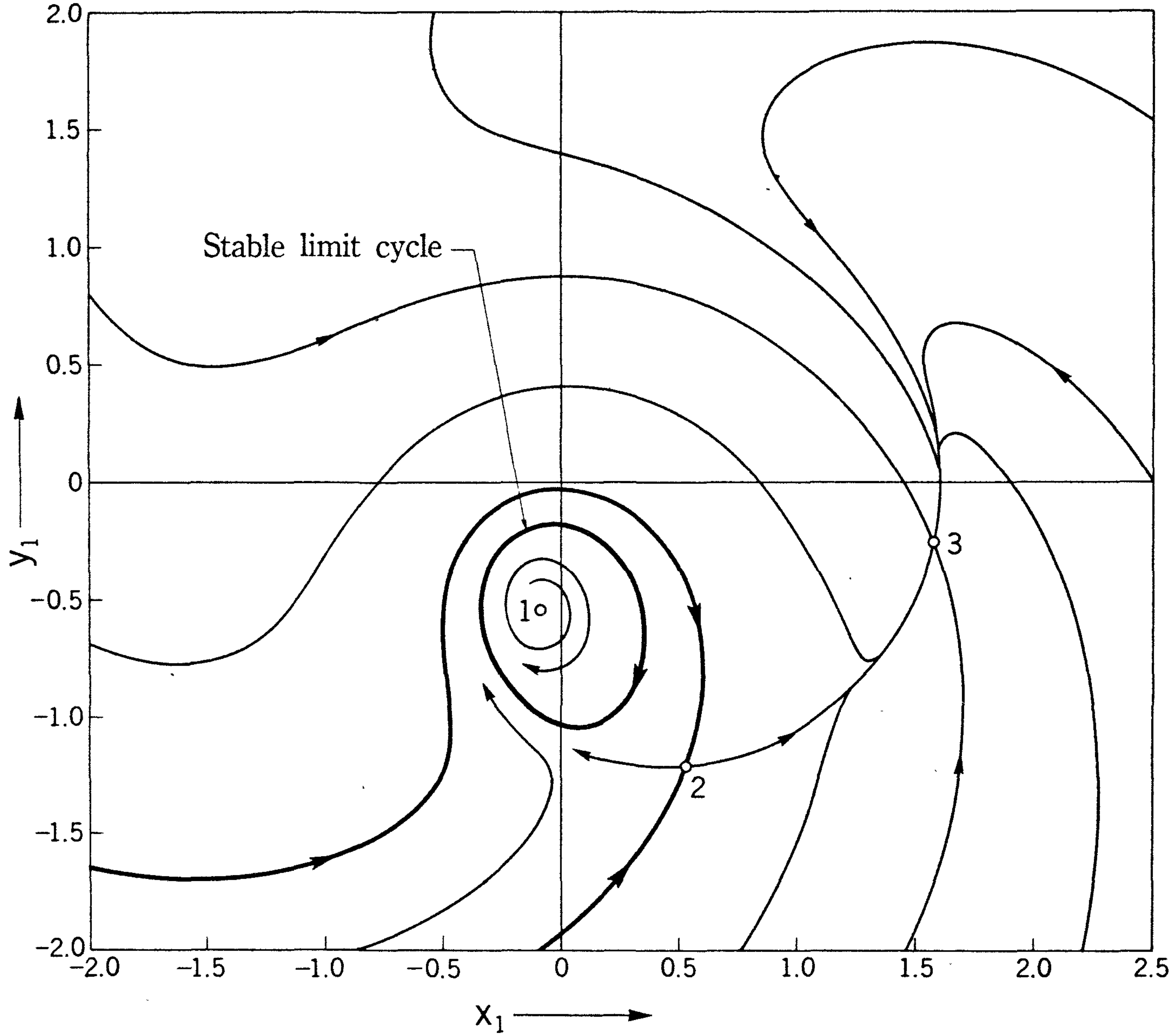


Fig. 4.3. Example of the phase portrait of the system as given by Eqs. (4.5).

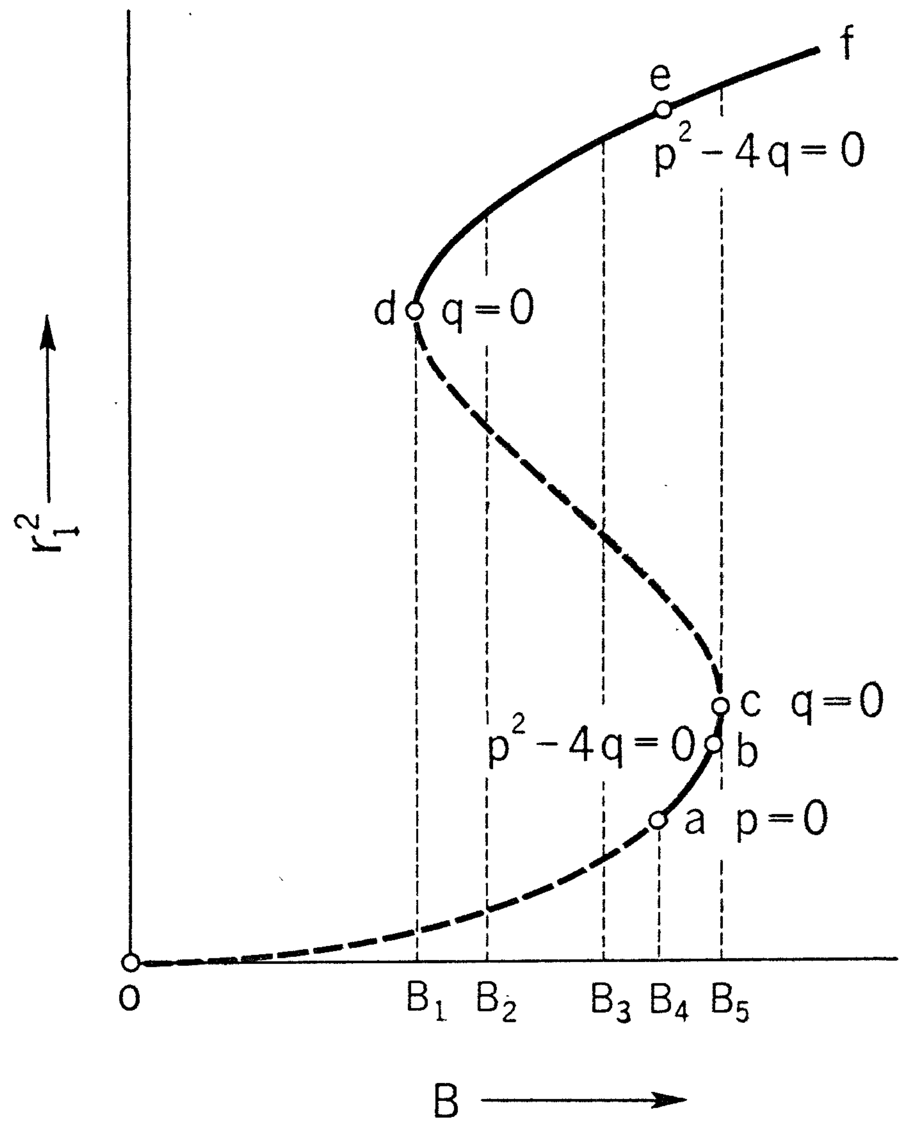


Fig. 4.4. Amplitude characteristic of the harmonic oscillation when $\nu$ is kept constant.

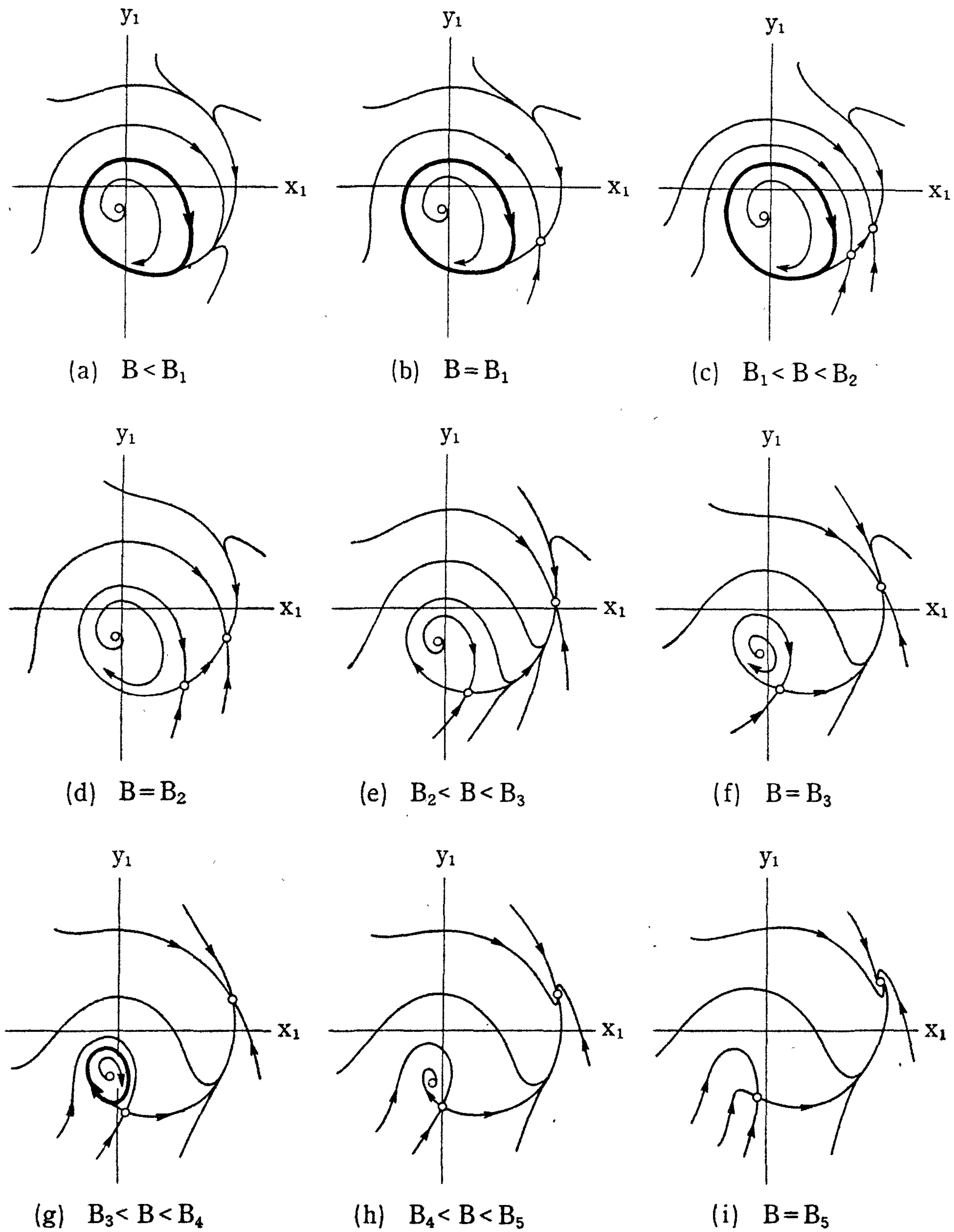


Fig. 4.5. Phase portraits of Eqs. (4.5) for various values of B.

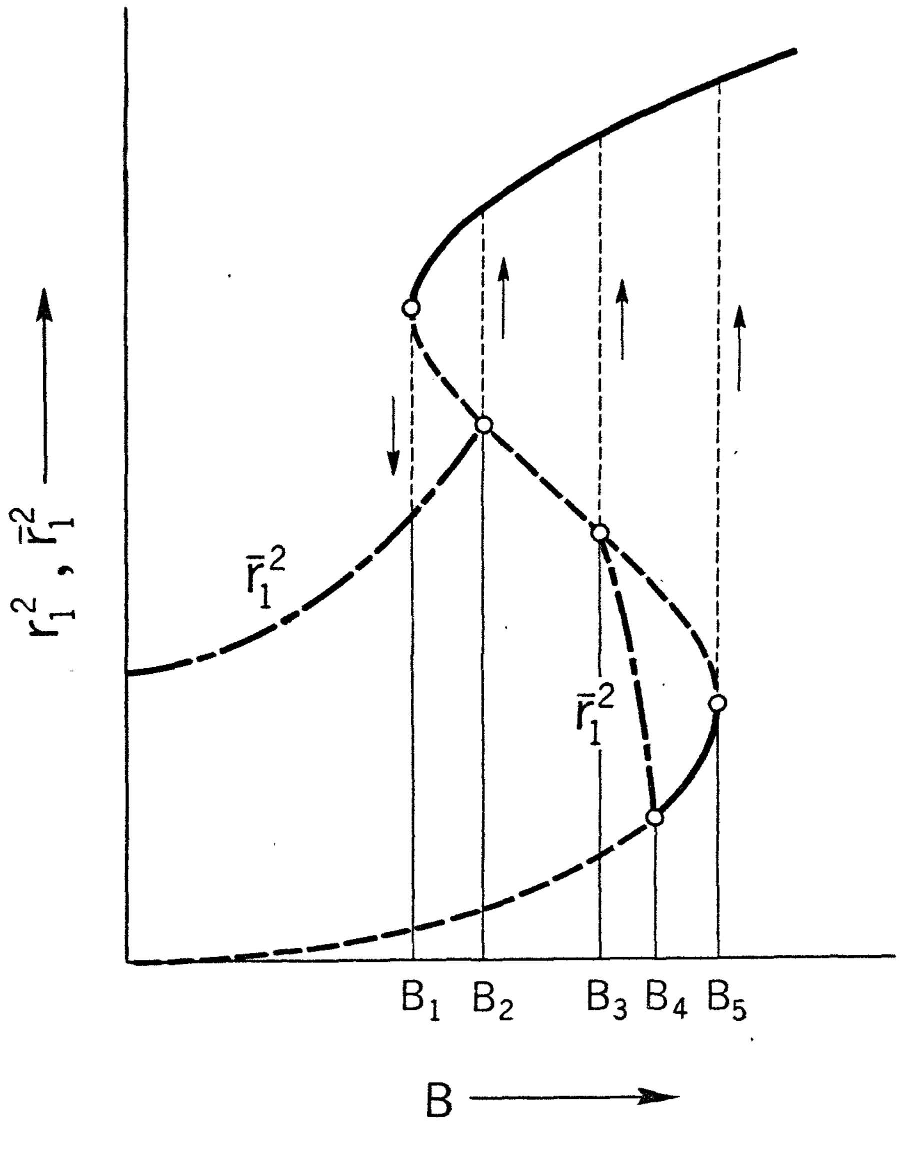


Fig. 4.6. Amplitude characteristic with mean-square amplitude of the almost periodic oscillation, showing the transition between entrained and almost periodic oscillations.

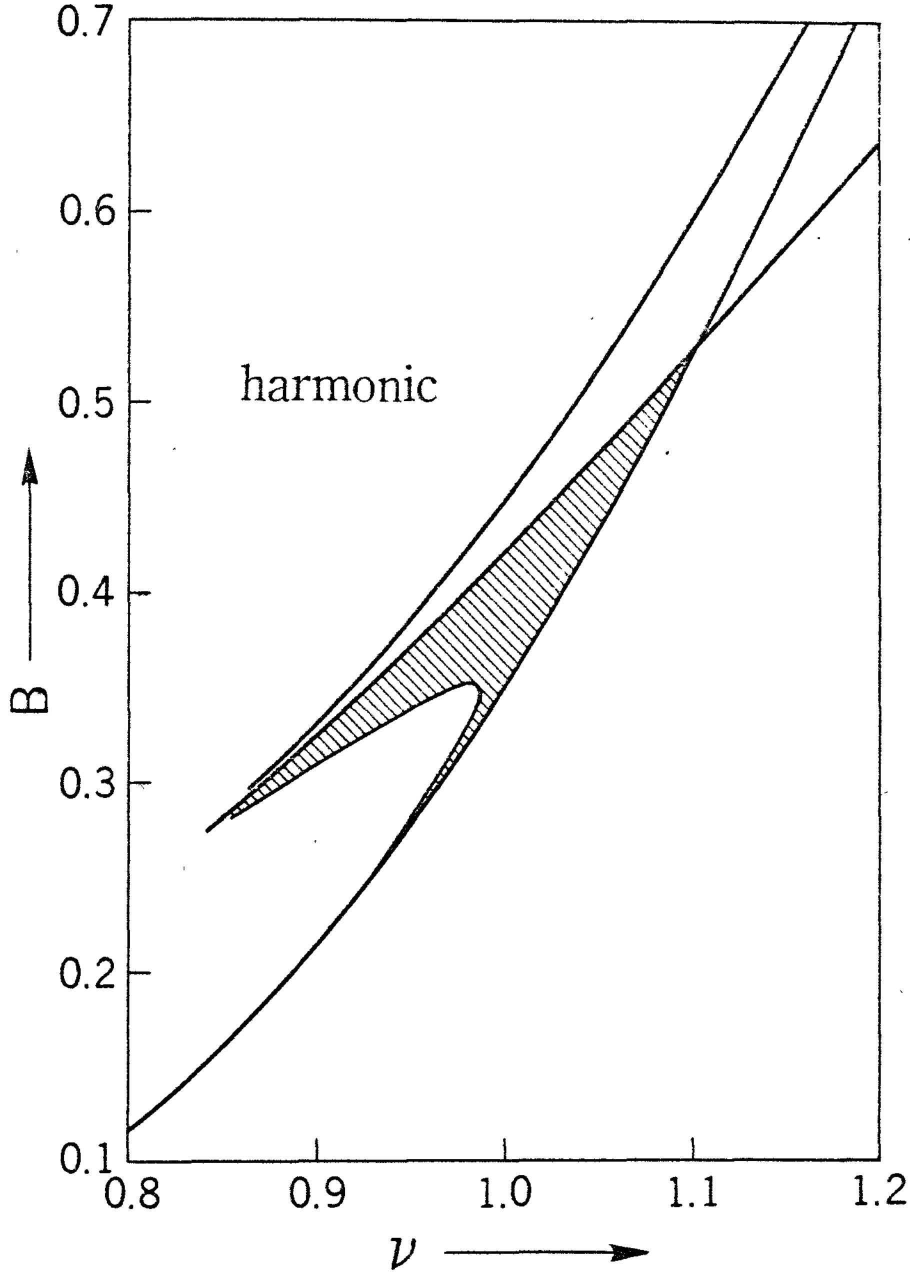


Fig. 4.7. Region of harmonic entrainment obtained by analog-computer analysis.

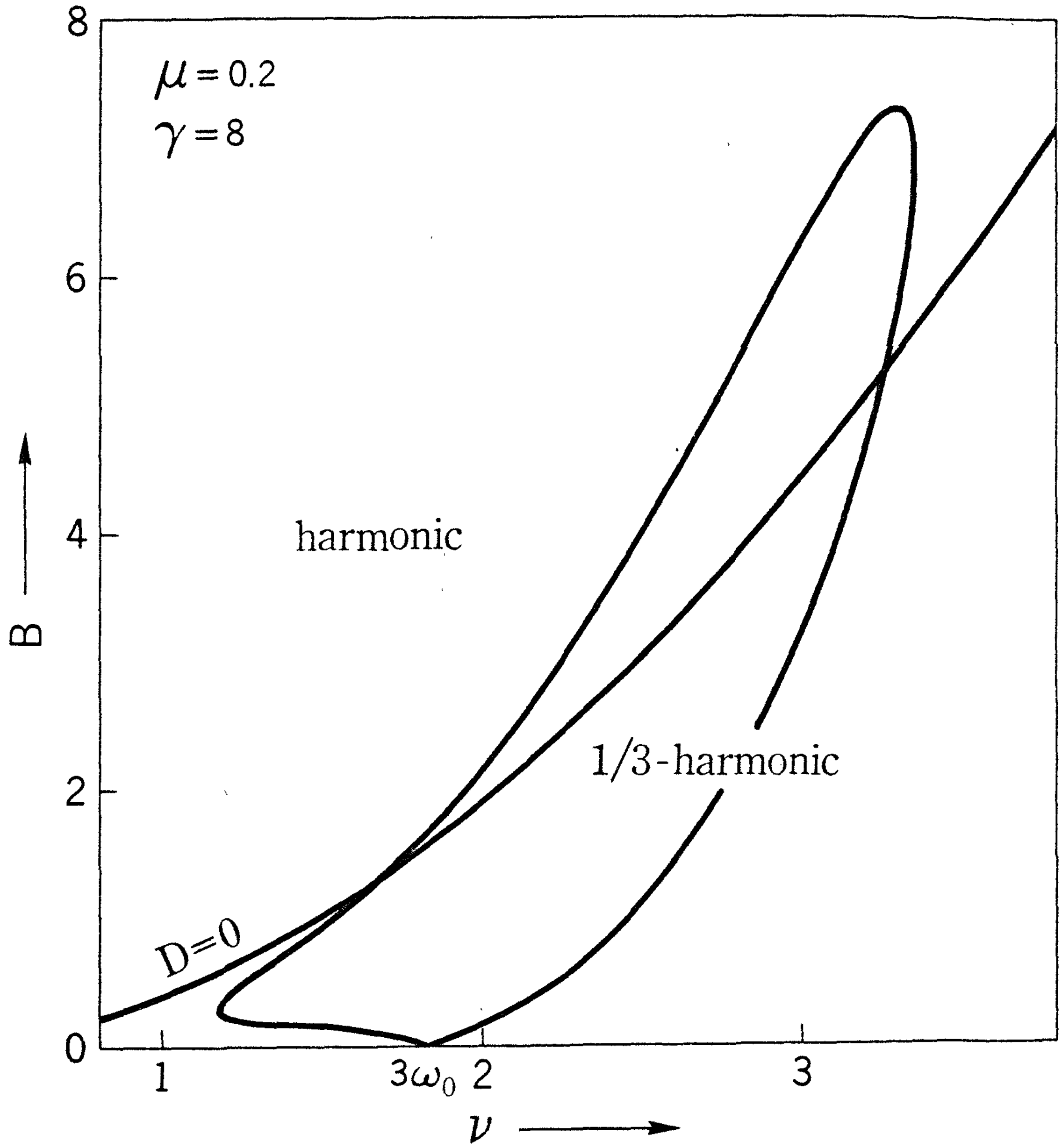


Fig. 4.8. Regions of harmonic and 1/3-harmonic entrainments.

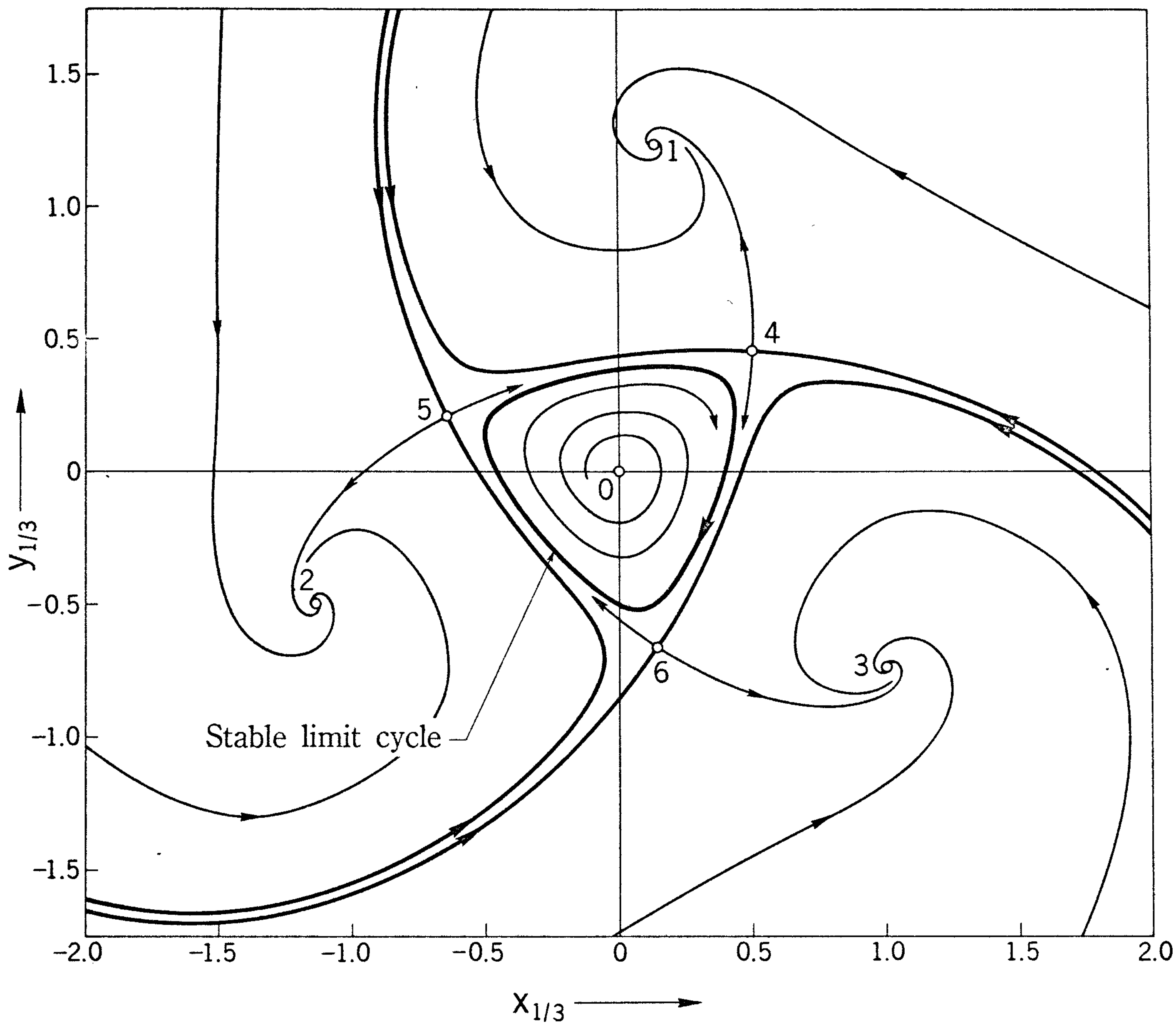


Fig. 4.9. Example of the phase portrait of the system as given by Eqs. (4.14).

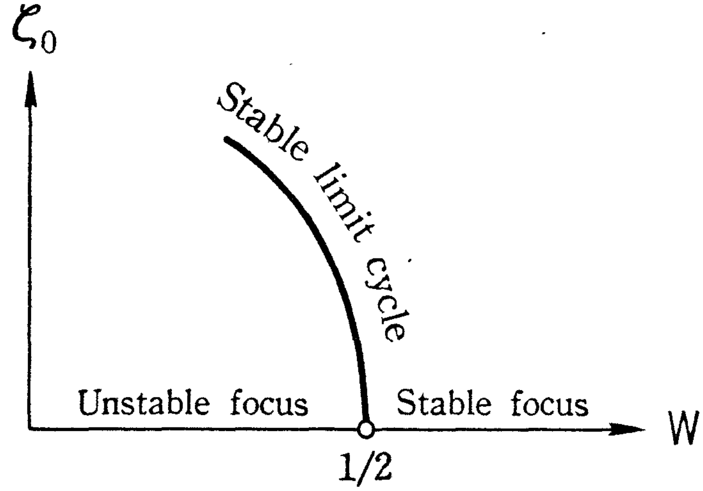


Fig. 4.10. Change of the stability of focus.

CHAPTER 5

# THE SINGULARITIES AND LIMIT CYCLES OF SOME AUTONOMOUS SYSTEM

## 5.1 Introduction

In the present chapter we consider an autonomous system governed by the simultaneous differential equations

$$\begin{aligned} \frac{dx}{d\tau} &= (1 - \gamma\nu^2 r^2)x - \sigma y + \frac{B}{\mu\nu a_0} \equiv X(x,y) \\ \frac{dy}{d\tau} &= \sigma x + (1 - \gamma\nu^2 r^2)y \equiv Y(x,y) \end{aligned} \tag{5.1}$$

where

$$\begin{aligned} r^2 &= x^2 + y^2 & \sigma &= \frac{\omega_0^2 r^2 - \nu^2}{\mu\nu} \\ a_0^2 &= \frac{4}{3\gamma} & \omega_0^2 &= \frac{1}{\gamma} \end{aligned} \tag{5.2}$$

The system (5.1) arises as the fundamental equations determining the in-phase and quadrature amplitudes of the forced oscillation in a self-oscillatory system with external force.* In Eqs. (5.1) and (5.2) $\mu$ and $\gamma$ are the system

---

* The system to be considered is

$$\frac{d^2v}{dt^2} - \mu\left[1 - \gamma^2\left(\frac{dv}{dt}\right)^2\right]\frac{dv}{dt} + v^3 = B\cos\nu t \qquad 0 < \mu \ll 1$$

By assuming an approximate solution for the above equation of the form

$$v(t) = b_1(t)\sin\nu t + b_2(t)\cos\nu t$$

and by making use of the method of harmonic balance under the analogous assumptions made on $b_1$ and $b_2$ in the preceding chapters, we obtain Eqs. (5.1) with the relations $x = b_1/a_0$, $y = b_2/a_0$, and $\tau = \frac{\mu}{2}t$. The constants $a_0$ and $\omega_0$ represent the first approximating values of the amplitude and frequency of the free oscillation, respectively.

parameters; B and $\nu$ are proportional to the amplitude and frequency of applied force; that is, the same symbols as in the preceding chapter are used.

The system (5.1) also describes the phenomenon of frequency entrainment. Region of harmonic entrainment, in which an entrained oscillation is represented by a stable singular point, has on either side regions in each of which an almost periodic oscillation, represented by a stable limit cycle, occurs. Between these two regions, rather complicated transitions take place such as already explained in the preceding chapter.

In the present analysis, we show the example of transition which occurs involving as many as three singular points and two limit cycles.

## 5.2 Quantitative Investigation

Equations (5.1) cannot be integrated by known methods, and there are a few theorems regarding the existence of limit cycles. We are therefore compelled to resort to the numerical methods, which can prove very laborious and possibly unreliable in critical regions, however.

### (a) Singular Points and Conditions for Stability

In Eqs. (5.1) x and y, regarded as cartesian coordinates of a point on xy phase plane, are functions of the time $\tau$. The singular point of Eqs. (5.1), determining solution x = constant and y = constant, may be obtained by putting $dx/d\tau = 0$ and $dy/d\tau = 0$, i.e.,

$$X(x,y) = 0 \qquad\qquad Y(x,y) = 0 \tag{5.3}$$

By eliminating x and y from the above equations, we obtain the relation

$$[(1 - \gamma\nu^2 r^2)^2 + \sigma^2]\, r^2 = \left(\frac{B}{\mu\nu a_0}\right)^2 \tag{5.4}$$

which yields the squared radius $r^2$ from the origin to a singular point. The coordinates of the singular point are written as

$$x = -\frac{\mu\nu a_0}{B}(1 - \gamma\nu^2 r^2)r^2 \qquad y = \frac{\mu\nu a_0}{B}\sigma r^2 \tag{5.5}$$

In physical systems, the equilibrium states determined by Eqs. (5.5) are not always sustained, but are only able to last so long as they are stable. These conditions for stability of the singular point may also be derived by the same procedure as already used in Secs. 3.3b and 4.2b. The results are:

$$\begin{aligned} p &= 2(2\gamma\nu^2 r^2 - 1) > 0 \\ q &= (1 - \gamma\nu^2 r^2)(1 - 3\gamma\nu^2 r^2) + \sigma^2 + 2\frac{\omega_0^2}{\mu\nu}\sigma r^2 > 0 \end{aligned} \tag{5.6}$$

Figure 5.1 shows the resonance curves given by the relation (5.4) for the following values of the system parameters:

$$\mu = 0.2 \qquad \text{and} \qquad \gamma = 2$$

The stability limits $p = 0$ and $q = 0$ given by Eqs. (5.6) are also shown in the figure. Hence the dotted-line portions of the resonance curves are unstable. One sees that Fig. 5.1 is similar to Fig. 4.1 except the shape of the stability limit $p = 0$. From this result the region of harmonic entrainment is reproduced on the $B\nu$ plane as illustrated in Fig. 5.2, which is also analogous to Fig. 4.2. In the figure the curvilinear triangle BGD corresponding to that of Fig. 4.2 is broader than that of before. Therefore, we can, somewhat easily, deal with the behavior of integral curves when the external force is given in the vicinity of this region.

(b) Example of the Phase Portrait

In this section we show an example of phase portrait having three singularities and two limit cycles. The special case we have in mind is that specified by the following value of the external force;

$$B = 0.065 \qquad \text{and} \qquad \nu = 0.57$$

The other system parameters are the same as in Sec. 5.2a.

By substituting these values into Eqs. (5.1) and (5.2), the phase portrait is plotted in Fig. 5.3. As illustrated in the figure, there are three singularities in this case. As in the case of the preceding chapter, the details of the singularities are readily known and are shown in Table 5.1. We see in the figure an unstable limit cycle which encircles the stable focus 3, and outside this a stable limit cycle enclosing three singular points. The unstable limit cycle divides the whole plane into two regions, inside this limit cycle all integral curves tend to the stable focus 3, outside to the stable limit cycle. Thus both the stable singular point and limit cycle exist in this system.

Table 5.1. Singular points of Fig. 5.3

| Singular point | x | y | $\lambda_1, \lambda_2$ | $\mu_1, \mu_2$* | Classification |
|---|---|---|---|---|---|
| 1 | -0.089 | -0.239 | $0.915 \pm 2.261i$ | — | Unstable focus |
| 2 | -0.474 | -0.507 | 2.006, -1.260 | -0.249, -2.027 | Saddle (unstable) |
| 3 | -0.551 | 0.698 | $-0.027 \pm 2.084i$ | — | Stable focus |

* $\mu_1, \mu_2$ are the tangential directions of the integral curves at the singular points.

(c) Transformation of Singularities and Limit Cycles When the External Force is Varied

In this section we consider the transformation of singularities and limit cycles of Fig. 5.3 when B is varied. By substituting $\nu = 0.57$ into Eq. (5.4), the $Br^2$ relation is calculated and plotted in Fig. 5.4. As in the case of Sec. 4.2e, the singularities are classified and the results are listed in Table 5.2.

Table 5.2. Classification of singular points along the amplitude characteristic of Fig. 4.4

| Interval | p | q | $p^2 - 4q$ | Classification |
|---|---|---|---|---|
| oa | - | + | - | Unstable foci |
| ab | - | + | + | Unstable nodes |
| bc | - | - | + | Saddles (unstable) |
| cd | - | + | + | Unstable nodes |
| de | - | + | - | Unstable foci |
| ef | + | + | - | Stable foci |

Figure 5.5 shows the phase portraits of Eqs. (5.1) for various values of B. The phase portrait of Fig. 5.3 is again sketched in Fig. 5.5d. When B is decreased the unstable limit cycle diminishes in size and shrinks up to the unstable focus when $B_2$ of Fig. 5.4 is passed. This state is shown in Fig. 5.5c. Further decrease in B brings the coalescence of singular points at $B = B_1$ and then this higher-order singularity disappears (see Fig. 5.5a and b). When B is increased from Fig. 5.5d the unstable limit cycle grows large and the higher-order singularity is formed between two limit cycles at $B = B_3$. Two limit cycles

persist for values of B between $B_3$ and $B_4$ but one singular point, and B reaches $B_4$ they overlap one another and form higher-order limit cycle which is semi-stable (Fig. 5.5h), and then disappear still subsisting only one stable focus.

Hence it is concluded that a stable limit cycle appears for $B < B_4$, an unstable limit cycle for $B_2 < B < B_4$ and a stable singular point for $B_2 < B$ in this particular case.

As we have already used in Sec. 4.2e, we again introduce the mean-square radius of the limit cycle defined by

$$\bar{r}^2 = \frac{1}{T}\oint_C r^2 d\tau \tag{5.7}$$

where C is an integration path being taken round the limit cycle and T is a period for the representative point $(x(\tau), y(\tau))$ to complete one revolution along the limit cycle.

By using Eqs. (5.1) and (5.7), we have

$$\oint_C \left(\frac{\partial X}{\partial x} + \frac{\partial Y}{\partial y}\right) d\tau = 2\int_0^T (1 - 2\gamma\nu^2 r^2) d\tau = 4T\gamma\nu^2\left(\frac{1}{2\gamma\nu^2} - \bar{r}^2\right) \tag{5.8}$$

From the Poincaré's criterion for orbital stability [24, pp. 253-258], we see that a stable limit cycle has mean-square radius greater than $1/2\gamma\nu^2$, an unstable limit cycle less than $1/2\gamma\nu^2$, and a limit cycle of higher order has mean square radius equal to $1/2\gamma\nu^2$.

The results above obtained are summarized and sketched in Fig. 5.6. In the figure the mean-square radii $\bar{r}^2$ of the limit cycle are plotted by chain lines, and the arrows show the jump phenomena between stable steady-states when B is varied.*

That is to say, in physical term, an entrained oscillation is sustained for $B_2 < B$, an almost periodic oscillation for $B < B_4$, and hysteresis occurs between $B_2$ and $B_4$.

## 5.3 Concluding Remarks

Singularities and limit cycles of the system governed by Eqs. (5.1) have been investigated. Particular attention has been directed to the transformation of the phase portraits on the left hand transitional region ( $\nu < \omega_0$) on the $B\nu$ plane, and the example illustrating such transformation has been given.

The application of this result to an original differential equation (given in the footnotes on page 96 ) requires further examination, since the representative point moves along the stable limit cycle rather quickly.

In addition such a region represented by the curvilinear triangle BGD in Fig. 5.2 is nonexistent in the case of linear restoring force [cf. Eq. (3.6)].

---

* When $B = 0$, Eqs. (5.1) are easily integrated; that is,

$$r^2 = \frac{\omega_0^2 r_0^2}{(\omega_0^2 - \nu^2 r_0^2)e^{-2\tau} + \nu^2 r_0^2}$$

where $$r_0^2 = r^2 \Big|_{\tau = 0}$$

We see that the limit cycle of this particular case is a circle centered at the origin with the radius $r^2 = 1/\gamma\nu^2$.

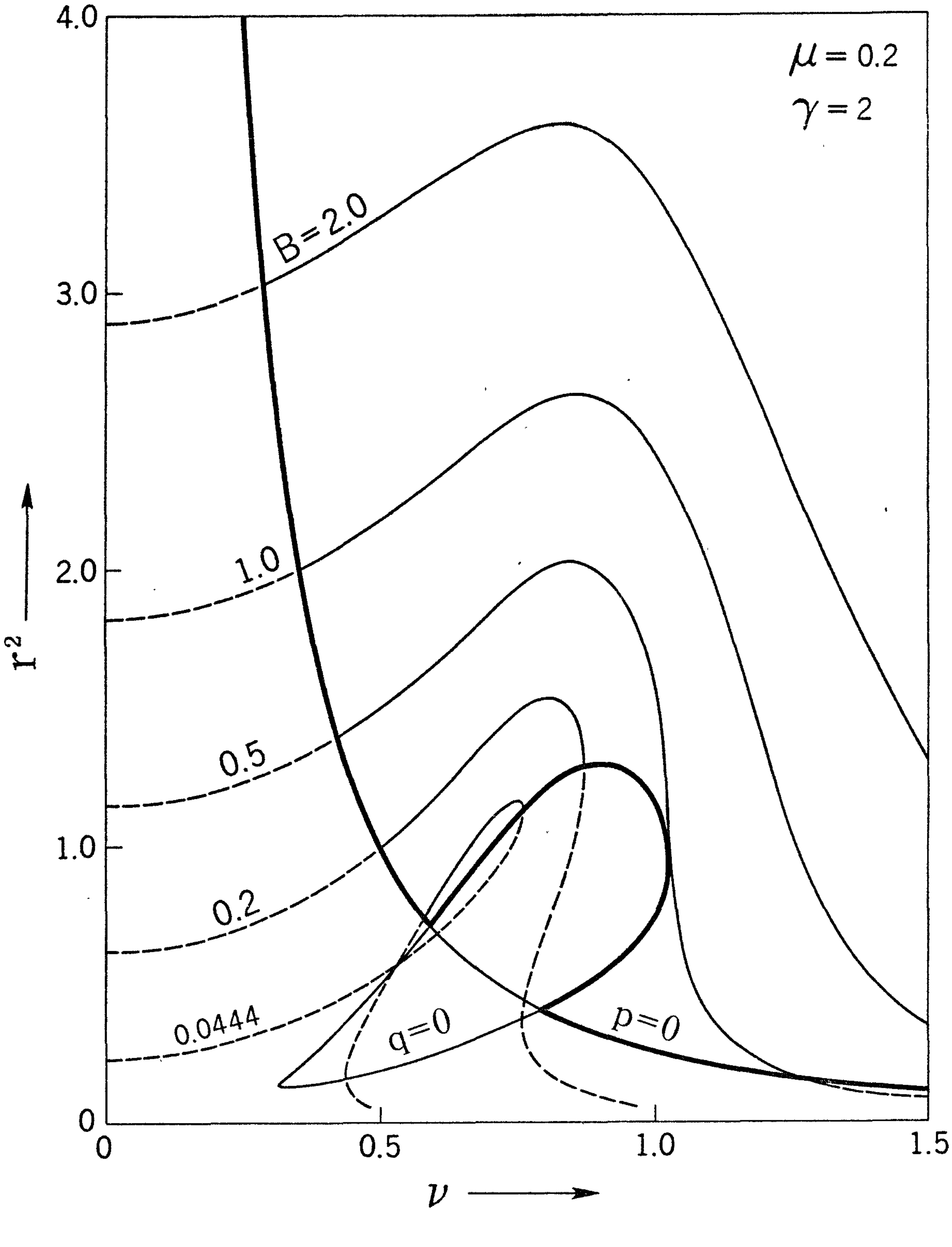


Fig. 5.1. Resonance curves of the system (5.1).

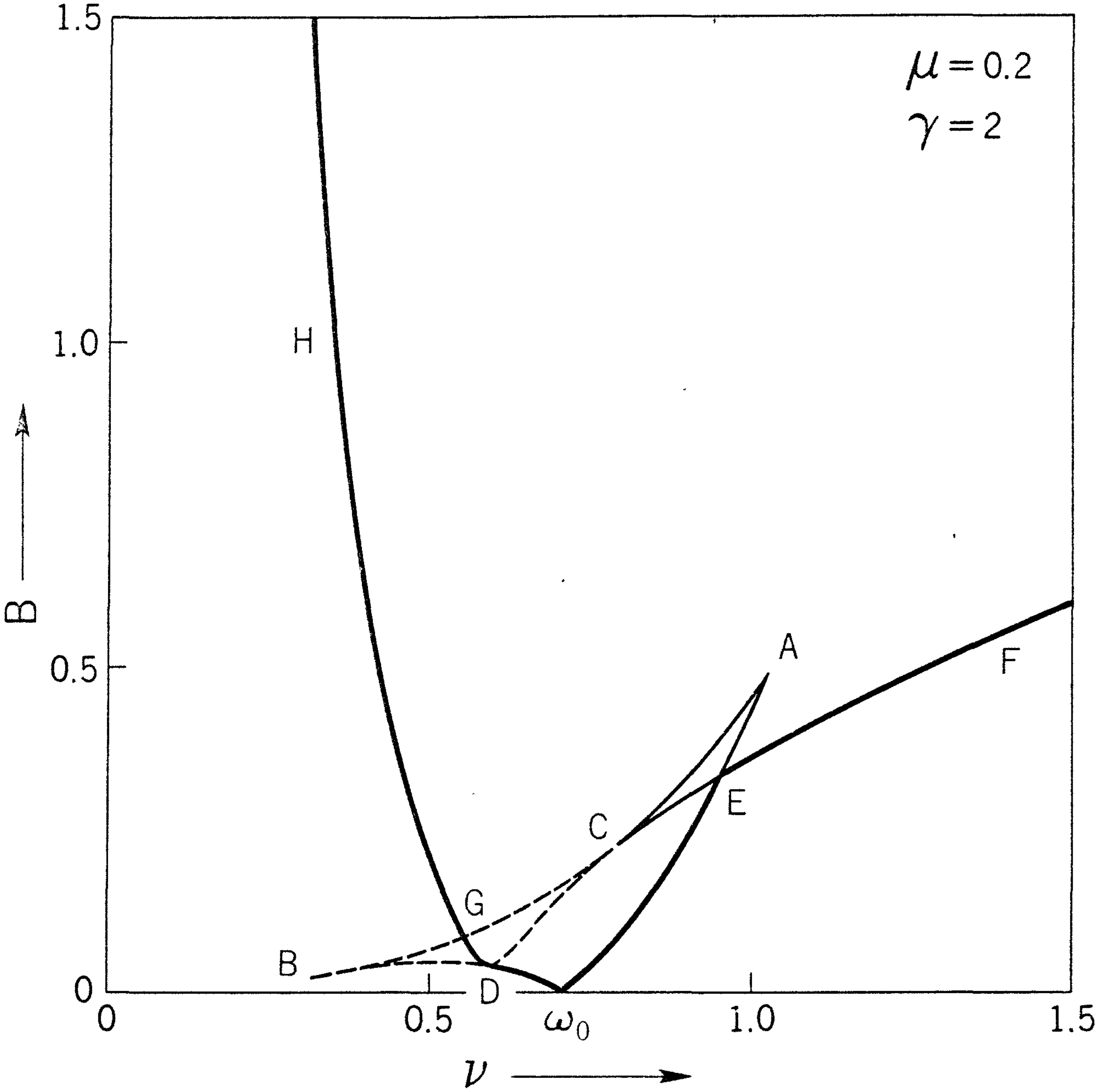


Fig. 5.2. Region of harmonic entrainment.

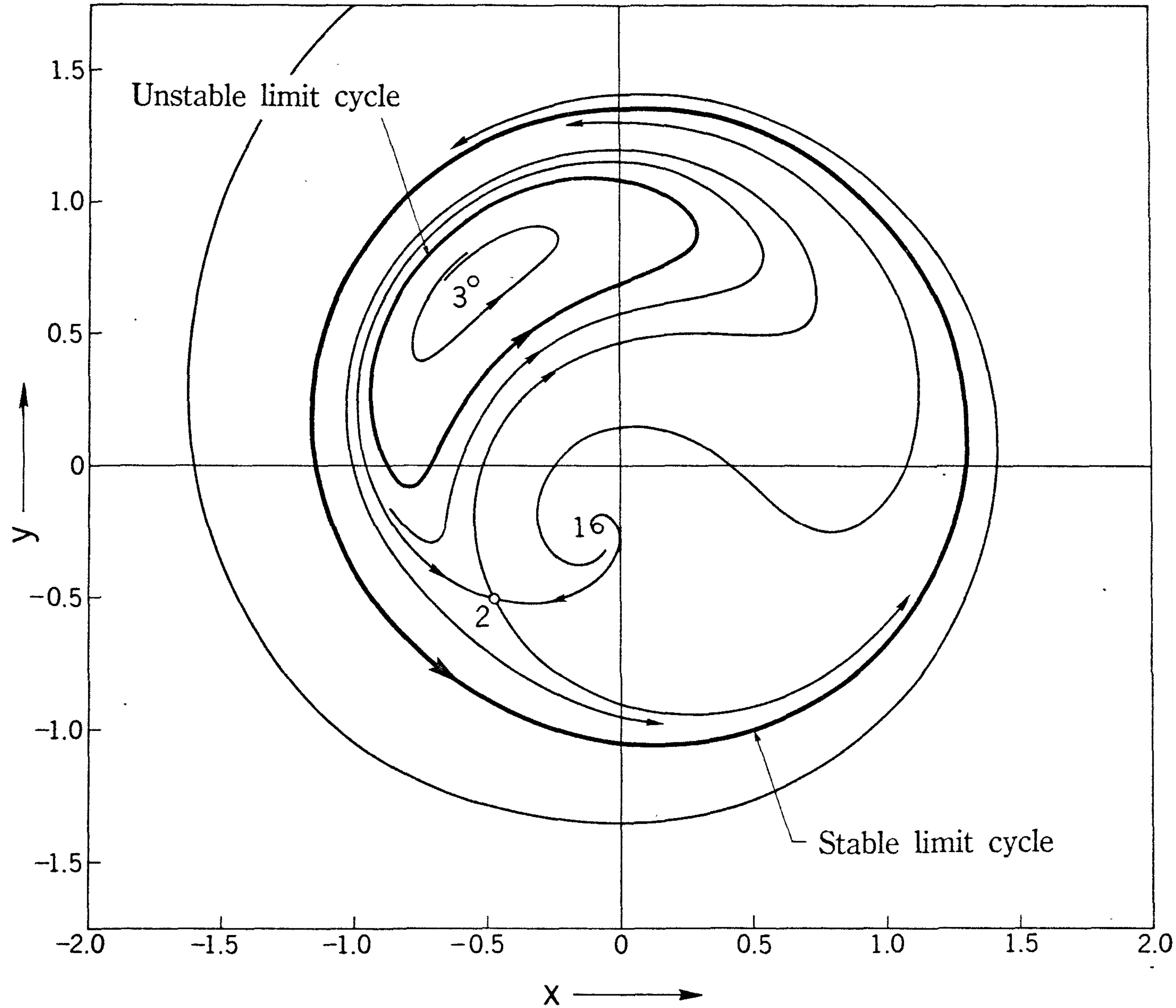


Fig. 5.3. Example of the phase portrait of the system as given by Eqs. (5.1).

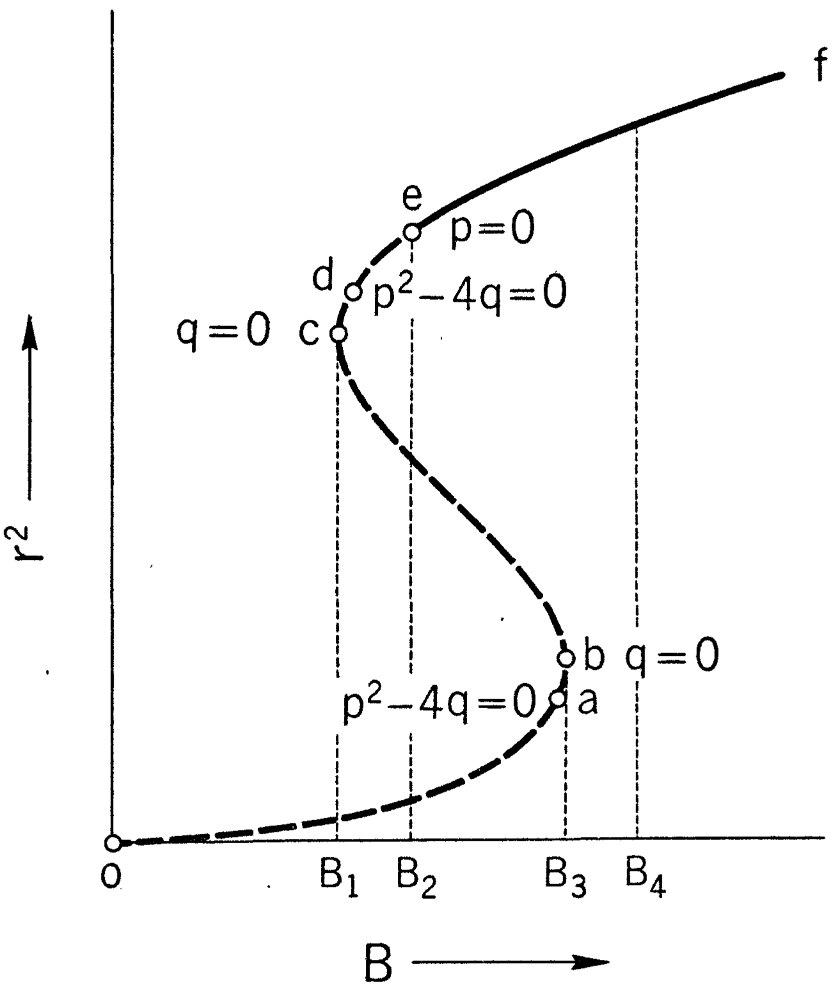


Fig. 5.4. Amplitude characteristic of the harmonic oscillation
when $\nu$ is kept constant.

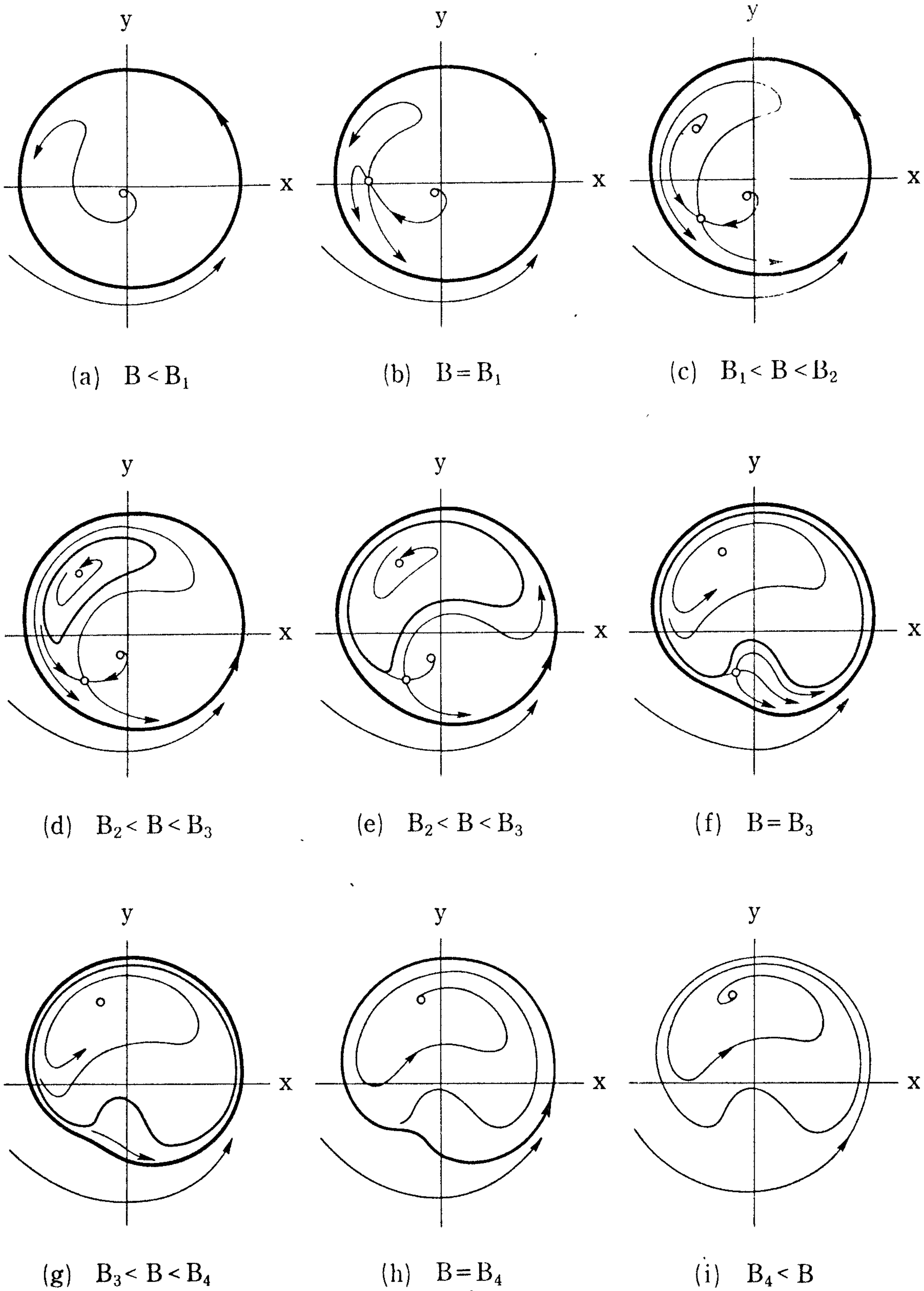


Fig. 5.[illegible]. Phase portraits of Eqs. (4.5) for various values of B.

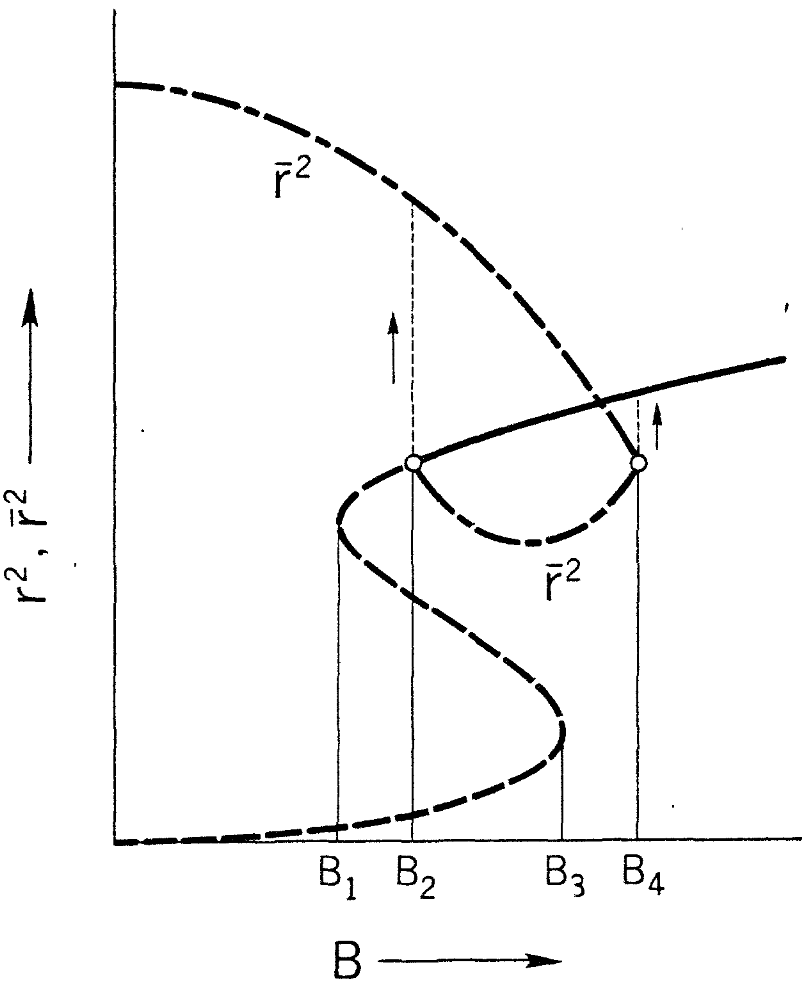


Fig. 5.6. Amplitude characteristic with mean-square amplitude of the almost periodic oscillation showing the transition between entrained and almost periodic oscillations.

## APPENDIX I

## THE THEOREMS OF BENDIXSON

The following theorems* are due to Bendixson and cited in our investigation of integral curves in chapter 3.

1°. First theorem of Bendixson

We consider a system of differential equations

$$\frac{dx}{dt} = X_m + X_{m+1}$$
$$\frac{dy}{dt} = Y_m + Y_{m+1} \tag{I.1}$$

where $X_m$ and $Y_m$ are polynomials which are homogeneous and of degree m in x and y; $X_{m+1}$ and $Y_{m+1}$ are analytic functions containing terms of degree higher than m.

The theorem of Bendixson states that the integral curves of the system (I.1) tend to the origin without any definite direction, thus in the manner of spirals, or with the definite direction as determined by the equation

$$xY_m - yX_m = 0 \tag{I.2}$$

2°. Second theorem of Bendixson

We deal with the differential equation

$$x^m \frac{dy}{dx} = ay + bx + B(x,y) \tag{I.3}$$

---

* For the proofs of these theorems see Bendixson [2, pp. 34, 45].

where $B(x,y)$ is a polynomial containing terms of degree higher than the first in $x$ and $y$, and we assume that $a \neq 0$.

Bendixson has obtained the following conclusions.

Case 1. $a > 0$, m: even number.

There is one and only one branch of integral curves tending to the origin on the left side of the y axis, while integral curves on the other side constitute a nodal distribution, i.e., they form a nodal region for $x > 0$. These integral curves are schematically illustrated in Fig. I.1.

Case 2. $a < 0$, m: even number.

By the substitution $x = - x'$, this case may be transformed to the foregoing case; thus we have a nodal distribution of integral curves for $x < 0$, and a saddle distribution for $x > 0$.

Case 3. $a > 0$, m: odd number.

The origin is a nodal point.

Case 4. $a < 0$, m: odd number.

The origin is a saddle point.

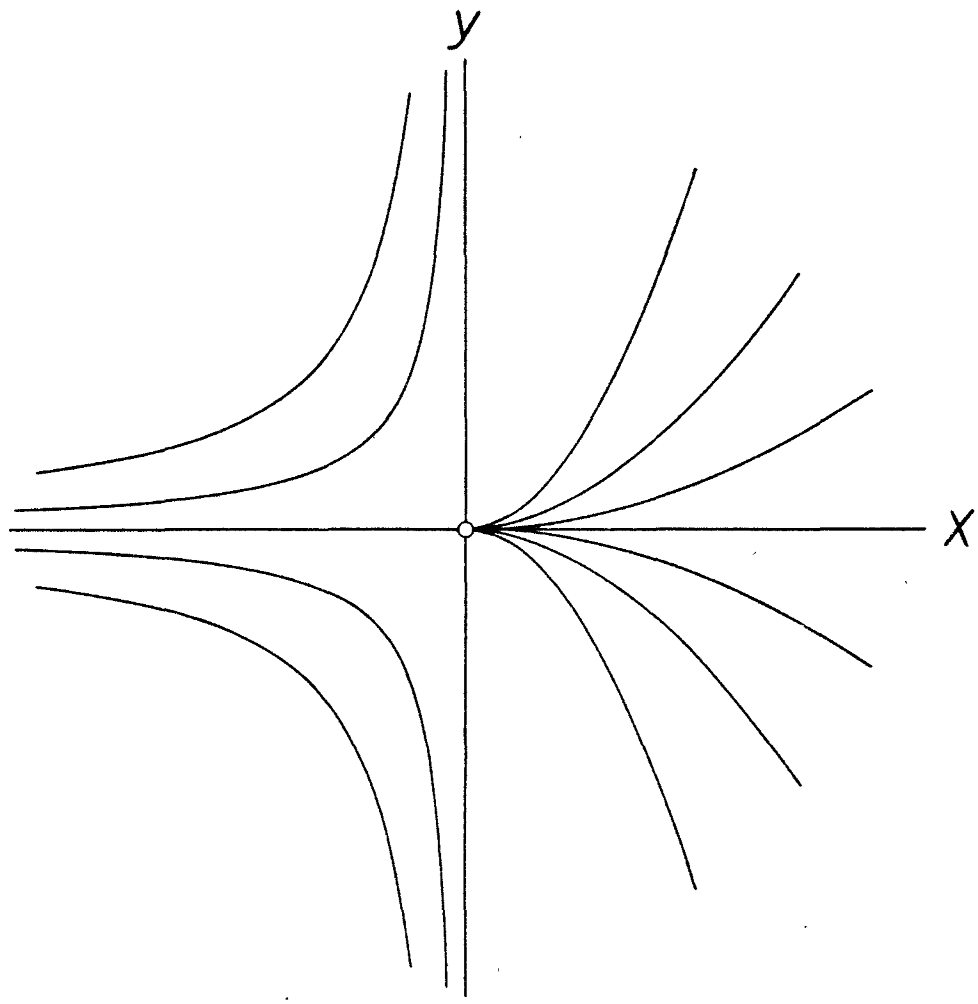


Fig. I.1. Coalescence of node and saddle.

# APPENDIX II

## THEORY OF CENTERS (POINCARÉ)

The types of singular points have been classified according to the roots of the characteristic equation (see Sec. 3.3b). If, in particular, the roots are purely imaginary, so that

$$p = -(a_1 + b_2) = 0$$
$$p^2 - 4q = (a_1 - b_2)^2 + 4a_2b_1 < 0 \tag{II.1}$$

the singularity will be either a center or a focus. The following procedure due to Poincaré [20, pp. 32-38] will distinguish between these two types of singularity when the conditions (II.1) are satusfied.

We consider a set of differential equations

$$\frac{dx}{dt} = X_1 + X_2 + \cdots + X_n \equiv X$$
$$\frac{dy}{dt} = Y_1 + Y_2 + \cdots + Y_n \equiv Y \tag{II.2}$$

where $X_m$ and $Y_m$ $(m = 1, 2, \cdots, n)$ are homogeneous polynomials of degree m in x and y. Since both X and Y vanish for $x = y = 0$, the origin is a singular point of the system (II.2).

In order to investigate the behavior of integral curves near the singularity, we consider a family of closed curves around the origin defined by

$$F(x,y) = C \tag{II.3}$$

where F(x,y) is a positive definite function of x and y, and C is a sufficiently small positive constant. We write

$$F(x,y) = F_2 + F_3 + F_4 + \cdots \tag{II.4}$$

where $F_i (i = 2, 3, 4, \cdots)$ is a homogeneous polynomial of degree i in x and y. Then, using Eqs. (II.2) and (II.4), we obtain

$$\frac{dF}{dt} = \frac{\partial F}{\partial x}\frac{dx}{dt} + \frac{\partial F}{\partial y}\frac{dy}{dt}$$
$$= (\frac{\partial F_2}{\partial x} + \frac{\partial F_3}{\partial x} + \cdots)(X_1 + X_2 + \cdots) + (\frac{\partial F_2}{\partial y} + \frac{\partial F_3}{\partial y} + \cdots)(Y_1 + Y_2 + \cdots)$$

If we write

$$\phi_{ik} = \frac{\partial F_i}{\partial x} X_k + \frac{\partial F_i}{\partial y} Y_k \tag{II.5}$$

then

$$\frac{dF}{dt} = \phi_{21} + (\phi_{31} + \phi_{22}) + (\phi_{41} + \phi_{32} + \phi_{23}) + \cdots \tag{II.6}$$

Following the analysis due to Poincaré, the unknown functions $F_i$ will be sought by equating zero the polynomials of the same degree in the right side of Eq. (II.6); namely,

$$\begin{aligned} \phi_{21} &= 0 \\ \phi_{31} &= -\phi_{22} \\ \phi_{41} &= -\phi_{32} - \phi_{23} \\ &\cdots\cdots \end{aligned} \tag{II.7}$$

When the conditions (II.1) are satisfied, an appropriate linear transformation of the variables and a change in the time scale will enable to choose $X_1$ and $Y_1$ in Eqs. (II.2) such that

$$X_1 = y \qquad \text{and} \qquad Y_1 = -x$$

Then $F_2 = x^2 + y^2$, and Eqs. (II.7) may be written in the form

$$\frac{\partial F_q}{\partial x} y - \frac{\partial F_q}{\partial y} x = H_q \qquad q = 2, 3, 4, \cdots \tag{II.8}$$

Introducing polar coordinates $x = r\cos\varphi$ and $y = r\sin\varphi$, we have

$$\frac{\partial F_q}{\partial x} y - \frac{\partial F_q}{\partial y} x = - \frac{\partial F_q}{\partial \varphi}$$

Equation (II.8) may be rewritten as

$$\frac{df_q}{d\varphi} = - h_q(\varphi) \qquad q = 2, 3, 4, \cdots$$

where
$$F_q = r^q F_q(\cos\varphi, \sin\varphi) = r^q f_q(\varphi) \qquad \text{(II.9)}$$

$$H_q = r^q H_q(\cos\varphi, \sin\varphi) = r^q h_q(\varphi)$$

A necessary condition for the solution of this equation is

$$\int_0^{2\pi} h_q(\varphi)d\varphi = 0 \qquad \text{(II.10)}$$

It is clear that this condition is also sufficient because, if it holds, we have

$$\frac{df_q(\varphi)}{d\varphi} = - h_q(\varphi) = \sum_{\nu=1}^{q} (a_\nu \cos\nu\varphi + b_\nu \sin\nu\varphi)$$

and, therefore,

$$f_q(\varphi) = \sum_{\nu=1}^{q} [\frac{a_\nu}{\nu} \sin\nu\varphi - \frac{b_\nu}{\nu} \cos\nu\varphi] + \text{const.}$$

If q is odd, the condition (II.10) is obviously satisfied. If, however, q is even, it may happen that the integral does not vanish and thus we are stopped in our procedure. We consider the following two cases.

Case 1. When the condition (II.10) ceases to hold as q increases.

Suppose that $f_2, f_3, \cdots, f_{q-1}$ are determined such that they satisfy the first (q - 2) equations of (II.9), but $f_q$ does not satisfy the (q - 1)th equation. In this case we replace the (q - 1)th equation by

$$\frac{df_q(\varphi)}{d\varphi} = - h_q(\varphi) + c_0$$

where
$$c_0 = \frac{1}{2\pi}\int_0^{2\pi} h_q(\varphi)d\varphi \tag{II.11}$$

and thus achieve the integrability for $f_q$. Returning to the cartesian coordinates, we obtain, after multiplication by $r^q$,

$$\frac{\partial F_q}{\partial x} y - \frac{\partial F_q}{\partial y} x = H_q(x,y) - c_0(x^2 + y^2)^{q/2} \tag{II.12}$$

It is noted that q is even in this case. We stop our procedure at this point and consider the polynomial

$$F(x,y) = F_2 + F_3 + \cdots + F_{q-1} + F_q \tag{II.13}$$

Then, for a sufficiently small value of C, F = C represents a closed curve encircling the singularity. If $c_0$ is negative, we see, from Fqs. (II.6), (II.12), and (II.13), that

$$\frac{dF}{dt} = \frac{\partial F}{\partial x} X + \frac{\partial F}{\partial y} Y > 0$$

so that the representative point on the integral curve will cross the closed curve from the inside to the outside as t increases. Hence the singularity is an unstable focus. If $c_0$ is positive, on the other hand, the representative point will cross the closed curve in the reversed direction, so that the singularity is a stable focus.

Case 2. When the condition (II.10) holds for all values of q.

In this case Eqs. (II.8) are solved for all values of q; thus we obtain

$$F(x,y) = F_2 + F_3 + \cdots + F_q + \cdots \tag{II.14}$$

which satisfies

$$\frac{\partial F}{\partial x} X + \frac{\partial F}{\partial y} Y = 0 \tag{II.15}$$

The solution of Eqs. (II.2) is given by

$$F(x,y) = C \tag{II.16}$$

which represents a family of closed curves encircling the singularity. Hence the singularity is a center.

# REFERENCES


1. Andronow, A. A., and S. E. Chaikin: "Theory of Oscillations," Princeton University Press, Princeton, N.J., 1949; enlarged 2d ed. by A. A. Andronow, A. A. Witt, and S. E. Chaikin, Fizmatgiz, Moscow, 1959 (in Russian).
2. Bendixson, I.: Sur les courbes définies par des équations différentielles, Acta Math., **24**: 1-88 (1901).
3. Cartwright, M. L.: Forced Oscillations in Nearly Sinusoidal Systems, J. Inst. Elec. Engrs. (London), **95**(3): 88-96 (1948).
4. Floquet, G.: Sur les équations différentielles linéaires à coefficients périodiques, Ann. Ecole Norm. Super., **2-12**: 47-88 (1883).
5. Gillies, A. W.: On the Transformations of Singularities and Limit Cycles of the Variational Equations of Van Der Pol, Quart. J. Mech. and Appl. Math. (London), **7**(2): 152-167 (1954).
6. Gillies, A. W.: The Singularities and Limit Cycles of an Autonomous System of Differential Equations of the Second Order Associated with Nonlinear Oscillations, Symp. Nonlinear Oscillations (Intern. Union Theoret. Appl. Mech.), Kiev, 1961.
7. Hayashi, C.: "Forced Oscillations in Nonlinear Systems," Nippon Printing and Publishing Co., Ltd., Osaka, Japan, 1953.
8. Hayashi, C.: Subharmonic Oscillations in Nonlinear Systems, J. Appl. Phys., **24**: 521-529 (1953).
9. Hayashi, C.: Initial Conditions for Certain Types of Nonlinear Oscillations, Symp. Nonlinear Circuit Analysis, **6**: 63-92 (1956), Polytechnic Institute of Brooklyn, New York.
10. Hayashi, C.: Quasi-periodic Oscillations in Nonlinear Control Systems, Autom. Remote Control (First Intern. Congr. IFAC), vol. 2, 889-894, Butterworth Scientific Publications, London, 1961.

11. Hayashi, C., Y. Nishikawa, and M. Abe: Subharmonic Oscillations of Order One-half, *Trans. IRE Circuit Theory*, **CT-7**: 102-111 (1960).

12. Hayashi, C., H. Shibayama, and Y. Nishikawa: Frequency Entrainment in a Self-oscillatory System with External Force, *Trans. IRE Circuit Theory*, **CT-7**: 413-422 (1960).

13. Hayashi, C., and Y. Nishikawa: Initial Conditions Leading to Different Types of Periodic Solutions for Duffing's Equation, *Symp. Nonlinear Oscillations* (*Intern. Union Theoret. Appl. Mech.*), Kiev, 1961.

14. Hayashi, C., H. Shibayama, and Y. Ueda: Quasi-periodic Oscillations in a Self-oscillatory System with External Force, *Symp. Nonlinear Oscillations* (*Intern. Union Theoret. Appl. Mech.*), Kiev, 1961.

15. Hayashi, C.: "Nonlinear Oscillations in Physical Systems," McGraw-Hill Book Company, Inc., New York, 1964.

16. Hill, G. W.: On the Part of the Motion of the Lunar Perigee, *Acta Math.*, **8**: 1-36 (1886).

17. Hurwitz, A.: Uber die Bedingungen, unter Welchen eine Gleichung nur Wurzeln mit negativen reellen Teilen besitzt, *Math. Ann.*, **46**: 273-284 (1895).

18. McLachlan, N. W.: "Theory and Application of Mathieu Functions," Oxford University Press, London, 1947.

19. Mathieu, E.: Mémoire sur le mouvement vibratoire d'une membrance de forme elliptique, *J. Math.*, **2-13**: 137-203 (1868).

20. Minorsky, N.: "Nonlinear Oscillations," D. Van Nostrand Company, Inc., Princeton, N.J., 1962.

21. Nishikawa, Y.: "A Contribution to the Theory of Nonlinear Oscillations," Nippon Printing and Publishing Co., Ltd., Osaka, Japan, 1964.

22. Poincaré, H.: Sur les courbes définies par les équations différentielles, *J. Math.*, **4-1**: 167-244 (1885); **4-2**: 151-217 (1886).

23. Poincaré, H.: "Oeuvres," vol. 1, Gauthier-Villars, Paris, 1928.

24. Stoker, J. J.: "Nonlinear Vibrations," Interscience Publishers, Inc., New York, 1950.

25. Strutt, M. J. O.: Lamésche, Mathieusche, und verwandte Funktionen in Physik und Technik, Ergeb. Math. Grenzg., 1-3: 207-322, Springer-Verlag, Berlin, 1932.

26. Whittaker, E. T., and G. N. Watson: "A Course of Modern Analysis," Cambridge University Press, London, 1935.